THE EXPRESSION AND FUNCTION

OF

STRETCH-ACTIVATED

2P-4TMD K^+ CHANNELS IN THE HEART

A THESIS SUBMITTED TO THE UNIVERSITY OF ADELAIDE AS THE REQUIREMENT OF THE DEGREE OF DOCTOR OF PHILOSOPHY

BY

ZHU HAIPENG

M App Sc, M Busi Oper MGT, MBBS

DEPARTMENT OF PHYSIOLOGY

SCHOOL OF MOLECULAR & BIOMEDICAL SCIENCE

THE UNIVERSITY OF ADELAIDE

May 2006

TABLE OF CONTENTS

GENERAL DISCUSSION

APPENDIX

SUMMARY

2-Pore-4-Transmembrane domain (2-P-4-TMD) potassium channels are first cloned in mouse and have been shown to be expressed in a widely variety of animals. To the humans, 2P potassium channels are not only expressed in central nervous system but are also found in peripheral organs. 2P potassium channels are the members of KCNK gene family that control background potassium conductance for regulating resting membrane potential and cell excitability. Similar arrangement of conservative amino acid sequence (T-x-G-x-G) is shown on the pore structure, which contributes to a typical K^+-selective ionic propensity. Based on the unique physiological and pharmacological characteristics, TREK-1 (Twik-RElated K^+ channel; KCNK2), TREK-2 (KCNK10) and TRAAK (Twik-Related Arachidonic Acid-stimulated K^+ channel; KCNK4) are distinguished from other members of 2P potassium channels.

TREK-1, TREK-2 and TRAAK are sensitive to membrane stretch, pH, temperature and polyunsaturated fatty acids. TREK-1 is also activated by lysophospholipids and inhaled anaesthetics. The functions of TREK-1 are regulated by neurotransmitters and receptor-dependent signalling mechanisms, which include TREK-1 activity is enhanced by phosphorylating Ser-351 of C-terminus by a cGMP-activated protein kinase (PKG); TREK-1 is inactivated by phosphorylating Ser-300 and Ser-333 of C-terminus by protein kinase A (PKA) and C; The action of $G\alpha_s$-couple receptors pathway preventing TREK-1 activity is similar as PKA whereas inhibition of $G\alpha_q$-couple receptors to TREK-1 is similar as PKC. TREK-1 is also

largely inhibited by prostaglandin E_2 (PGE_2). In addition, TREK-1 is notably insensitive to typical potassium channel inhibitors such as tetraethylammonium (TEA), 4-aminopyridine (4-AP) and Ba^{2+}. Furthermore, TREK-1 is not inactivated by Gd^{3+}. TREK-1 knockout mouse shows that polyunsaturated fatty acid-activated neuroprotection is weakened in ischemia area and the sensitivity of TREK-1 to volatile anaesthetics is reduced. 3 splice variants have been identified for TREK-2 including Variant A (Va) (Genebank AF279098), Variant B (Vb) (AF385399) and Variant C (Vc) (AF385400). The coding areas of Va, Vb and Vc encode 539, 544 and 544 amino acids respectively. TREK-2 has 7 exons (as does TREK-1), and the splice variants arise because of alternative sequences in the first exon. However, distribution of TREK-2 in human tissues is different from TREK-1 and TRAAK. Va is mainly expressed in kidney and pancrease, and Vb is largely expressed in kidney and pancreas whereas Vc mainly in brain. Vb and Vc expressed in human embryonic kidney 293 cell line show similar characteristics as a single channel and alternative sensitivity to antagonist of PKC and PKA. In spite of sharing 78% sequence homology, the distribution of TREK-1 and TREK-2 in human brain is different.

With TREK-1 expressed in cardiomyocytes of mice and rat and TREK-1-like potassium currents found in human atrial tissue, these observations strongly indicate the existence of TREK-1, TREK-2 or TRAAK in human heart. To investigate the expression of TREK-1, TREK-2 and TRAAK in human, PCR, nested PCR and sequencing are essential to be used in the illustration of the homology of TREK channels in human heart and other TREK-expressed organs. Sequencing is applied to

decide whether TREK in human heart is identical to any published TREK sequence in Genebank. To TREK-1 and TRAAK, primer design focuses on showing at least one pore structure in sequencing. To TREK-2, primer design is concentrated on exhibiting the unique arrangement of exon 1 of each variant in sequencing. Due to the likely functions of TREK channels under different physiological and pathological conditions, Western blot, real-time PCR and immunohistochemistry are applied in the quantification and localization of TREK channels in normal and diseased human heart.

The results presented in this thesis show the existence of TREK-1, variant A and C of TREK-2 and TRAAK in human heart; the localization of TREK-1 and variants of TREK-2 on the membrane and in cytoplasmic areas of human cardiomyocyte; the notably high-level expression of TREK-1 in diseased human heart; the reverse expression of variant A and C of TREK-2 in normal and diseased human heart. These observations strongly indicate TREK channels play important roles in arrhythmia genesis and TREK-sensitive cardiac remodeling within the development of cardiac hypertrophy, ischemia cardiomyopathy and idiopathic dilated cardiomyopathy.

Despite TREK channels are first discovered in human heart and the current lack of TREK-specific agonists and antagonists have restricted the research of the function of TREK channels in human heart, it is postulated that TREK may be a practical target for clinically relevant applications.

DECLARATION

This work contains no material that has been accepted for the award for any other degree or diploma in the University or other tertiary institution and, to the best of my knowledge and belief, contains no material previously published or written by another person, except where due reference has been made in the text.

I authorize this copy of my PhD thesis to the University of Adelaide, when deposited in the University Library, being available for loan and photocopying.

Zhu Haipeng

May 2006

ACKNOWLEDGEMENTS

This thesis is achieved successfully with the support and resources provided to me through the Department of Physiology of The University of Adelaide. I am sending my truthful thanks to Department of Cardiac Surgery of Royal Adelaide Hospital, Department of Cardiac Surgery of Saint Vincent Hospital, Sydney and Prof. Cris dos Remedios, Department of Anatomy of The University of Sydney for supporting human atrium, ventricle and testicles. I am so grateful that Australia Commonwealth Government provides Scholarship of Australia Postgraduate Award for me to achieve such great progress in my academic life. I am also sincerely appreciated for Traveling Fellowship supported by Australia National Heart Foundation assisting me to enter Annual Meeting of European Society of Cardiology in Stockholm, Sweden, 2005.

This study would not have been accomplished without the guidance of my principle supervisor A. Prof. David Saint. I am deeply indebted and honestly grateful to him for the assistance, suggestion and encouragement throughout my PhD candidature. I am also giving my thanks to his support in the preparation of this thesis and patent application. I wish to thank A. Prof. Michael Roberts, as my co-supervisor, for his enlightenment in solving the difficulties of my experiments. I would like to express sincere appreciation to Prof. Caroline McMillen for all her efforts on my major review and annual reviews.

I express sincere thanks to Dr. Kathy Saint, Dr. Jacob Ross, Dr. Weihong Liu, and Dr. Shiyong Yuan for the assistance of PCR, Western blot and immunohistochemistry. These thanks are also expanded to Dr. Daniel Ninio for obtaining human atrial tissues, Miss. Janet Smith for helping to prepare the experiments and Dr. Justin Dibbens for reviewing and finalizing the provision patents of TREK-1 and TREK-2 in PCT

Finally, I dedicate this thesis to my parents, my sister, my brother-in-law and my nephew and thank them for their patience, encouragement and support over the years especially during the difficult periods in my PhD candidature and thesis writing.

PAPERS & PATENTS

The papers that have been finished and being sent to the journals:

Expression of the Tandem-pore potassium channel TREK-1 in human heart ***Zhu H-P,*** *Yuan S-Y and Saint. D. A.*

Expression and localization of TREK-2 in normal and diseased human heart ***Zhu H-P,*** *Yuan S-Y and Saint.*

Expression and localization of TREK-1 in normal and diseased human heart ***Zhu H-P,*** *Yuan S-Y, Diniol D and Saint. D. A.*

Patents

TREK-1 in human and the possible applications of TREK-2 in arrhythmia and cardiac hypertrophy have been patented in PCT (PCT/AU2005/001937) by The University of Adelaide on 22-Dec-2005, where ***Mr. Haipeng Zhu*** is shown as an inventor.

Conference Presentation

Poster

European Society of Cardiology, 2005. Expression of 2-Pore Potassium Channel TREK-1 in Human Heart ***Zhu H-P,*** *Yuan S-Y and Saint. D. A.*

Scientific Session of American Heart Association, 2005. Expression of 2-Pore Potassium Channel TREK-2 in Human Heart ***Zhu H-P,*** *Yuan S-Y and Saint. D. A.*

Figures & Tables

Figure 1. MEF affects the interaction of action potentials and contraction. After normal excitation contraction coupling, a mechanical change associated with the next normal excitation is produced. This perturbation generated by drop in venous return or blood- decreased stretch prolongs the action potential, which increases the force of excitation (Lab, 1999).

Figure 2. Altering cell length or tension acts on the process of excitation and mechano-electric feedback, which are independent of a mechanical effect caused by cardiac contraction, or by the changes of the mechanical background in the heart (Kohl et al., 1996).

Figure 3. MEF acts on the action potentials of two segments in series during mechanical interaction with one segment contracting abnormally (Lab, 1999).

Figure 4. Monophasic action potential recorded from the right endocardium of the patient undergoing pulmonary valvuloplasty. A is control whereas B is response to acute obstruction of right ventricular outflow tract. Premature beats were produced (Levine et al., 1988).

Figure 5. Mechanoactivated ectopic excitation occurred in a Langendorff rabbit heart model. Upper curve is normal monophasic action potential whereas lower curve shows that changing volume of fluid volume injected in left ventricle causes depolarization of the diastolic membrane potential under a critical value (Franz et al., 1992).

Figure 6. ECG illustrates that early ventricular fibrillation is corrected by a single chest thump (Barrett et al., 1971). When expanding of ventricular fibrillation is fallen in refractory period produced by mechanical stimulation, ventricular fibrillation is prevented and normal rhythmus reoccurred.

Figure 7. ECG and left ventricular pressure recording obtained from an anaesthetised pig show that due to a pre-cordial impact that coincides with the upstroke of the T-wave, mechanical- induced ventricular fibrillation occurred and contractility disappeared (Link et al., 1998).

Figure 8. illustrates that normal heart is kept in uniformly systolic and diastolic phases (A and B); a region of acute ischemia in left ventricle (C) moves paradoxically during systole, which may cause the production of a number of MEFs (Taggart et al., 1999).

Figure 9. shows that the formation of a secondary depolarization (EAD) during the phase 3 of action potential whereas the formation of DAD after the phase 3. Tthe amplitudes of both EAD and DAD reaching threshold activate a premature action potential (Taggart et a.l, 1999).

Figure 10. Left shows that excitation from point A blocks at points B and C in an area of inexcitability and then passes the blocked area by D. Right shows that excitation through point D re-excites point A (Taggart et al., 1999).

Figure 11. illustrates that different mechanochemical stimulations are transferred from cell membrane to intact heart. Stimulation felt by Mechanosensor and chemosensor acted on the local adhesion complexes of the membrane, which includes stretch-activated channels (SAC), chemical receptors, integrins and focal adhesion kinase (FAK). SACs have effects on cell electrophysiology by changing ion concentration. Stimulation produces electrophysiological and biochemical alterations by cytoskeleton system and signal transduction system, which affect cardiovascular function at molecular level. Mechanochemical stimulation activates immediate early genes (IEGs) and relative protein kinase

cascade, which function on the distant cardiac tissue and the whole heart and remodel myocardium in cardiac hypertrophy and chronic heart failure (Lab et al., 1999)

Figure 12. illustrates that a 21pS stretch-activated ion channel is recorded by single-channel technique from a fresh-isolated 17-day-old embryonic chick ventricular cell under a pipette suction of 25mmHg. The channel is activated during the application of suction in the recording pipette, and inactivated after removing the suction. Time scale magnification of a segment of the recording shown in the upper panel, as indicated. Time scale bar: 1s fro the upper panel and 100ms for the lower panel. Recording conditions: pipette and bath solutions in mM, 150 NaCl, 5 KCl, 2 $CaCl_2$, 1 $MgCl_2$, 10HEPES, pH 7.4 titrated with NaOH. Pipette holding potential, +60mV (Hu et al., 1994).

Figure 13. shows that membrane potential responding to artificial long-lasting stretch in left ventricle with myocardial infarction. With increasing stretch, stretch-activated depolarization occurs near to APD50 whereas withdrawing stretch results in disappearance of the stretch-induced effect (n=7) (Irina et al., 2000).

Figure 14. shows that stretch-activated depolarisations near to APD90 in left ventricle with myocardial infarction are suppressed by applying 40μM Gd^{3+} (n=9). The effect of Gd^{3+} is produced within 5 and 10 min after application (Irina et al., 2000).

Figure 15. Distribution of K_{2P} channels in adult human tissue. DNA fragments are PCR amplified by using specific primers and analyzed by Southern blot by using internal ^{32}P-labeled oligonucleotides. PBL: peripheral blood leukocytes; GAPDH: glyceraldehydes-3-phosphate-dehydrogenase (Lesage and Lazdunski, 2000).

Figure 16. shows molecular structures of K^+ channel families. Transmembrane domain and pore structure are recognized from the N-terminus. 2-pore channels are composed of an extended extracellular loop with the first TM domain (O'Connell et al., 2002).

Figure 17. shows membrane morphology and diversity of 2P-K^+ channel subunit. M_1-M_4 are four transmembrane domains and P_1 and P_2 were 2P domains. The potential amphipathic α-helix involved in the formation of homodimers is in the self-interacting domain (SID). K_{2P} channels are cloned in mice and humans, which have been coded in Genebank (Lesage and Lazdunski, 2000).

Figure 18. shows that mRNA from other human tissue and brain are hybridised at high stringency with a ^{32}P labelled HKT4.1b cDNA (β-actin as control). The blots are exposed to X-ray film for 36h for HKT4.1 and 6h for β-actin. Andres et al., (2002).

Figure 19. shows a clear band, (theoretic size 697bp), is amplified by specific primers of TREK-1 on 1.2% Agarose gel.

Figure 20. demonstrates that nested PCR produces one band (theoretical size 372bp). Sequencing shows nested PCR product is 100% homologous to the published human TREK-1 sequence.

Figure 21. shows that normal PCR for TRAAK in human atrial tissue give a single band (theoretical size 477bp), in which human testicular tissue is chosen as a positive control.

Figure 22. shows that 250-bp nested PCR product is obtained, whose sequencing result is 100% homologous to the published sequence of TRAAK

Figure 23. A and B shows that the primers of TREK-1 and TRAAK applied in real-time PCR are specific and valid. The results of real-time PCR are suitable to represent the expression level of

TREK-1 and TRAAK in human atrial and ventricular tissues. TREK-1, TRAAK and GAPDH are synthesized in 84, 86 and 87 degree, respectively (A) whereas their fluorescence is dectected by Laster Reader in 27 cycles, 16 cycles and 14 cycles, respectively (B). All curves of the same pair of primers can be traced in a fix initial point that means regression of a single curve is valid to calculate the initial mRNA concentration from a given sample.

Figure 24. A, Ratio of expression levels of TREK-1 and TRAAK to GAPDH in fresh human testicular tissue (left panel, n=1), frozen human atrial tissue (middle panel, n=7) and fresh human atrial tissue (right panel, n=3). B, Comparison of TREK-1 and TRAAK expression in frozen atrial and ventricular tissue samples. Left panel; fresh human testicular tissue (n=1), middle panel; frozen human atrial tissue (n=7) and right panel; frozen ventricular tissues (n=5). C, Comparison of expression of TREK-1 and TRAAK in fresh human testicular tissue (left panel, n=1), 3-month-frozen human testicular tissue (middle panel, n=1) and fresh human atrial tissues (right panel, n=3).

Figure 25. Western Blot analysis of human ventricular samples. 4 ventricular samples are selected from human donor group. GAPDH (36.6KDa) as positive control and TREK-1 (55KDa) are recognized by relative specific antibody. Botanic tissue is selected as negative control (NC). Sample concentration is 20μg/30μL; $[\text{primary Ab}]_{\text{TREK-1}}$=1:500; $[\text{secondary Ab}]_{\text{TREK-1}}$=1:1000; $[\text{primary Ab}]_{\text{GAPDH}}$=1:1000; $[\text{secondary Ab}]_{\text{GAPDH}}$=1:2000.

Figure 26. TREK-1 immunoreactivity in paraffin section of human heart. A. Labeled TREK-1 channels in longitudinal section of cardiac myocytes in atrial appendage. TREK-1 immunoreactivity is observed as bright punctate granules in most of cardiac myocytes. Many of them are found along the membrane of the cardiac myocytes (unfilled arrows) and some in the cytoplasm. Connective tissue between the muscle bundles (arrow heads) and the center of nuclear region in cardiac myocytes (filled arrows) are not labeled. No immunoreactivity is found in negative control preparation after omission of primary antibody (B). C: Labeled TREK-1 channels in cross-section of cardiac myocytes in ventricular tissue. Similar distribution of TREK-1 immunoreactivity in atrial tissue is observed in ventricular tissue. Labelled TREK-1 channels can also be found along membrane of cardiac myocytes and in the cytoplasm. No connective tissue and centre of nuclear region of cardiac myocytes are labelled. No positive labelling was observed in negative control preparation (D). Calibration bar: 25 μm for A and B and 50 μm for C and D.

Figure 27. PCR results of real-time primer. Human testicle tissue is selected as positive control.

Figure 28. Western blot of TREK-1 and GAPDH in human donor, IDC and IC groups. A: TREK-1 (55KDa) and GAPDH (37KDa) as positive control are identified by specific antibodies from normal human ventricular samples (n=4). [Supernatant concentration]=20μg/30μL. [Primary Ab] =1:500; [Secondary Ab] =1:1000; B and C: TREK-1 and GAPDH were expressed in idiopathic dilated cardiopathy samples (n=7) and ischemia cardiopathy samples (n=7). [Supernatant concentration]=20μg/30μL. $[\text{primary Ab}]_{\text{TREK-1}}$=1:500; $[\text{secondary Ab}]_{\text{TREK-1}}$=1:1000; $[\text{primary Ab}]_{\text{GAPDH}}$=1:1000; $[\text{secondary Ab}]_{\text{GAPDH}}$=1:2000.

Figure 29. The expression of TREK-1 in Donor, IC and IDC at mRNA and protein levels. A: summary data of real-time PCR of TREK-1 in Donor, IC and IDC; B: data collection of Western blots of TREK-1 in Donor, IC and IDC, in which density ratio of TREK-1 and GAPDH obtained by Gel Dock System is used to represent the amount of TREK-1 protein in each group. Mean values of TREK-1 protein in IDC and IC are compared with those in Donor.

Figure 30. Southern blot of TREK and TRAAK in human cDNA library, Lesage et al., (2000).

Figure 31. mRNA of TREK-2 is hybridized with human cDNA library, Gu et al., (2002).

Figure32. PCR and nested PCR of Va, Vb and Vc in human testicular tissue. A shows that one predicted size band was expressed by PCR for Va, Vb and Vc. (sizes were 948bp, 945bp and 760bp respectively). B shows nested PCR results for Va, Vb and Vc. One single-optimal band (255bp) was present in PCR products of Va, Vb and Vc.

Figure33. PCR and nested PCR of Va, Vb and Vc in human atrial and ventricular tissues. A illustrates PCR products for Va, Vb and Vc in human atrial tissue. A 948bp-product of Va and a 952bp-product of Vc PCR were expressed in human atrial tissue. No Vb expression could be detected. B: PCR products for human ventricular tissue. Similar to atria, Va and Vc variants were detected, but no Vb. Nested PCR results of Va and Vc were shown in C. A single 255bp band occurred in Va and Vc PCR products from human atrial and ventricular tissue.

Figure 34. Western Blot of Va and Vc in human atrial tissue. 6 human atrial samples from patients undergoing coronary artery bypass are used for Western Blot experiments. Va (59KDa) and Vc (61KDa) can be readily detected in all the samples. Supernatant concentration of each sample was 25μg/30μL. [primary Ab] =1:500; [secondary Ab] =1:1000.

Figure 35. Western Blot of Va and Vc in human ventricular tissue. A shows the expression of Va and Vc in 4 human ventricular samples from donor hearts with sample concentrations of 20μg/30μL. B demonstrates that only Vc was found in 6 human ventricular samples from donor hearts under the sample concentration of 6μg/20μL. [primary Ab] =1:500; [secondary Ab] =1:1000.

Figure 36. Western Blot of Va and Vc in human disease ventricular tissue. Western blot result of variant A and variant C in 2 ventricular samples of ischemic cardiomyopathy (sample 1&2) and 5 ventricular samples of idiopathic dilated cardiomyopathy (samples 3 to 7) with identical sample concentrations of 20μg/30μL. [primary Ab] =1:500; [secondary Ab] =1:1000.

Figure 37. The expression levels of Va and Vc in normal and pathological human ventricular samples. Diagram shows the comparison of expression level of variant A and C between normal human ventricular samples and pathological ventricular samples from Western blot experiments.

Figure 38. Immunohistochemistry of Va and Vc in human atrial and ventricular tissues. Panel A: TREK-2 immunoreactivity in paraffin section of human atrial appendage. Within the muscle bundle the cardiac myocytes are different in diameter and some of them show an empty area without myofibrils in the nuclear region (filled arrows). Punctate fine granules of TREK-2 immunoreactivity were located in most of cardiac myocytes. Some of TREK-2 positive granules were located along the membrane of the cardiac myocytes (hollow arrow). Connective tissue between the muscle bundles (arrow head) and centre of nuclear region in cardiac myocyte (filled arrows) were not labelled. No immunoreactivity was found in negative control preparation (Panel B). Calibration bar: 50 μm. Panel C: TREK-2 immunoreactivity in paraffin section of human cardiac ventricle. TREK-2 immunoreactivity was located in most of cardiac myocytes and their locations were similar to that in atrial myocytes, along the membrane (hollow arrow) and in the cytoplasm. Connective tissues

between the muscle bundles (arrow head) were not immunoreactive. In an expanded view (Panel D) the immunoreactivity appeared to be spaced in striations. No immunoreactivity was found in negative control preparation (Panel E). Calibration bar: 50 μm.

Figure 39. The expression of TREK-1 in guinea pig heart, rabbit heart and pig heart. The bands similar to 720bp are shown on A, B and C, respectively. D shows that the products similar to 194bp are expressed on nested PCR gel.

CHAPTER 1

LITERATURE REVIEW

1. GENERAL INTRODUCTION

During the earlier stages of embryogenesis, mechanical factors are involved in stimulating and regulating excitation and contraction of cardiac tissues (Rajala et al., 1976). Furthermore, Patten (1949) showed that at the end of the 3rd week of embryogenesis, mechanical regulation in electrophysiological activity has occurred in the heart, which is much ahead of the regulation of the autonomic nervous system. Bainbridge (1915) demonstrated that heart rate was increased by the distension of the right atria in an anaesthetised dog. He concluded that increasing the volume of fluid flowing back to the heart caused a reflex acceleration of heartbeat. This phenomenon is regarded as a feedback mechanism of the heart to the change of increasing load returning from veins. Decreasing or increasing heart load may lead to a stretch of myocardium that produces mechanical stimuli resulting in changes in electrophysiological behaviour of human heart.

Over 100 years researchers have been devoting their energy and enthusiasm into finding how stretch makes a great modification in excitation of the heart and how stretch acts as a cause of arrhythmias. The mechanisms and roles of stretch in producing abnormal cardiac electrophysiology, such as arrhythmias, have eluded physiological researchers. With the development of electrophysiological techniques and the progress of research methods, the effects of stretch on electrophysiological behaviours of the myocardium are being slowly unravelled. In this chapter, literature reviewed is classified into three subtopics, which are described as the importance of mechanoeletric feedback, stretch-activated channel and 2P-4MD-K^+channel, a group of specific stretch-activated channels.

1.1 MECHANOELECTRIC FEEDBACK (*MEF*)

1.1.1 THE CONCEPT OF *MEF*

The phenomenon of influencing the electrical properties of ventricular muscle by the process of MEF and its potential functions in arrhythmogenesis has been discussed extensively (Lab, 1982). Two questions are raised (1) whether mechanoelectric feedback occurs in the normal heart as a common electrophysiological behaviour (2) What is the importance of mechanoelectric feedback? Generally, mechanoelectric feedback is one kind of electrophysiological change that is produced when mechanical stimuli acted on myocardium. It is described as a transduction from a mechanical stimulus to an electrical signal. Mechanoelectric feedback is found not only in sinoatrial fibroblast and in atrium but also in ventricular myocardium (Kohl et al., 1996; Nazir et al., 1996). More reviewers have suggested that this process produces mechano-induced ventricular arrhythmia (Lab et al., 1982; Dean et al., 1989; Lab, 1991; Taggart et al., 1996).

MEF alters electrophysiological activity depending on changes in myocardial segment length. Franz (1996) reviewed that the following changes were produced: a shortening of the action potential duration; a decrease in the resting diastolic potential; a decrease in the maximum systolic action potential amplitude; development of early afterdepolarization; ectopic beats originating from afterdepolariztion in myocardium.

All these factors mentioned above may affect normal electrophysiological activity and are integrated into the generation of MEF. Also a variety of clinical data and previous studies have shown that MEF is involved in the situations such as acute

stretch, chronic stretch, myocardial infarction, myocardial hypertrophy, the changes of ionic concentration, direct or indirect factors leading to apoptosis and remodelling.

1.1.2 THE FUNCTION OF MEF

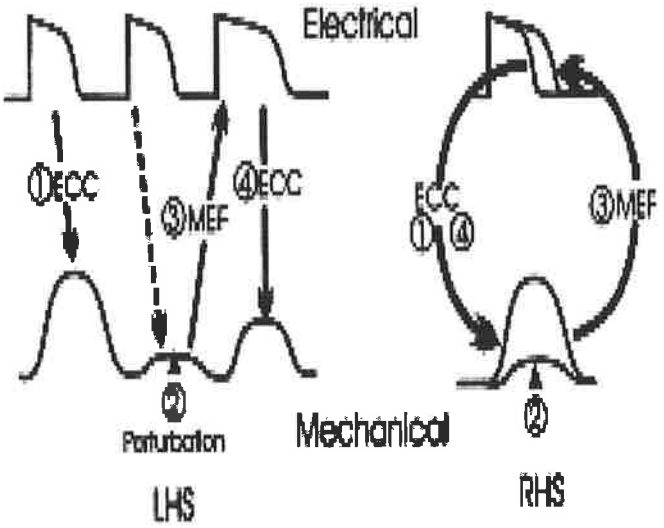

Figure1. MEF affects the interaction of action potentials and contraction. After normal excitation contraction coupling, a mechanical change associated with the next normal excitation is produced. This perturbation generated by drop in venous return or blood- decreased stretch prolongs the action potential, which increases the force of excitation (Lab, 1999).

Although MEF has an effect on normal electrophysiological action potential, it is possible that MEF may play a fine tuning role in the regulatory procedures of myocardium. Fig 1 illustrates a possible feedback situation occurring in both an initial stretch and the subsequent events in cardiomyocytes. As above, left hand panel is described in time series whereas right hand panel shows a feedback loop.

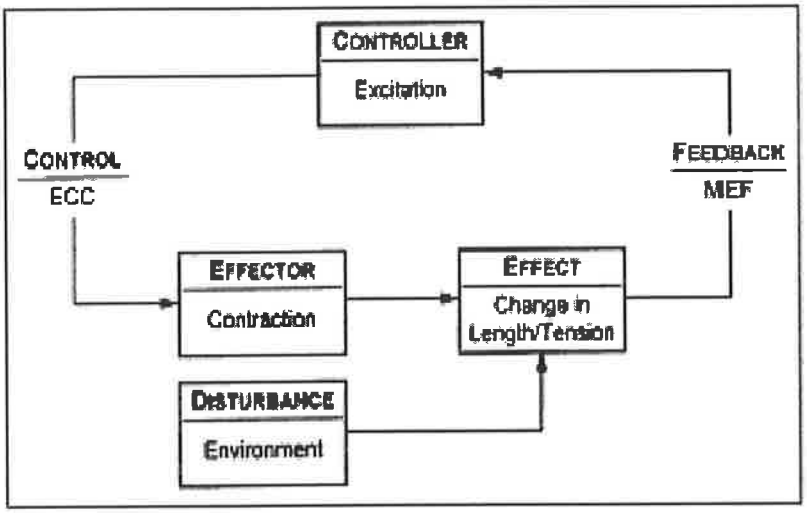

Figure2. Altering cell length or tension acts on the process of excitation and mechano-electric feedback, which are independent of a mechanical effect caused by cardiac contraction, or by the changes of the mechanical background in the heart (Kohl et al., 1996).

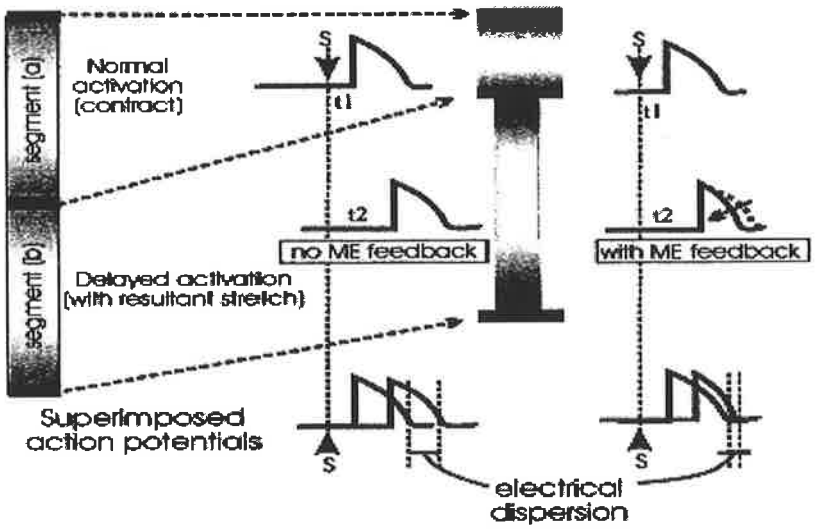

Figure3. MEF acts on the action potentials of two segments in series during mechanical interaction with one segment contracting abnormally (Lab, 1999).

Myocardial segments exhibit uniformly synchronous electrical and mechanical activity in a normal and intact heart. However, under certain cardiac pathological situations, for example an area of infarction, these interactions are altered. Figure 2 shows that environmental disturbance and efforts of contraction cause the changes in length or tension of cardiac muscle, which lead to the production of MEF. The time

difference of transferring excitation between two segments may be longer than normal. Fig 3 shows that if segment (a) contraction stretches segment (b) or segment (b) contraction is against an existed contracted segment, which meant segment (b) contracts with a high load this activates stretch-dependent channels and the duration of segment (b)'s repolarization is shortened ; Under such conditions, a decrease in the action potential duration and repolarization of segment (b) protects the myocardium from a dangerous arrhythmic situation.

1.1.2.1 MEF EFFECTS AND ALTERING PRELOAD AND AFTERLOAD

It is well known that the initial length of cardiac tissue influences resting membrane potential (Duel et al., 1954; Penefsky et al., 1963) and produces changes in duration (Lab, 1980) and amplitude (Penefsky et al., 1963) of the monophasic action potential. Many reviews yield various results on the effects of initial length on action potential duration. Hennekes et al., (1981) showed that gradual stretch of cat papillary muscle did not influence action potential duration, however gradual stretch of frog ventricular strips shortened the action potential duration (Lab, 1980). In an isolated canine ventricle, Franz et al., (1989) found that the action potential was shortened if the end-diastolic volume was increased during equal-load beating.

Davidson (1993) demonstrated significant MEF generated by altering preload in ventricles during normal ejection against constant levels of afterload. It was shown that the plateau phase of the monophasic action potential was shortened and repolarization became slow after the end-diastolic volume was increased from 20ml to 40ml. These results confirm that monophasic action potential duration measured at 20% repolarization is notably reduced if the end-diastolic volume is increased.

Significant reductions in monophasic action potential duration persist at 70-90% repolarization in spite of repolarization of the plateau phase being slow. At present, there are not enough details for showing the effects of MEF on altering preload in the ejecting heart.

Based on the data of afterload between cat papillary muscle and intact canine ventricle, the results demonstrate that in cat papillary muscle, during a quick release, the loaded contraction is reduced. This results in larger shortening of the muscle than occurred in physiologically loaded ventricles. In studies of intact canine ventricle, shortening deactivation has been demonstrated by using the end-systolic clamp technique (Sugiura et al., 1989). In cat papillary muscle experiments, quick release results in an immediate decrease in tension. Also the number of shortening deactivations found during lightly loaded contractions of the quick release experiments in papillary muscle is much more than that observed in the isolated canine ventricle during normal loaded contractions. These details reveal that monophasic action potential duration is unchanged by altering the ventricular afterload in canine ventricle. Without any changes associated with preload, alterations in afterload have not modulated action potential duration in the canine left ventricle.

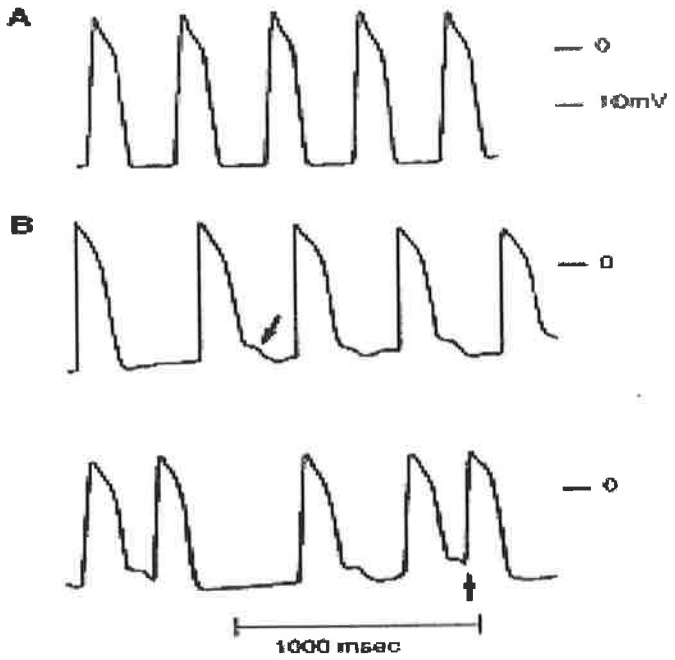

Figure4. Monophasic action potential recorded from the right endocardium of the patient undergoing pulmonary valvuloplasty. A is control whereas B is response to acute obstruction of right ventricular outflow tract. Premature beats were produced (Levine et al., 1988).

Although Fig 4 shows that monophasic action potential recorded from human right ventricles was shortened as right ventricular pressure rose in transient obstruction of the right ventricular outflow (Levine et al., 1988), it does not clarify the potential role of afterload in modulating electrophysiology in the intact heart. Due to increasing afterload, the ventricle preload keeps rising. This suggests that amplifying preload is more likely responsible for MEF effects. With increasing intraventricular pressure, myocardial length becomes more elastic and longer than before. Time-dependent ventricular distension is parallel to intraventricular pressure (Calkins et al., 1989), which protected myocardium against stretch during mechanical systole. During the period of diastole, increasing preload leads to the changes of myocardial length that makes myocardium more sensitive to stretch. This may explain the effects of altered preload with a few of the changes of afterload on time and amplitude of the action potential.

1.1.2.2 MEF AND EARLY/DELAYED AFTERDEPOLARIZATION

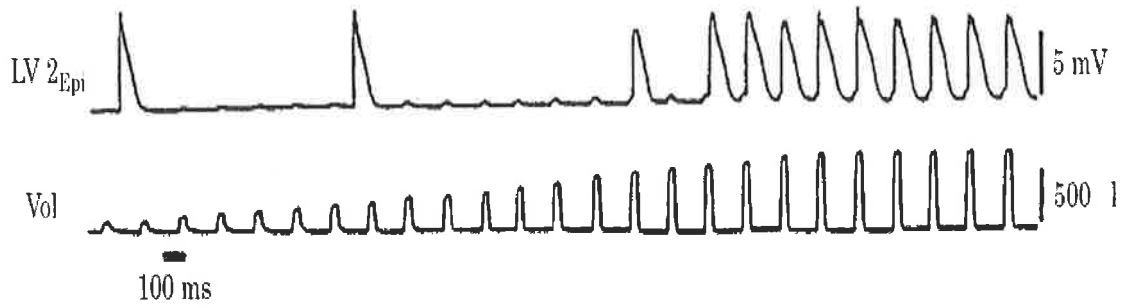

Figure5. Mechanoactivated ectopic excitation occurred in a Langendorff rabbit heart model. Upper curve is normal monophasic action potential whereas lower curve shows that changing volume of fluid volume injected in left ventricle causes depolarization of the diastolic membrane potential under a critical value (Franz et al., 1992).

Franz et al., (1992) showed that rapid stretch caused premature ventricular excitation with the increase of volume. A number of rapid volume pulses with step-by-step increasing amplitude produce diastolic depolarizations. Above a certain value of amplitude each transient depolarization is accompanied with a premature ventricular excitation (Fig 5). These data show that the magnitude of stretch is the most powerful predictor for stretch-induced arrhythmias whereas the velocity of stretch is recognized as the second most important signal.

Davidson (1993) and Franz et al., (1989) found that Early AfterDepolarization (EAD) was produced as ventricular volume remained high and was clamped at the end of diastole without changing preload. An EAD occurs in the monophasic action potential from the final beat and disappears as ejection is apparent. This phenomenon is transient due to EAD of the initial ejection being minimal. Ventricular volume at the end of systole is recognized as the important factor to regulate MEF. In a hypertrophic ventricle, ventricular distension has always existed in the whole cycle with large end-diastolic volumes and largely decreasing ejection fractions. The production of a large number of EAD may be an optimal environment to trigger the

formation of arrhythmias whereas the normal ventricle is less susceptible since normal end-systolic volume is small relative to that of failing heart.

Stretch-activated depolarization in diastole produces Delayed-AfterDepolarization (DAD). During the plateau phase of action potential, short stretch causes an immediate dip in the repolarization (Calkins et al., 1991). Zabel et al., (1996) noted that stretch applied in the plateau state of action potential had a little or no effect on the repolarization contour. These results are consistent with a computer-based study of specific stretch-activated channel characteristics (Sachs et al., 1994).

Stretch-induced depolarization is similar to EAD and DAD at amplitude and timing of short stretch. Despite showing similar morphology, it is essential to understand that stretch-induced depolarization was not a standard EAD or DAD, which is produced in the aftermath of a preceding monophasic action potential (Cranefield, 1977; January et al., 1992).

1.1.3 CLINICAL CORRELATES TO MEF

1.1.3.1 MEF AND SUDDEN CARDIAC DEATH

Commotion cordis described as a phenomenon of Sudden Cardiac Death (SCD) has been recorded since it was reported over 120 years ago (Meola, 1879; Nelaton, 1876). The importance of such a case focuses on transient and powerful mechanical stimulus acting on the pre-cardiac location causes serious dysrhythmia, even without any damage to the heart and other organs in chest. Subsequently Schlomka and Hinrichs (1932) showed that the arrhythmogenic effect of precordial mechanical stimulation depended on the region of impact to the heart, the size of the contact area,

and the time of the impact. They believed that the mechanical stimulus was the important factor in producing cardiac rhythm perturbation, and that the compliance of the chest would be a key point to this transition. Presently, more and more reports emphasize that MEF is the cause of spontaneously occurring arrhythmias in patients. Many SCD cases show rhythm disturbance and an altered mechanical loading of the heart (Taggart, 1996) (Fig 6 & 7).

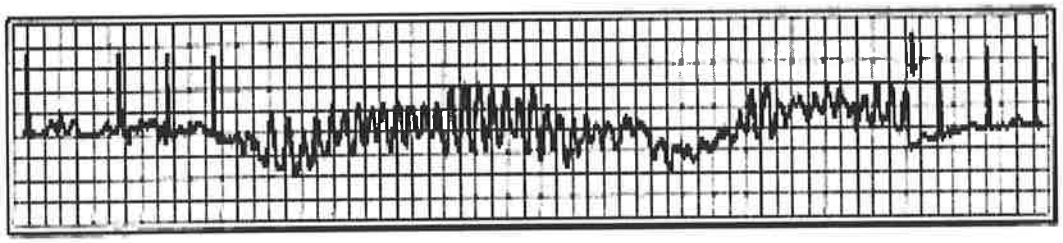

Figure6. ECG illustrates that early ventricular fibrillation is corrected by a single chest thump (Barrett et al., 1971). When expanding of ventricular fibrillation is fallen in refractory period produced by mechanical stimulation, ventricular fibrillation is prevented and normal rhythmus reoccurred.

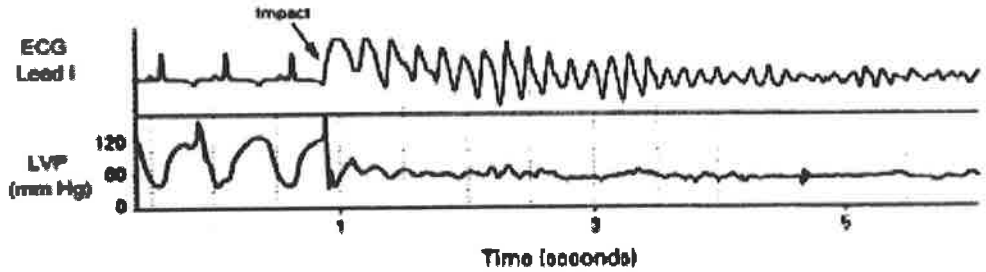

Figure7. ECG and left ventricular pressure recording obtained from an anaesthetised pig show that due to a pre-cordial impact that coincides with the upstroke of the T-wave, mechanical- induced ventricular fibrillation occurred and contractility disappeared (Link et al., 1998).

Pathological effects of MEF are classified as active and passive. In the active mechanism, the amplitude of abnormal MEF is expressed higher than that in normal myocardium. It includes ventricular outflow tract obstruction and arterial hypertension, sudden intraventricular volume shifts, congestive heart failure, and

similar conditions that elevate intraventricular volume or pressure and generate abnormal strain on the ventricular wall. Mechanical stimulation in cardiac hypertrophy generates higher-amplitude MEF between normal and hypertrophic areas, which induces fatal ventricular arrhythmias (Calvert et al., 1977; Califf et al., 1978; Meizlish et al., 1984; White et al., 1987), and incidence of high-amplitude MEF by abnormal wall motion that is one of the most obvious signals to SCD (Weaver et al., 1976). Almost half of congestive heart failure and dilated myocardial patients die suddenly in ventricular tachycardia and fibrillation produced due to similar reasons (Swerdloe et al., 1983; Holmes et al., 1985; Gradman et al., 1989; Kjekshus, 1990).

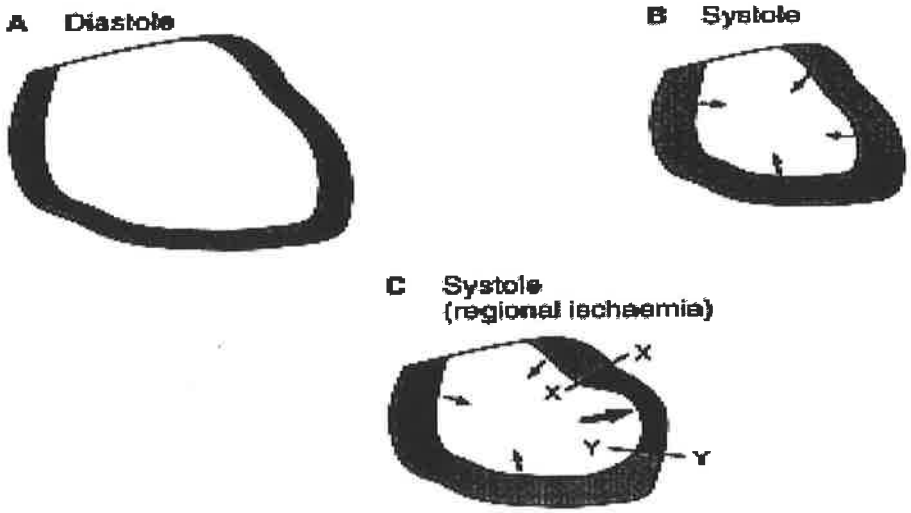

Figure8. illustrates that normal heart is kept in uniformly systolic and diastolic phases (A and B); a region of acute ischemia in left ventricle (C) moves paradoxically during systole, which may cause the production of a number of MEFs (Taggart et al., 1999).

In the passive mechanism, MEF increases the sensitivity of myocardium to arrhythmias. This includes regional myocardial ischemia, post-infarction stunning or border area of a post-infarct scar or ventricular aneurysm. Taggart et al., (1999) (Fig 8) demonstrated that during systole, intraventricular pressure increased contraction of healthy myocardium that forced the blood into the ischemic location, a non-contractile

segment. Due to non-uniform wall contraction, the ischemic region expands and becomes more convex. The part between normal and ischemic region is tethered to surrounding normally contracting myocardium. MEF is frequently produced in such area, which increases the sensitivity of myocardium to MEF-induced arrhythmia. The properties of the non-infarcted myocardium are inhomogeneous post myocardial infarction. Abnormal myocardial cells and dysfunction of regions adjacent to the scar interact with each other in the process of remodeling (Olivetti et al., 1991; Kramer et al., 1993; Lima et al., 1984; Gallagher et al., 1986), which has been shown to be more sensitive to produce arrhythmias than normal tissues (Pye et al., 1992; Hart, 1994). Clearly, MEF plays an important role in the above situations (Lab et al., 1996; Dick et al., 1998; Franz, 1996).

1.1.3.2 MEF AND ARRHYTHMIA

1.1.3.2.1 MECHANISMS OF ARRHYTHMIA

At present, the mechanisms of the production of arrhythmias are classified into automaticity, re-entry and triggered activity (Janse and Wit, 1989). The results based on clinical and pathological cases show that triggered activity and re-entry are widely applied to explain the production of serious ventricular arrhythmias and fibrillation due to altered mechanical loading (Franz, 1996; Lab, 1996).

Triggered activity is defined as a premature action potential occurring during the phase of repolarization or between two normal depolarizations. The morphology is similar to EAD and DAD. Taggart et al., (1999) illustrated that based on the changes in repolarization produced by previous mechanical stimulation the incoming mechanical stimuli with enough amplitude generated the depolarization like EAD (Fig

9A). In a normal action potential, the depolarization equal to threshold was produced in repolarization, which triggered abnormal action potential similar to DAD (Fig 9B). Janse and Wit (1989) found that whenever triggered activity arose from EAD or later from DAD, both had different mechanisms. Both result in tachycardia by individual activation or repetitive premature action potentials.

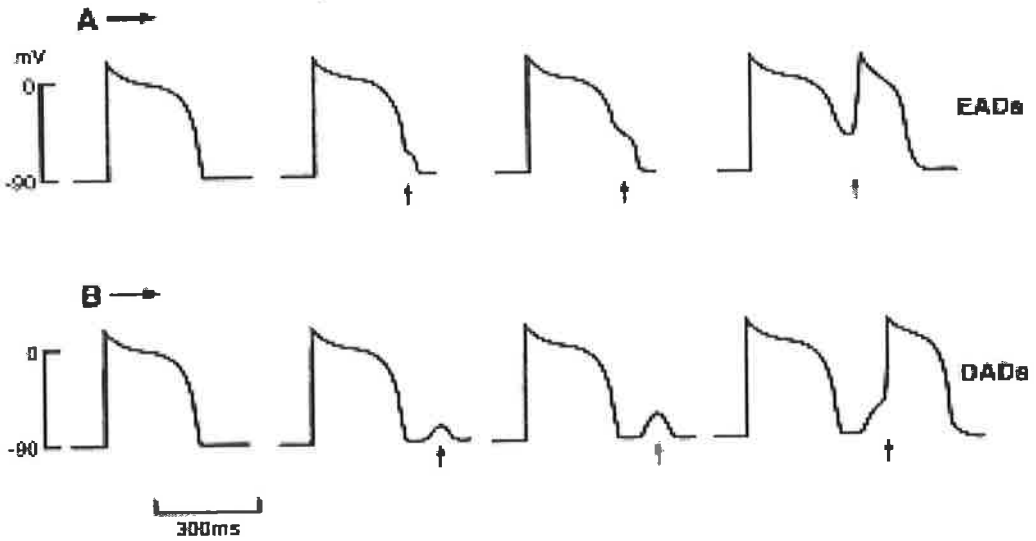

Figure9. shows that the formation of a secondary depolarization (EAD) during the phase 3 of action potential whereas the formation of DAD after the phase 3. Tthe amplitudes of both EAD and DAD reaching threshold activate a premature action potential (Taggart et a.l, 1999).

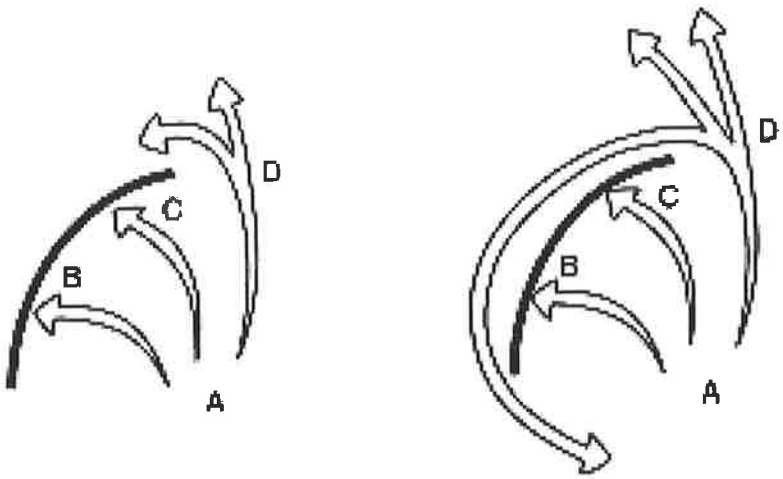

Figure10. Left shows that excitation from point A blocks at points B and C in an area of inexcitability and then passes the blocked area by D. Right shows that excitation through point D re-excites point A (Taggart et al., 1999).

Janse and Wit (1989) found that the mechanism of re-entry was essential in the majority of sustained ventricular tachycardia and fibrillation cases caused by pathological factors. Fig 10 shows excitation traveling through an area of intact heart, but propagation being prevented at point C and B. Excitation passes around the region of block by point D and acts on unexcited tissues, which re-excite proximal myocardial tissue. This produces a reentry circuit. One single circuit produces one ectopic beat. Lots of circuits occurring simultaneously in the ventricle lead to ventricular tachycardia. As a large amount of re-entry circuits are generated in the ventricle, fibrillation is formed. Time and amplitude of excitation through the block region are key factors to the mechanism of re-entry. If enough amplitude of excitation extends slowly through the block region, time difference permits the myocardial cells in proximal and around the block region to regain their excitation. If the action potential becomes shorter, the myocardium is easier to be re-excited. Therefore, delayed conduction and shortening action potential may stimulate the formation of re-entry mechanisms.

1.1.3.2.2 MEF AND THE PRODUCTION OF ARRHYTHMIAS

MEF generates arrhythmias (Franz, 1996; Reiter, 1996). Clinical data have demonstrated a close correlation between different overloads of ventricle and arrhythmias. Patients with chronic heart failure have higher occurrence of non-sustained and sustained tachycardia and are more susceptible to sudden cardiac death than normal people. As above described, it is not likely that chronic overload or chronic ventricular dilation share the same mechanism with acute, transient stretch forces in producing arrhythmias. It is less possible to produce regional MEF during the period of end-systole. Contraction force in congestive heart failure and dilated

myocardial diseases is more reduced compared to the healthy heart. Therefore, MEF-induced arrhythmias are much more likely to occur in the situation of acute, transient volume or length increases than those stable and chronic loading changes.

Although other factors exist in the production of ventricular arrhythmias, MEF is more responsible for mechanical-induced lethal arrhythmia in cardiac hypertrophy and chronic heart failure than in the normal physiological environment. By reducing diastolic and systolic membrane potential, MEF causes a shortened action potential duration, refractory duration, and the velocity of myocardial propagation (Lerman et al., 1985; Franz et al., 1989; Reiter et al., 1988; Franz et al., 1992; Zabel et al., 1996). Ventricular overload affects different regions of ventricle depending on different wall thickness, non-uniform curvature and autonomically intrinsic regulation to myocardial contraction.

It is more and more obvious that MEF is an important mechanism for the understanding of the production of arrhythmias and the treatment of lethal ventricular arrhythmias. Fig 11 shows the discoveries and theories found, which correlate between MEF and arrhythmiogenesis described as a more complicated model at molecular level.

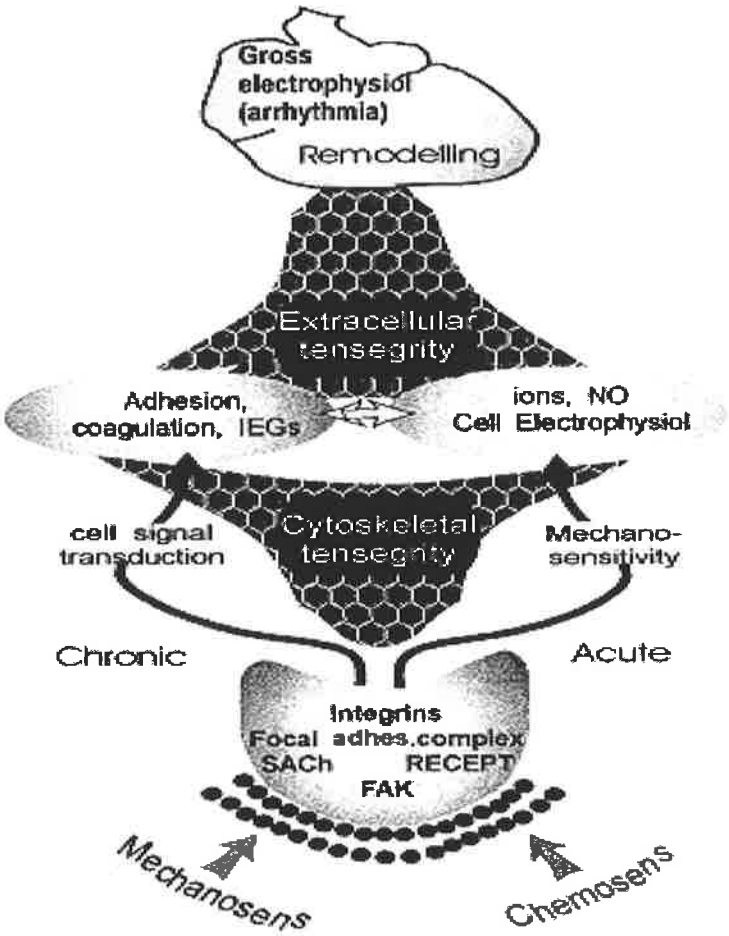

Figure11. illustrates that different mechanochemical stimulations are transferred from cell membrane to intact heart. Stimulation felt by Mechanosensor and chemosensor acted on the local adhesion complexes of the membrane, which includes stretch-activated channels (SAC), chemical receptors, integrins and focal adhesion kinase (FAK). SACs have effects on cell electrophysiology by changing ion concentration. Stimulation produces electrophysiological and biochemical alterations by cytoskeleton system and signal transduction system, which affect cardiovascular function at molecular level. Mechanochemical stimulation activates immediate early genes (IEGs) and relative protein kinase cascade, which function on the distant cardiac tissue and the whole heart and remodel myocardium in cardiac hypertrophy and chronic heart failure (Lab et al., 1999)

1.2 THE STRETCH-ACTIVATED CHANNELS (SAC) IN THE HEART

1.2.1 SAC

Mechanical stimulation, such as stretch, acting on the mechanosensors on the cardiomyocyte membrane changes ion concentration inside and outside

cardiomyocyte. Alteration of ion concentration results in depolarization of cell membrane and produces MEF. This theory has been reviewed widely (Riemer et al., 1998; Kohl et al., 1999). Stretch-activated channels are the most important group of mechanosensors due to the activation of SAC directly leading to the production of MEF in myocardium. Recording by patch clamp, Hamill et al., (1981) showed one group of SAC and Sachs (1988) confirmed that this kind of SAC was different from voltage-induced and ligand-induced channels. Computer models have been used to describe the function of stretch-activated channels in the stretch-induced arrhythmias (Zabel et al., 1996; Riemer et al., 1998; Kohl et al., 1999). This model is based on the data from embryonic chicken heart myocardial cells, in which mechanical stimulation induces single current by SAC and increase cytosolic Ca^{2+} concentration (Sigurdson et al., 1992; Hu et al., 1994; 1997). Hansen et al, (1992) and Suleymanian et al., (1995) demonstrated that stretch-activated channel was an important factor in stretch-induced arrhythmias and volume regulation of cardiomyocytes.

Lots of experimental and clinical evidence have shown that SAC plays the key role in the production of arrhythmia under the situations such as ischemic cardiac diseases, dilated myocardial pathology and chronic heart failure especially in myocardial infarction and myocardial hypertrophy.

Since SAC was first discovered in chicken skeletal muscles by Guharay and Sachs (1984), SAC have now been described in more than 30 types of cells. Stretch-activated currents have been shown in different animals in the studies of a single channel in an intact heart. With the development of biophysics techniques, standard patch-clamp technique has been used to exhibit electrophysiological features of the

single channel (Hamill et al., 1981). Briefly, pressure acting on the cell membrane increased the membrane surface tension and then activated stretch-activated channels. The larger the pressure was on the cell membrane, the greater the probability of being open. Sachs (1991) reported that his group applied suction to a single channel of SAC and successfully recorded physiological behavior of such channel.

Table1. Stretch-activated channels in the different animals (Hu and Sachs, 1997)

Cell type	G (pS)	V_r (mV)	Selectivity	Gd^{3+} block	Reference
Chicken Ventricle (cultured)	25	-50	CAT	Y	Ruknudin et al., (1993)
	25R	10	CAT	Y	Ruknudin et al., (1994)
	50	-35	CAT	Y	Ruknudin et al., (1995)
	100	-70	K^+	Y	Ruknudin et al., (1996)
	200	-40	K^+	Y	Ruknudin et al., (1997)
Chicken Ventricle (freshly-isolated)	21	-2	CAT	Y	Hu and Sachs (1996)
	90	-70	K^+	Y	Hu and Sachs (1996)
Rat Atrium	52	N/A	K_{ATP}	N	Van Wagoner (1993)
Rat Atrium	64-94	N/A	K^+	N	Kim (1992)
Rat Atrium	21	N/A	CAT	N	Kim (1993)
Rat Atrium	36	N/A	CAT	N/A	Fu and Kim (1993)
Rat Ventricle (cultured)	46	N/A	CAT	Y	Sadoshima et al., (1992b)
Rat Ventricle (freshly isolated)	120	$V_{resting}$+31	CAT	N/A	Craelius et al., (988)
Guinea pig	N/A	N/A	CAT	Y	Bustamante et al., (1991)
Porcine Right Atrium	32 (mono-)	N/A	CAT	N/A	Hoyer et al., (1994)
	13 (divalent)	N/A	N/A	N/A	Hoyer et al., (1994)
Molluscan Ventricle	33	−70	K^+	N/A	Sigurdson et al., (1987)

(N/A: Not Applicable; CAT: Cation; Y: Yes; N: No;)

1.2.1.1 SINGLE CHANNEL

SAC are a group of ion channels that are activated directly by mechanical stimulation. Fig 12 shows the evidence that a single channel of SAC is activated in chicken

embryonic ventricular cell. As the suction acts on the recording pipette, SACs are opened whereas with low pressure, the channels close. The duration of action lasts for a few seconds to a couple of minutes (Sigurson et al., 1987; Van Wagoner, 1993; Hu and Sachs, 1997).

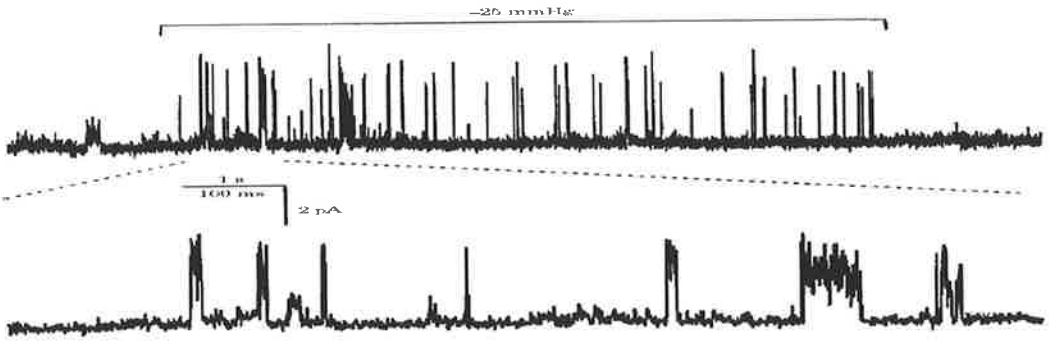

Figure 12. illustrates that a 21pS stretch-activated ion channel is recorded by single-channel technique from a fresh-isolated 17-day-old embryonic chick ventricular cell under a pipette suction of 25mmHg. The channel is activated during the application of suction in the recording pipette, and inactivated after removing the suction. Time scale magnification of a segment of the recording shown in the upper panel, as indicated. Time scale bar: 1s fro the upper panel and 100ms for the lower panel. Recording conditions: pipette and bath solutions in mM, 150 NaCl, 5 KCl, 2 $CaCl_2$, 1 $MgCl_2$, 10HEPES, pH 7.4 titrated with NaOH. Pipette holding potential, +60mV (Hu et al., 1994).

SACs exist extensively in chicken ventricular and atrial cells. The majority of SAC are weakly permeable to monovalent cations and strongly permeable to divalent cations. Additional SACs are K^+-selective. SACs can be activated by hypotonic swelling and trans-patch hydrostatic gradients (Kim, 1992; 1993). The details show that different kinds of SACs co-exist in the same ventricular cells. Kim (1993) demonstrated that at least two kinds of non-selective cationic SAC were expressed in neonatal rat atrial cells, one of which was sensitive to stretch and the other was more responsive to swelling.

1.2.1.2 WHOLE CELL STUDIES

Compared with hypotonic inflation and positive pressure, pipette method of direct stretch is more suitable to single channel application. Using guinea-pig

ventricular cells, Sasaki et al., (1992) made recordings of mechanosensitive current from the whole cell with a reversal potential of -15 mV under normal physiological conditions. Hu and Sachs (1997) showed that according to the increased extent of the stimulation, the amplitude of mechamosensitive current was increased in a dose-dependent manner. Under normal physiological situations, the linear current-voltage relation has a reversal potential of -17 mV. These discoveries may suggest that two kinds of SAC, which are K^+-selective and cation-selective channels, control the whole-cell current. In 20% of ventricular cells the current shows a time-dependent inactivation. Stretch does not affect Na^+ current significantly in chicken ventricular cells. Sasaki et al., (1992) demonstrated that mechanical stimuli did not affect voltage-dependent Ca^{2+} current or inward rectifier K^+ current.

Hypotonic stimulation has also been used as an experimental method. Under hypotonic conditions, ventricular cells increase their permeability to Cl^- or K^+ (Sasaki et al., 1992; Sorota, 1992; Tseng, 1992; Van Wagoner, 1993; Zhang et al., 1993a). Hypotonic swelling increases delayed-rectifier potassium current whereas a time-independent non-selective cation current is activated by direct mechanical stimulation (Sasaki et al., 1992). As the hypotonic condition induces an anionic current, direct mechanical stretch causes a cation-selective current (Hu and Sachs, 1997). But some of these currents are coupled with Ca^{2+}, ATP and cAMP (Zhang et al., 1993b; Oike et al., 1994; Hall et al., 1995), which may suggest that induced currents be relative to the second messenger system.

1.2.2. THE PHARMACOLOGY OF SAC

Paintal et al., (1964) showed that drugs activating or inactivating the specific mechanosensory receptors did not affect mechanotransduction but rather function on action potential, muscular and vascular tone. Mechanotransduction shows a low susceptibility to chemical stimulation and the capacity of regulating cell volume (Hamill, 1983a; Christensen, 1987; Sackin, 1989; Medina and Bregestovski, 1988; Wilkinson et al., 1996a; 1996b). Actually, SACs exhibit the diverse properties depending on different types of cells, which include the alterations in mechanosenstitives, gating dynamics and channel opening (Howard et al., 1988; Sachs, 1988; Morris, 1990; French, 1992; Petrov and Usherwood, 1994; Sackin, 1995; Hamill and McBride, 1995).

1.2.2.1 OPEN CHANNEL PROPERTIES

Although SACs present a variety of open channel characteristics with different ion selectivity and single channel conductance from 20 to 2000pS, other channels with similar ion selectivity and conductance are not mechanosensitive (Opsahl and Webb, 1994). Some cells show the existence of only one type of SACs whereas some cells display five types or more, whose functions are classified depending on their open channel features (Berrier et al., 1992; Ruknudin et al., 1993). And the drugs that especially bind to these types of channels either open or block the channels depending on the type of pore the channels contain. Such changes reflect the variations of the structure and function of the pore on the different kinds of SAC.

1.2.2.2 GATING CHARACTERISTICSS

SACs demonstrate quick and complete adaptation to continuous stimulation. SAC activities are refractory from one adaptation to another in the duration of patch clamp

recording (Hamill and McBride, 1992). Certain types of SACs are activated by random thermal changes (Denk and Webb, 1989) whereas other types need mechanical changes such as membrane-damaged and cell-ruptured stimuli (Vandorpe et al., 1994; Morris and Horn, 1991). Hamill and McBride (1994a) concluded that most of SACs were activated under modest stimulation.

Generally, different categories of stimulations have diverse effects on SACs within cells. At the molecular level, one kind of SACs is only sensitive to a certain category of stimulation such as direct stretch, hypotonic swelling, shear stress or pressure (Olesen et al., 1988; Sasaki et al., 1992). Some SACs are responsive to multiple-selective mechanical stimulations (Christensen, 1987; Ubl et al., 1988; Sackin, 1989; Oliet and Bourque, 1993). These observations may suggest that integrity of mechanical transduction system existing among extracellular, membrane, and intracellular environment is important to the sensitivity of SAC to mechanochemical stimulation.

Some SACs are also activated by non-mechanical stimulation rather than membrane stretch, such as ligands (Kirber et al., 1992; Vandorpe and Morris, 1992; Van wagoner, 1993; Paolettis and Ascher, 1994; Vandorpe et al., 1994) and membrane voltage (Hisads et al., 1991; Kirber et al., 1992; Chang and Loretz, 1992; Davidson, 1993; Langton, 1993; Ben-Tabou et al., 1994; Hamill and McBride, 1995b).

1.2.2.3 THE ACTIVATORS OF SAC

Activators of SACs include lipid metabolites, free fatty acids, lipids and amphipathic molecules. These compounds directly affect channel activity by

interacting with the channel protein or the lipid environment rather than by interacting directly with active components of various enzymatic pathways that functioned on the channels (Meves, 1994). Three possible mechanisms of activation include adding into the bilayer to change the surface tension of the membrane (Martinac et al., 1990; Martin and Martinac, 1991); altering cellular capacity of maintaining a normal morphology (Lundbaek and Andersen, 1994); interacting with allosteric sites on the channel protein (Petrou et al., 1994; Kirber et al, 1992; Kim et al., 1995).

1.2.2.3.1 FATTY ACIDS AND LIPIDS

Fatty acids are lipid molecules which have a polar head with hydrophobic tail. Some reviews demonstrate that fatty acids activate different types of SAC without the involvement of the fatty acid metabolism cycle (Kirber et al., 1992; Kim, 1992; Petrou et al., 1994; Kim et al., 1995). Kirber et al., (1992) showed that arachadonic acid modulated the activity of Ca^{2+}-dependent K^+ channels in rabbit arterial smooth muscle to produce a large current. Petrou et al., (1994) showed another case of K^+-selective SACs that was activated by fatty acid in gastric smooth muscle of rabbit. This K^+-selective SACs have been suggested as an example of indirect mechanism due to occurrence of stretch activation being in seconds rather than milliseconds (Ordway et al., 1991). Such activations are also blocked by Al^{3+}, which is well known to remove fatty acids from the membrane (Ordway et al., 1995). These results may suggest that stretch induces the production of fatty acid that causes the alteration of SACs. The process is similar to the activation of stretch-sensitive phosphatase on the membrane (Jukka et al., 1995).

However, some K^+-selective SACs in encephalic and hypothalamic regions of rat brain and cardiac muscle show the opposite results, in which Al^{3+} does not prevent stretch sensitivity (Kim, 1992; 1995). This indicates that there is a different mechanism between stretch-induced SACs and fatty acid-dependent SACs. These details may suggest that either fatty acid has the specific binding sites for different types of cells or fatty acid does not participate in the activation of SACs.

Fatty acid-sensitive SACs show three characteristics including time of activation is short (only in a few seconds); mediated role rather than direct activation (Martinac, 1990); the activity of SAC depending more on the polarization of fatty acid (Martinac, 1990). It is not clear whether stretch and fatty acid interact with each other or they function separately. Brophy et al., (1993) and Jukka et al., (1995) did not find that stretch sensitivity resided in a SAC or a stretch-sensitive phospholipase produced fatty acid, but Sukharev et al., (1994) made it clear that in *E coli*, mechanical sensitivity was based on interaction between channel protein and its surrounding bilayer environment.

1.2.2.4 BLOCKERS OF SAC

1.2.2.4.1 GADOLINIUM (Gd^{3+})

Gd^{3+} is the most commonly applied blocker of SAC and often used to check the putative role of SAC in the process of mechanosensitivity. The mechanism of Gd^{3+} blocking SAC has been reviewed by Millet and Pickard (1988), in which Gd^{3+} (10-250 μ M) blocked both thigmotropism and geotropism in plants. Edwards and Pickard (1987) hypothesized that the blocking mechanism was based on the inactivation of the permeability of Ca^{2+} of SAC. Patch clamp confirmed that Gd^{3+} blocked SACs in plant

cells (Alexandre and Lassalles, 1991; Ding and Pickard, 1993a; Garrill et al., 1993), in fungi (Zhou et al., 1991), in bacteria (Berrier et al., 1992; Martinac, 1992; Cui et al., 1995; Hase et al., 1995), and in animal cells.

Table2. Inactivation of SAC by Gd^{3+} in different types of cells

Cell	Ion	G_{pS}	$[C]_{\mu M}$	Reference
E. coli	NS	300-2000	100	Berrier et al., (1992)
E. coli	NS	350-1100	100	Cui et al., (1995)
Sacchromyces (yeast)	NS	40	10	Gustin et al., (1988)
Schizosacchar (yeast)	+	180	1000	Zhou et al., (1995)
Uromyces (fungi)	+	600	50	Zhou et al., (1991)
Hyphae (fungi)	+	-	100	Garrill et al., (1993)
Necturus kidney	+	18	20	Filipovic and Sackin, (1991)
Xenopus oocyte	+	50	10	Yang and Sachs, (1989)
Xenopus kidney	+	70	10	Kawahara and Matsuzaki, (1993)
Bone cell line	+	40	20	Duncan et al., (1992)
Guinea pig bladder	+	80	20	Wellner and Isenberg, (1994)
Mouse skeletal muscle	+	20-50	>10	Franco and Lansman, (1990)
Rat hepatoma cells	+	40	50	Bear and Li, (1990)
Rat supraoptic neurons	+	30	100	Oliet and Bourque, (1994)
Rat cardiocytes	+	42	1	Sandoshima et al., (1992a)
Chick cardiocytes	+	20/50	20	Ruknudin et la., (1993)
Chick cardiocytes	K^+	100/200	20	Ruknudin et la., (1993)
Human demyelinated axon	K^+	52	1000	Quasthoff, (1994)
E.coli	-	100-250	-	Berrier et al., (1992)
Rat astrocyte	K^+	70	-	Yang and Sachs, (1989)
Mouse Ehrlich ascites	+	15-40	-	Christensen and Hoffmann, (1992)
Rat artial cells	+	20	-	Kim, (1993)
Rat atrial cells	K^+	50-100	-	Kim et al., (1995)
Snail neur (*Lymnaea*)	K^+	44	-	Small and Morris, (1995)

NS: NO SELECTIVE; +: POSITIVE ION; -: NEGATIVE ION; I_{pS}: CHANNEL CONDUCTANCE; $[C]_{\mu M}$: THE CONCENTRATION OF BLOCKERS.

Yang and Sachs (1989) concluded that Gd^{3+} (10 μ M) in the outside solution inactivated completely or reversibly the activity of cation SAC on the surface of *Xenopus* oocytes whereas higher concentration (10x) of La^{3+} or Lu^{3+} displayed the same results to block SAC. Cui et al., (1995) demonstrated that in *E. coli,* Gd^{3+} (20 μ M) increased the activity of SACs (350-1100pS); however, with the increase of $[Gd^{3+}]$, Gd^{3+} blocked the activity of SACs. Berrier et al., (1992) showed that Gd^{3+} (100 μ M) inhibited the activity of SACs (300-2000pS) whereas did not affect the activity of SACs (100-220pS). There are some exceptions in the studies, which include the relatively high concentration ($\leq$ 1mM) inactivated a K^+-selective SAC in human myelinated nerve (Quastoff, 1994) and in lymphocytes (Schlicter and Sakellaropoulos, 1994) but blocked cation SAC in atrial cardiomyocyte (Kim, 1993). Boland et al., (1991) demonstrated that the presence of anion such as CO_3^{2-}, PO_4^{3-} and EGTA interacting with Gd^{3+} altered the effective concentration of blocking SAC.

The mechanism of Gd^{3+} behavior on SACs is not well understood. An explanation is that Gd^{3+} function is complex due to multiple-site binding at different concentrations. Lehrmann and Seeling (1994) reviwed that La^{3+} showed specific interactions with membrane channel proteins similar to Gd^{3+} interplaying with bilayer. Yu et al., (1996) confirmed that increasing phase transition temperature or decreasing the membrane fluidity and dipole potentials by different $[Gd^{3+}]$ altered the extrinsic environment of membrane channel proteins, which affected the acitivity of SACs. Yang and Sachs (1989) used three likely mechanisms to explain the roles of Gd^{3+} under the concentration in a range of 5-10 μ M . (1) At the concentration of 5 to 10μM, Gd^{3+} reduces the amplitude of single channel current. Gd^{3+} possibly connects with the

negative surface charges in or near the vestibule of the channel. (2) At the same concentration, the voltage-independent reduction in open channel duration is caused by Gd^{3+} interacting with an external allosteric site, which produces a transition to a shortened close state. (3) At 10 μ M, channel activity is inactivated completely since high concentration Gd^{3+} keeps the channels in a long-lived close state.

1.2.2.4.2 GsMtx-4

GsMtx-4 is a peptide found in two kinds of spider venoms. It has 34 amino acids with 3 disulfids and the sequence has been cloned and expressed in *E. coli* (Sachs, 2002). It is firstly described by Suchyna (2000) to block cationic SACs in several types of cells. GsMtx-4 shows high specificity to cationic SACs located in astrocytes and the heart whereas it does not affect cationic SAC or K^+-selective TREK and TRAAK families in cochlear hair cells (Marcotti et al., 2001). GsMtx-4 inactivates SAC with K_d (500nM) and reduces hypotonic-induced Cl^- current, which is likely to participate in the regulation of SACs to cellular volume (Sachs, 2002). GsMtx-4 has not shown any cross reactivity or any effect on the action potential of voltage-dependent channels in acute-treated heart cells (Suchyna et al., 2000), however in hypertrophic ventricular cells, it reduces the cellular volume and related cationic currents. GsMtx-4 blocks atrial fibrillation caused by dilation, in which GsMtx-4 does not show any function on hemodynamics and monophasic action potential (Bode et al., 2001).

1.3 SAC CORRELATES TO DISEASE

It is essential to understand the function of SACs in different physiological environment. The following cases are used to discuss the importance of SACs in

pathophysiological situations. In the cases of myocardial hypertrophy, dilated cardiomyophathies and myocardial infarction, SACs are more sensitive to stretch, which produces a large amount of SAC-induced MEF. The Activation of a number of SACs results in opening of multiple signaling pathways that are involved in genetic modification in cardiac hypertrophy and heart remodeling. Both may participate in the generation of ventricular arrhythmias.

1.3.1 SAC AND ARRHYTHMIA

It is clear that MEF induces arrhythmia in heart under physiological or pathological conditions. Mechanism of MEF to produce arrhythmia is similar to generate EAD or DAD-like premature action potential in the duration of systole and diastole. The production of premature action potential is based on the changes of ionic concentrations and currents. According to correlative data mentioned, SACs may be a regulative trigger to control such changes. Presently, more and more results have confirmed that SACs play a key role in the transduction of MEF to arrhythmia in spite of the less understanding of the function of SACs in myocardium. One possibility is to modify cell growth and ventricular remodeling according to altering preload and afterload (Bustamante et al., 1991; Sadoshima et al., 1992b; Sadoshima et al., 1993). Some reports show that SACs affect intrinsic regulation of contractility, which is involved in alteration of autonomy of Purkinje fiber and sinus node (Kaufmann et al., 1970; Sigurdson et al., 1992). By changing [Ca^{2+}], it is likely to generate the changes of action potential. It includes an increase in cytosolic free ionic calcium that is possibly released from intracellular Ca^{2+} store (Lakatta et al., 1992); improving cytosolic calcium ion concentration that inhibits transmembrane Ca^{2+} influx (Le et al., 1991); the activation of K^+ outward current (Di et al., 1994). All these factors shorten

the duration of repolarization and action potential. Lab et al., (1984) recorded a load-induced shortening of action potential with a transient increase of cytosolic Ca^{2+} in an isolated ferret myocardium.

1.3.2 SAC IN CARDIAC HYPERTROPY AND CHRONIC HEART FAILURE

The experiment by Kamkin et al., (2000) showed that SACs in ventricular myocardium amplified arrhythmogenic effects in hypertrophic phase. In this study, stretch-induced current is insensitive to substitution of Cl^- by negative aspartate ions. However, cationic SAC-dependent current is inactivated by Gd^{3+} (100 μ M within 1 min or 5 μ M within 7-10 min). Under the application of stretch, the late currents measured with or without Gd^{3+} cross at a reverse potential of -1+/- 4 mV in ventricular hypertrophy. Stretch-activated currents are produced by non-selective cationic channels. Stretch-induced currents follow linear voltage dependence and reversed (-5+/- 3mV). The current is closer to 0mV in myocardium of healthy guinea-pig than in hypertrophic human heart due to the small size of healthy guinea pig heart. Other reports demonstrate that Ca^{2+} permeates through SACs and the permeability is smaller than Na^+, which suggests that Ca^{2+} interacts with SAC-protein during permeation. The details also show that Na^+-selective SACs result in retarded repolarization and diastolic depolarization. The sensitivity of myocardium to stretch is increased with the development of hypertrophy, which is established in the case of young healthy rats undergoing left ventricular hypertrophy (Bing et al., 1995).

Clive and Henry (2002) concluded that cationic SACs were blocked by Gd^{3+} and GsMTx-4, which were expressed in ventricular myocardium of osmotic shrinkage heart failure. In the animal models of chronic heart failure (mainly in canine and

rabbit), cationic SACs are responsible to produce ventricular arrhythmias by random depolarizations in ventricular myocardium. However, due to pre-treating with Gd^{3+} or GsMTx-4, this phenomenon disappears.

1.3.3 SAC IN MYOCARDIAL INFARCTION

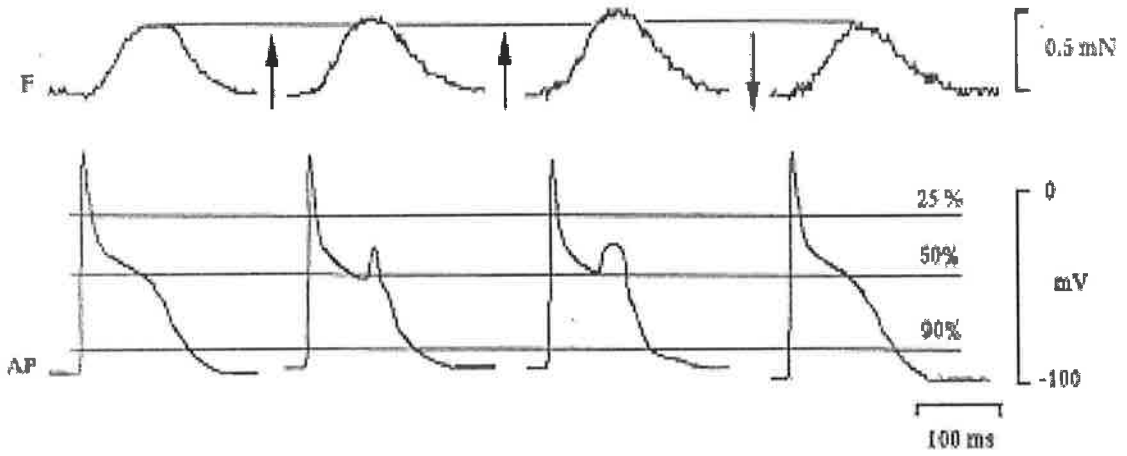

Figure13. shows that membrane potential responding to artificial long-lasting stretch in left ventricle with myocardial infarction. With increasing stretch, stretch-activated depolarization occurs near to APD50 whereas withdrawing stretch results in disappearance of the stretch-induced effect (n=7) (Irina et al., 2000).

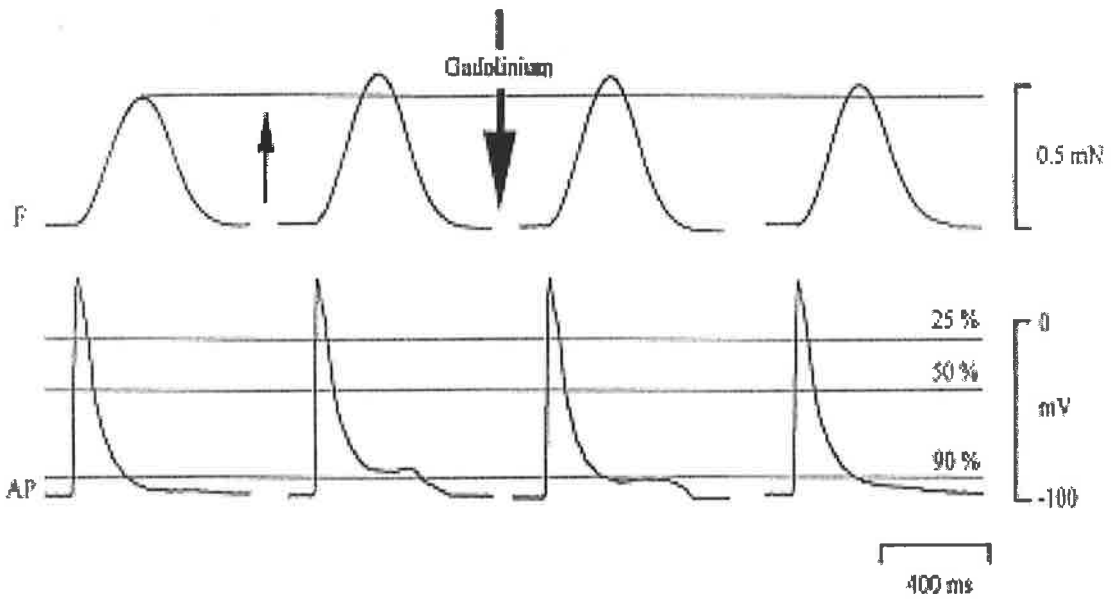

Figure 14. shows that stretch-activated depolarisations near to APD90 in left ventricle with myocardial infarction are suppressed by applying 40μM Gd^{3+} (n=9). The effect of Gd^{3+} is produced within 5 and 10 min after application (Irina et al., 2000).

Irina et al., (2000) imitated left ventricular infarction in rats. The results demonstrate that long-lasting stretch to the ventricle causes an increased in active force. Action potential remains constant without stretch at -25mV, however, at -50mV stretch-induced depolarization occurs obviously (Fig 13). SAC-dependent stretch-activated depolarization is similar to EAD. The results show that Gd^{3+} has a significant effect on active force development and stretch-induced depolarization in myocardial infarction (Fig 14). Stretch-induced depolarization at -90mV is inactivated within 10min after the application of 40 μ M Gd^{3+}. However Gd^{3+} does not affect resting membrane potential, amplitude of action potential and frequency of contraction. These results strongly suggest that stretch-induced depolarization only change the duration of depolarization and repolarization, which causes ventricular arrhythmias.

1.4 2-PORE-4 TRANSMEMBRANE DOMAIN (TMD) K^+ CHANNELS

2-P-4MD K^+ channel is a distinct group of SAC. It was only one group of SAC, which has been cloned and sequenced. This provides us a great opportunity to identify the presence of SAC by molecular biology techniques. Fig 15 shows that these channels existed extensively in human tissues. Basic knowledge of K^+ channels is essential to understand 2-P-4MD K^+ channels completely.

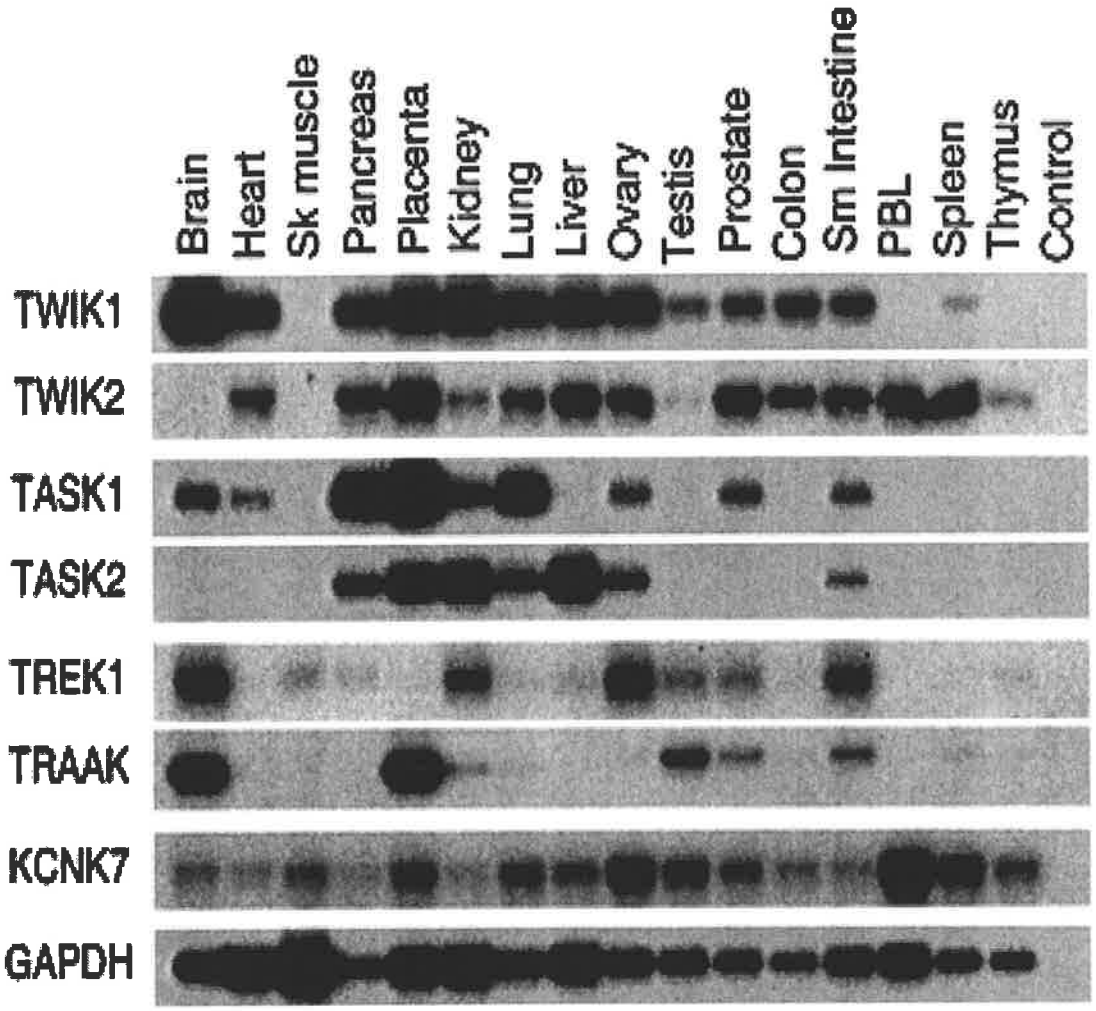

Figure 15. Distribution of K_{2P} channels in adult human tissue. DNA fragments are PCR amplified by using specific primers and analyzed by Southern blot by using internal ^{32}P-labeled oligonucleotides. PBL: peripheral blood leukocytes; GAPDH: glyceraldehydes-3-phosphate-dehydrogenase (Lesage and Lazdunski, 2000).

1.4.1 BACKGROUND MATERIALS OF K^+ CHANNELS

K^+ channels have been broadly found in cellular membranes of plants and animals. They are used to maintain primary cellular functions, which include cell growth, cellular volume and cellular excitability. There are three groups of K^+ channels, which are voltage-dependent, inward rectifier and two-pore domain channels (Fig 16). Voltage-dependent channels allow efflux of K^+ during depolarization and influx of K^+ during repolarization of action potential. They are

inactivated by Mg^{2+} or polyamine molecules. Inward rectifier channels allow influx of K^+ at negative potentials as a result of inward rectification. 2-pore K^+ channels are more sensitive to alteration of pH value, fatty acid, stretch, and anesthetic reagents than voltage. The existence of 2-pore channels sensitive to stretch in human heart provides more details for the understanding of arrhythmogenesis caused by SACs.

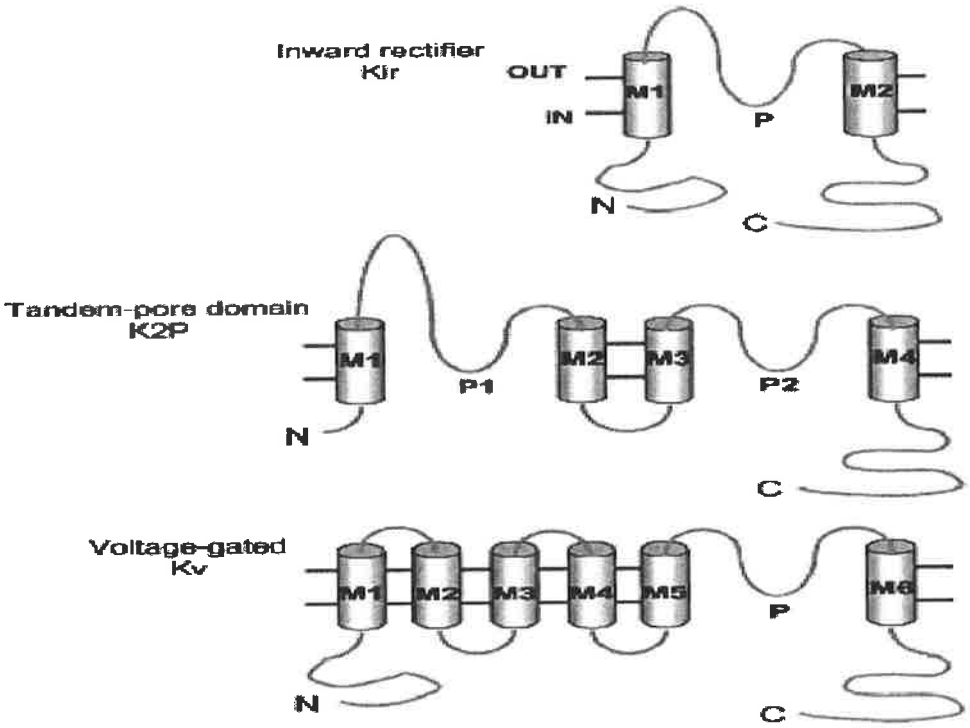

Figure16. shows molecular structures of K^+ channel families. Transmembrane domain and pore structure are recognized from the N-terminus. 2-pore channels are composed of an extended extracellular loop with the first TM domain (O'Connell et al., 2002).

In conductance and molecular structure, there are obvious differences in K^+ channels families (Fig 16). Six transmembrane domains existed in voltage-dependent group whereas two domains in inward rectifier group and four domains in 2-P group. All their subunits have intracellular N- and C-terminate, however, there is little homology to the terminates and pore structures. Due to specific pore organization, K^+ channels exhibit remarkable ability to facilitate transmembrane conductance of more

than one million ions per second. 2-P K^+ channels have two pore regions per subunit whereas the others have one. T-X-G-X-G, conserved amino acid sequence is expressed in each pore structure of 2-P K^+ channels. Experimental data demonstrate that all functional K^+ channels are multimeric complex that is homomeric or heteromeric (Hille, 2001). Functional voltage-dependent group and rectifier group contain four subunits whereas 2-P group holds two subunits (Lesage and Lazdunski, 2000; Biggin et al., 2000; Goldstein et al., 2001).

1.4.2 THE CHARACTERISTICS OF 2-P-4 DOMAIN K^+ CHANNELS

2-P group contains four transmembrane domains and two-pore structure (Fig 17). At present, eight types of 2-P K^+ channels have been cloned in rodent and human. Lesage and Lazdunski, (2000) classified 2-P K^+ channels into four different categories, which included TWIK-1 and TWIK-2 that were weak inward rectifiers and were named from Tandem of P domains in Weak Inward rectifier K^+ channels; TASK for TWIK-related Acid-Sensitive K^+ channel, which were sensitive to pH values; TREK-1 for TWIK-RElated K^+ channel and TRAAK for TWIK-Related Arachidonic Acid-sensitive K^+ channel, both of which were activated by polyunsaturated fatty acids and stretch; KCNK6 and KCNK7 were silent subunits likely to be activated with a partner. In mammalian cells, membrane conductance of 2-P channels is equal in both directions with the absence of concentration gradient.

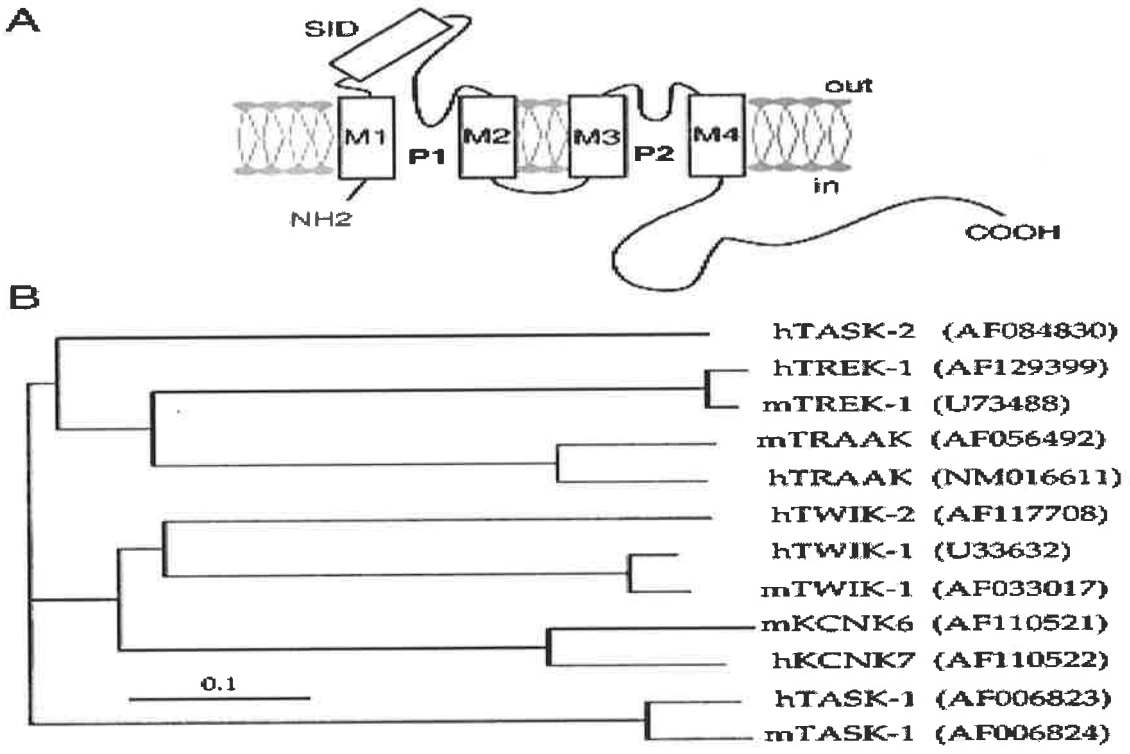

Figure17. shows membrane morphology and diversity of 2P-K^+ channel subunit. M_1-M_4 are four transmembrane domains and P_1 and P_2 were 2P domains. The potential amphipathic a-helix involved in the formation of homodimers is in the self-interacting domain (SID). K_{2P} channels are cloned in mice and humans, which have been coded in Genebank (Lesage and Lazdunski, 2000).

Notable structural features of 2-P domain K^+ channels are four potential transmembrane domains, two pore regions, short NH_2-terminal and long COOH-terminal cytoplasmic parts with an extended extracellular loop between M1 and P1. These subunits are composed of 307-499 amino acids. Except for pore area, the subunits have no significant homological sequence with those of 1-P-6TMD and 1-P-2TMD K^+ channels. To 2-P K^+ channels, homology of the subunits is lower (not more than 45% in human). However, homology between TWIK-1 and TWIK-2 is 58% whereas 54% between TREK-1 and TRAAK (Lesage and Lazdunski, 2000). In nematode, more than 50% genes encode 2-P K^+ channels, in which 70 to 80 genes construct the formation of pore subunits in the animal models. Amino acid sequence

comparison between animal and human demonstrates that homology is as low as no more than 35% similarity in the subunits of 2-P K^+ channels (Wang et al., 1999).

Experimental results indicate that the structure of 2-P K^+ channels is the formation of a dimer (Chavez et al., 1999; Lesage et al., 1996a; Lesage et al., 1997; Lesage et al., 1996b), in which TWIK-1 forms disulfide-bridge homodimers with 4-P regions that is also important to K^+-selective pore of 1-P-6TMD and 1-P-2TMD K^+ channels. TWIK-1 channels have a cysteine residue in the extracellular loop between M1 and P1 at the position of 69 where there are two cysteine residues forming a di-sulfide bridge in each α−subunit to balance the channel. When a cysteine is substituted by a Serine, the currents disappeared. The study of immunolabeling M1 and P1 on the surface of non-permeable cells confirms that N-linked glycosylation of asparagines 95 of TWIK-1 presents in the extracellular location between M1 and P1 region. The same biochemical methods have been applied in other 2-P K^+ channels. The details of the secondary structures show that all cloned subunits except TASK-1 have a cysteine residue equivalent to cysteine 69 of TWIK-1 and form covalent homodimers expressed in heterologous tissues. TREK-1 and TRAAK are also expressed in synaptic membranes by the formation of covalent dimerization. Due to lower conservation in M1 and P1 region of 2-P K^+ channels, the secondary structure of 2-P K^+ channels is proposed to be an amphipathic α−helix. It may suggest that M1 and P1 region play the same function in the 2-P K^+ channels, however the sequence of the extracellular part between M1 and P1 in the different types of 2-P K^+ channels are always diverse. The relative data about 2P-4D-K^+ channels are shown in Table 3 & 4.

Table 3. 2P-4D-K^+ channels located in animal and human.

Name	Synonym	Cloned	Localization	Reference
TWIK-1	KCNK-1	Human	Heart, brain, placenta, lung, liver, kidney, pancreas	Lesage et al., (1996c)
TWIK-2	KCNK-6	Human	Placenta, pancreas, heart, colon, spleen, peripheral blood leukocytes, lung, liver, kidney, thymus, brain.	Salinas et al., (1999)
TREK-1	KCNK-2	Human, Rat, mouse	Brain, lung, kidney, heart, skeletal muscle.	Fink et al., (1996); Bockenhauer et al., (2001)
TREK-2	KCNK-10	Human, Rat	Brain, pancreas, cerebellum, spleen, testis.	Bang et al., (2000)
TRAAK	KCNK-4	Human, mouse	Brain, skeletal muscle, liver, lung, kidney, testis.	Fink et al., (1998)

Table 4. The activity of 2P-4D-K^+ channels to different activators and blockers

Name	Q	TEA^+	4-AP	Cs^+	Ba^{2+}	S	AA	Ph 6_i	Ph 6_e	Reference
TWIK-1	-	-	0	0	-	0	0	-	0	Lesage et al., (1996)
TWIK-2	0	X	X	X	-	X	X	-	0	Chavez et al., (1999)
TASK-1	0	0	0	-	0	0	0	0	-	Duprat et al., (1997)
TASK-2	-	0	0	0	-	X	0	0	-	Reyes et al., (1998)
TASK-3	-	0	X	0	0	X	0	0	-	Rajan et al., (2000)
TASK-4	0	0	0	0	-	X	0	0	-	Decher et al., (2001)
TREK-1	0	0	X	0	-	+	+	+	X	Maingret et al., (2000)
TREK-2	X	0	X	X	-	+	+	+	X	Bang et al., (2000)
TRAAK	X	0	0	0	0	+	+	0	0	Fink et al., (1998)

Q: $[Quinine]_{100\mu M}$; $[TEA^+]$: 1mM; [4-AP]: 1mM; $[Cs^+]$: 100μM; $[Ba^{2+}]$: 100μM; S: Stretch; AA: $[Arachidonic\ Acid]_{10\mu M}$; $Ph6_i$: Internal Ph 6; $Ph6_e$: External Ph 6; 0: No Effect; +: Currents increased; -: Currents inhibited; X: no research.

1.4.3 THE WEAK INWARD RECTIFIERS OF 2-P K^+ CHANNELS (TWIK)

1.4.3.1 ELECTROPHYSIOLOGICAL PROPERTIES

TWIK-1 and TWIK-2 expressed in heterologous tissues show weak amplitude of K^+ conductance. The currents are transient and unblocked. Conductance of TWIK-1 is 34pS with [140 mM] K^+. Activation of TWIK-1/2 is time-dependent and reversal potential is equal to K^+ equilibrium potential (Chavez et al., 1999; Lesage et al., 1996a; Lesage et al., 1997; Lesage et al., 1996b).

1.4.3.2 PHARMACOLOGICAL CHARACTERISTICS

TWIK-1 is inactivated by Ba^{2+}, quinine and quinidine in a range of 50μM to 100 μM whereas TWIK-2 does not show any similarity. Both channels are slightly sensitive to tetraethyl ammonium (TEA), 4-aminopyridine (4-AP), and Cs^+. Despite TWIK-1 and 2 having similar molecular structure, they have different reactions to the same stimuli (Lesage et al., 1996a; 1996b). TWIK-1 and TWIK-2 are activated by protein kinase C and blocked with decreasing pH (Lesage et al., 1996b). These results are possibly explained by indirect mechanism. Altering the action site of protein kinase C does not change the activity of TWIK-1 and TWIK-2 to the activators. Acidic inactivation is not found in inside-out patch model, in which internal side of the channels is at a lower pH. Both TWIK-1 and TWIK-2 are not susceptible to the alteration of extracellular pH value even though this activates protein kinase C (Chavez et al., 1999; Lesage et al., 1996a).

TWIK-1 and TWIK-2 have been investigated in rat and human (Arrighi et al., 1998; Lesage et al., 1997). They are found in many tissues except skeletal muscle. This indicates that TWIK1/2 are involved in the control of background K^+

conductance in a variety of physiological environments such as sustaining resting membrane potential in pancreatic acinar cells (Schmid et al., 1995; Schmid et al., 1997). The weak inward rectifiers have been discovered in hepatic cells (Takanashi et al., 1994). TWIK-1 more often than TWIK-2 is reported in specific regions of the brain such as hippocampus, cerebellar granule and Purkinje cells (Lesage et al., 1997). This may suggest that TWIK-1 is mostly applied to keep resting membrane potential of neural cells. In these tissues and cells, the results demonstrate that intracellular acidification causes depolarization due to the inhibition of quinine-sensitive K^+ conductance.

1.4.4 TWIK-RELATED ACID-SENSITIVE K^+ CHANNELS (TASK)

1.4.4.1 BACKGROUND OF TASK

The TASK group of channels includes 5 subtypes. TASK-1 and TASK-3 are found in the neural tissue; TASK-2 is highly expressed in kidney and TASK-4 is described in many tissues; however TASK-5 does not show any known function. Altering extracellular pH, TASK1 to 4 exhibit different activities.

TASK-1 and TASK-2 are only regulated by extracellular pH under normal physiological conditions. TASK-3 has been shown to be open permanently, which is expressed in stomach where pH is approximately 4.5 (Hirst et al., 1989). At present, due to no accurate localization of TASK-3 in the gastric epithelium, its function is not clear. TASK-4 has a tendency of being active in alkaline situation and no activity is found in physiological environment. TASK-4 coexists with the subunits of other channels, which coordinate the sensitivity to different pH values (Decher et al., 2001).

Lopes et al., (2001) and Rajan et al., (2000) confirmed that histidine residue immediately distal to the first P region of TASK-1 and TASK-3 was responsible for pH sensitivity and altering this amino acid resulted in the prevention of pH sensitivity (Lopes et al., 2001; Rajan et al., 2000). Despite no histidine residue being present in TASK-2 and TASK-4, they are always sensitive to extracellular pH changes (Reyes et al., 1998; Decher et al., 2001).

1.4.4.2 ELECTROPHYSIOLOGICAL CHARACTERISTICS OF TASK-1 AND TASK-2

TASK-1 is the first cloned 2-P K^+ channel in mammalian cells (Duprat et al., 1997; Kim et al., 1998; Leonoudakis et al., 1998). Increasing external K^+ concentration increases the amplitude of time dependent outward currents, inactivation of which is not reopened by altering the concentration of external K^+, H^+ or voltage (Lopes et al., 2000). Conductance of single channel is between 12 and 16pS with different kinetics (Leonoudakis et al., 1998; Lopes et al., 2000; Kim et al., 1998; Kim et al., 1999) whereas TASK-2 currents showed rapid activation kinetics (Reys et al., 1998) in 60ms at +50mV. TASK-1 and TASK-2 have unitary conductance of 14 and 60pS at [150 mM] K^+ (Kim et al., 1999; Leonoudakis et al., 1998; Reyes et al., 1998). The sensitivity of TASK channels are notably changed by external pH in a narrow physiological range (Duprat et al., 1997; Kim et al., 1999; Leonoudakis et al., 1998; Reyes et al., 1998). 90% of TASK-1 current is shown at pH 7.7 and 10% at pH 6.7. 50% current is blocked at pH7.3 with 0mV (Duprat et al., 1997). 90% of TASK-2 current occurrs at pH 8.8 and 10% at pH 6.5. 50% current is inhibited at pH 8.3 with 0mV (Reyes et al., 1998). Acidic action depends on altering

the number of activated channels not on the conductance of single channel (Reyes et al., 1998).

1.4.4.3 THE PHARMACOLOGICAL CHARACTERISTICS OF TASK-1 & TASK-2

TASK-1 and TASK-2 are not sensitive to Ba^{2+}, Cs^{+}, TEA and 4-AP. TASK-2 is blocked by quinine (IC_{50}=22 μM) and quinidine (IC_{65}=100 μM). Zn^{2+} is a more effective inhibitor of TASK-1 (IC_{50}=175 μM) than of TASK-2 (IC_{15}=100 μM). Distribution of TASK-1 and TASK-2 is more restrictive than TWIK channels. TASK-1 and TASK-2 are applied to maintain resting membrane potential, the recycling and secretion of K^{+}. Both channels are found in excitable and non-excitable tissues, but TASK-1 is only shown in cortical tissue of brain, motoneurons and cardiac tissue (Duprat et al., 1997; Leohoudakis et al., 1998; Kim et al., 1998; Talley et al., 2000).

TASK-1 is cloned and identified by Kim et al., (1998). TASK-1 in human heart is sensitive to volatile anesthetics and thought to be responsible for cardiac malfunction in anesthetic patients (Goldstein et al., 2001; Patel et al., 1998). The study demonstrates that TASK-1 has similar kinetic characteristics with TASK-2 under the background current, I_{kp}, which affects amplitude and duration of plateau phase of action potential and contraction (Goldstein et al., 2001). RT-PCR technology shows the existence of TASK-1 in both atrial and ventricular myocardium of rabbit (Jones et al., 2002).

To neural tissues, Talley et al., (2000) demonstrated that TASK-1-dependent K^{+} conductance in hypoglossal motoneurone of rat was inhibited directly by acid,

serotonin, norepinephrine, substance P and thyrotropin-releasing hormone. Many experiments show that TASK-1 is the background current in rat cultured cerebellar granule neurons (Millar et al., 2000; Watkins et al., 1996; Patel et al., 1998). Brickley et al., (2001) indicated that TASK-like current occurred in $GABA_A$-deficient cerebellar granule neuron cells of mice. Investigators concludes that increasing TASK-like current in cerebellar granule neuron cells is a compensation mechanism for insufficiency of the current generated by the release of GABA from these cells. However, the background current is not likely to be produced by TASK-3 due to the absence of its mRNA after birth. Hougaard et al., (2001) and Niemeyer et al., (2001) revealed that the cellular volume undergoing an increase in Ehrlich ascites tumor cell was reduced due to TASK-like K^+ current (TASK-1 or TASK-2).

1.4.5 STRETCH- AND UNSATURATED FATTY ACID-ACTIVATED TREK-1 & TRAAK

1.4.5.1 THE ELECTROPHYSIOLOGICAL CHARACTERISTICS OF TREK-1 & TRAAK

TREK-1 and TRAAK are the first cloned polyunsaturated fatty acid and stretch-sensitive K^+ channels. In heterogeneous tissues, TREK-1 and TRAAK show lower activity with respect to TASK channels. TRAAK current is linear with highly symmetric $[K^+]$ whereas TREK-1 shows outward rectification for strong hyperpolarization. Carboxyl terminus of TREK-1 is responsible for voltage-dependent inactivation that leads to Mg^{2+}-independent outward rectification in the whole cell (Maingret et al, 2000). Both are flickery and unitary conductance is 100pS at 45mV with symmetric [150mM] K^+ (Fink et al., 1996; Patel et al., 1998; Fink et al., 1998; Maingret et al., 1999).

1.4.5.2 THE PHARMACOLOGICAL CHARACTERISTICS OF TREK-1 & TRAAK

TREK-1 in mice is mainly expressed in brain and heart whereas TRAAK is only found in neural tissues such as brain, spinal cord, and retina (Fink et al., 1996; Fink et al., 1998; Maingret et al., 1999). TREK-1 in human is found mainly in brain, ovary and small intestine whereas TRAAK is highly expressed in brain and placenta (Lesage et al., 2000). TREK-1 and TRAAK are activated by arachidonic acid and inhalation anesthesia, which is reversible and concentration-dependent. However, TREK-1 and TRAAK are resistant to saturated fatty acids and the activity is not changed by arachidonic acid and its inhibitors, which may suggest that the effect of arachidonic acid is a direct action (Fink et al., 1998; Lesage et al., 2000; Maingret et al., 1999; Patel et al., 1998). TREK-1 and TRAAK are susceptible to stretch such as shear stress, cell swelling and negative pressure. The activations of 50% TREK-1 and TRAAK by pressure are -36mmHg and -46mmHg, respectively (Maingret et al., 1999a; Maringret et al., 1999b; Patel et al., 1998).

TREK-1 and TRAAK are reversibly blocked by Gd^{3+} (Patel and Honore, 2001). Both channels are not sensitive to TEA and 4-AP and slightly inhibited by Ba^{2+} at high concentration. Quinine blocks the activity of TREK-1 (IC_{50}=100μM). TREK-1 is inhibited by a cAMP-dependent phosphorylation whereas TRAAK is not sensitive (Patel et al., 1999; Maingret et al., 1999). With the alteration of intracellular pH, TREK-1 is activated at normal atmospheric pressure (Maingret et al., 1999). The Studies show that carboxyl terminus of TREK-1 is involved in the transduction of

mechanosensitivity and the sensitivity to arachidonic acid and different intracellular pH (Maingret et al., 1999; Patel et al., 1998).

1.4.5.3 TREK-1 CHANNEL (KCNK2)

TREK-1 has been shown in mouse and rat heart and also been found in the different regions of their brains. Negative pressure activates TREK-1 (Kim et al., 1989; 1992; 1995). Stretch-activated currents are flickery. TREK-1 is also activated by arachidonic acid and other lipophilic reagents in cardiac and neural tissues. More importantly, TREK-1 is sensitive to mechanical stimuli at acidic intracellular pH between 5.6 and 7.2 (Lesage and Lazdunski, 1999). TREK-1 is inhibited by cAMP phosphorylations, which suggest that TREK-1 is involved in many biochemical activities. TREK-1 also responses to a major K^+ efflux in ischemia areas of brain and heart, where the efflux caused by Ca^{2+}-induced K^+ channel and ATP-dependent K^+ channel is prevented by specific inhibitors (Lesage and Lazdunski, 1999). In hypertrophic cardiac cells, the activity of TREK-1 is strengthened due to intracellular acidification in swelling cells (Patel et al., 1998).

1.4.5.4 TRAAK CHANNEL (KCNK4)

Andres and Eleazar (2002) demonstrated that KCNK4 included two transcript areas, HKT4.1a and HKT4.1b. Seven exons exist in HKT4.1a, which encode 393 amino acids whereas 11 exons in HKT4.1b, which encode 419 amino acids. HKT4.1a is 83% homologous to TRAAK in mice. RT-PCR suggests that cDNA of TRAAK in human and mouse is the product of orthological gene. The results of Andres and Eleazar (Fig 18) are completely different from what Lesage and Lazdunski (2000) described (Fig 15), in which Lesage and Lazunski found that no TRAAK was

expressed in human heart. The discovery of Andres and Eleazar indicates that some deficiencies and disadvantages exist in the experiment made by Lesage and Lazunski.

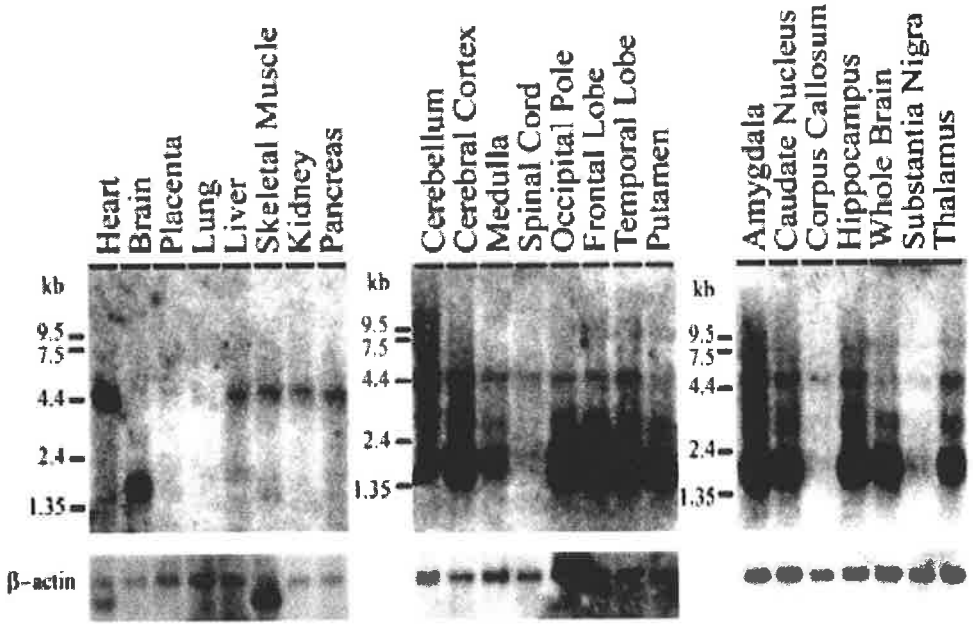

Figure18. shows that mRNA from other human tissue and brain are hybridised at high stringency with a ^{32}P labelled HKT4.1b cDNA (β-actin as control). The blots are exposed to X-ray film for 36h for HKT4.1 and 6h for β-actin. Andres et al., (2002).

1.4.6 KCNK6 AND KCNK7

KCNK6 is cloned from mouse (Salinas et al., 1999). KCNK6 is found in endoplasmic reticulum and shows ion channel activity on cell surface. It is not an intracellular channel but a subunit, which cooperates with another subunit to act on plasma membrane (Salinas et al., 1999). The major expression of KCNK6 is in the eyes with Ca^{2+}-binding site, which suggests that KCNK6 is responsible for the sensitivity or regulation of Ca^{2+}. It indicates that KCNK6 controls electrical signals in retina. Goldstein et al., (2001) concluded that TWIK-2 was indeed KCNK6 or KCNK8 in human beings. In humans and mice, KCKN6 is 94% homologous to KCNK7, which suggests that both are the product of orthologous gene. Additionally, the second pore region of KCNK7 is GYG instead of GFG in TASK-1, TASK-2,

TREK-1 and TRAAK, and GLG in TWIK-1 and TWIK-2. Also in KCNK7, GLE replaces GLG. This indicates that KCNK7 has the unique functions in the selection of different kinds of ions.

1.5 PURPOSE OF THIS THESIS

TREK channels have been found in rat and mouse heart. TRAAK splicing variants are discovered in human heart. Furthermore, TREK-1-like currents are found in human atrium. These discoveries are challenging the results published by Lesage and Lazdunski (2000) and makes the existence of TREK channels in human heart become more reasonable. Certainly, some unconfirmed factors may affect the expression of TREK channels in human heart in the previous publication.

In this thesis, we try to confirm the existence of TREK-1, TREK-2 and TRAAK in human heart and to evaluate the different distribution and quantification of TREK-1, TREK-2 and TRAAK between physiological and pathological human heart tissue. The difference in the localization and the quantity of channel protein between normal and abnormal cardiac tissues may open a new window for the understanding of the relationship between MEF, SAC and arrhythmia. And further the discoveries of stretch-sensitive channels in human heart may provide the clues that explain the mechanisms of cardiohypertrophy caused by stretch and the reason why the occurrence of arrhythmia in cardiohypertrophic patients is higher than other cardiac diseases at molecular level. These possibilities may result in the new treatments to arrhythmia and related cardiac diseases.

CHAPTER 2

GENERAL
MATERIALS AND METHODS

2.1 GENERAL MATERIALS

2.1.1 CHEMICALS AND REAGENTS

The following chemicals and reagents were ordered from Sigma Chemical Co. Ltd., St Louis MO, USA and ICN Chemical Co. Ltd., USA.

0.6% Triton X 100

10% Ammonium Persulphate solution

1-bromo-3-chloropropane (BCP)

40% Acrylamide/Bis solution

Bromophenol blue

Courmaric Acid

Diethyl pyrocarbonate (DEPC)

Ethanol

Ethidium bromide

Ethylenediaminetetra acetic acid (EDTA)

Ficol

Glycine

Hydrogen peroxide

Isopropanol Magnesium chloride

Luminol

Na Vanadate NaF

Sodium dodecyl sulphate (SDS)

ß-mercaptoethanol

TEMED

Tris[hydroymethyl]aminomethane (Tris base)

Tween-20

Xylene cyanol

Source of other chemicals and reagents used generally are as follows:

Agarose DNA ladder (Geneworks, Adelaide, Australia); Low melt agarose (Sigma, USA); dNTP (Life Technology, USA); Tri-reagent (Sigma, USA). Also all the chemicals and reagents used in this project are of molecular biology grade and analytic standards.

2.1.2 BUFFERS AND SOLUTIONS

10X DNA loading buffer	20% ficoll; 1.0% glycol; 0.1M EDTA (pH 8.0); 0.25% Bromophenol blue; 0.25% Xylene cyanol;
RNA loading buffer	50% formamide; 6.2% formaldehyde; 10% glycerol; 30µg ethidium bromide; 1X MOPS buffer;
10X PCR buffer	200mM Tris-HCl; 500mM KCl;
10X MOPS buffer	0.2M MOPS free acid;

	50mM Na acetate; 10mMEDTA;
5X first-strand buffer	250mM Tris-HCl; (pH 8.3 room temperature); 375mM KCl; 15mM $MgCl_2$;
Storage buffer of Reverse Transcriptase	20mM Tri-HCl (pH 7.5); 100mM NaCl; 0.1mM EDTA;1mM DDT; 0.01%(v/v) NP-40; 50%(v/v) glycerol;
Storage buffer of *Taq* Polymerase	20mM Tri-HCl (pH 7.5); 0.1mM EDTA;1M DDT; 50%(v/v) glycerol; stabilizers;
TBE buffer	90mM Tris base; 90mM boric acid; 0.5M EDTA (pH 8.0);
TE buffer	10mM Tris-HCl (pH 8.0); 1mM EDTA;

2.1.3 ENZYMES

The enzymes applied in this thesis were ordered from Invitrogen™, Carlsbad, California, USA and USB Corp. Cleveland, Ohio, USA.

SuperScript™ II Reverse Transcriptase	Concentration (200U/µl); Store at -20°C;
SuperScript™ III Reverse Transcriptase	Concentration (200U/µl); Store at -20°C;
Taq DNA Polymerase	Concentration (5U/µl); Store at -80°C;
ExoSAP-IT	Concentration (100 reactions); Store at –20°C;

2.1.4 KITS

Tri-Reagent RNA isolation reagent	SIGMA-ALDRICH, Australia
cDNA synthesis	*PE* Applied Biosystems, California, USA
DNA-free™	*Ambion* The RNA Company, USA
PCR synthesis	*PE* Applied Biosystems, California, USA
SYBR Green	*PE* Applied Biosystems, California, USA
IQ™ SYBR® Green Supermix	BIO-RAD, Hercules CA, USA
UltraClean GelSpin DNA purification	*MO BIO* Laboratories, Inc. USA

UltraClean PCR Clear-Up	*MO BIO* Laboratories, Inc. USA
BigDye Terminator v3.1 Cycle Sequencing	*PE* Applied Biosystems Company. USA

2.1.5 SYNTHETIC OLIGONUCLEOTIDE SEQUENCE

The following primers are designed by ABI PRISM primer design software for amplifying specific regions of mechano-stretch activated channels in the animal heart tissues and the human heart tissues. Abbreviations used: SP = Sense Primer; ASP = AntiSense Primer; r = rat; R = Rabbit; H = Human; GP = Guinea Pig.

2.2 GENERAL METHODS

The methods used in this thesis are described in Sambrook et al., (1989). These include quantitation of DNA and RNA; autoradiography; agarose gel electrophoresis; DNA and RNA precipitations and phenol/chloroform extraction.

All manipulations involving molecular biological techniques are carried out in accordance with the regulations and approval of the Australian Academy of Science Committee on Recombinant DNA and the Council of the University of Adelaide.

Handling and procedures of animals and the human heart tissues are carried out at

the animal house facilities of the University of Adelaide and the Royal Adelaide Hospital in accordance and approval from the Animal Ethics Committees of the University of Adelaide and the Royal Adelaide Hospital. Ventricular tissues were delivered in a container with liquid nitrogen and stored in a tissues-specific freezer (-80 °C) in the Department of Physiology, The University of Adelaide. Positive control and negative control used in PCR and Western blot will be described individually in the following chapters.

2.2.1 RNA EXTRACTION

General tissue preparation techniques were as described by Chomczynski et al., (1987). Tissue samples were homogenised in in tri-agent (1ml/ 50-100mg) until all large tissue pieces were broken down. Homogenised samples were transferred to labelled microfuge tubes, and allowed to stand at room temperature for 5 min. adding 0.1ml BCP per ml of tri-agent for each tube. Samples were shaken vigorously for 15 seconds and allowed to stand at room temperature for 2 to 15 min. before centrifuging at 12,000g for 15 min at 4°C. There are 3 phases in the liquid in which a lower organic phase contains protein, white interphase contains DNA and colourless upper aqueous phase is the RNA. The RNA layer was transferred into a new labelled microfuge tube and 0.5 ml of isopropanol/ml of tri-reagent added and mixed thoroughly. After being allowed to stand for 5 to 10min on ice, the sample was centrifuged at 12,000g for 10min at 4°C, supernatant removed and pellet washed by adding 1ml of 70% ethanol per ml of

tri-reagent used in the sample preparation. The sample was centrifuged again at 12,000g for 5min at 4°C, before adding TE buffer and being stored at -80°C.

2.2.2 DNAse TREATMENT TO mRNA SAMPLE

This protocol is designed to remove trace to moderate amounts of contaminating DNA (up to 50 µg DNA/ml RNA) from purified RNA to a level that is insignificant by RT-PCR. No RNA isolation method can extract RNA that is completely free from DNA contamination. To 50 µl RNA sample with contaminating DNA, was added 0.1 volume 10X DNAse I buffer and 1 µl rDNAse (2U/ µl); incubating at 37°C for 20-30 minutes; adding 0.1volume DNAse Inactivation Reagent and standing at room temperature for 2 minutes; and then spinning at 10,000g for 1.5 minutes at room temperature or at 4°C, transferring supernatant to a new tube.

2.2.3 FIRST-STRAND cDNA SYNTHESIS PROCESS

The first-strand cDNA synthesis reaction is catalyzed by SuperScript II and III RNAse H^- Reverse Transcriptase (RT) (Invitrogen). Although there are some different temperature requirements for the two enzymes the buffer and components are the same. Two tubes are used to SuperScript II process. First tube is RNA and Primer mix which includes Xµl up to 5µg RNA; 1 to 5µl random hexamers (50ng/µl); 1µl 10mM dNTP mix; DEPC-treated water up to 10µl. The second one is RT mix in which there are 2µl 10X RT buffer, 4µl 25mM $MgCl_2$, 2µl 0.1M DTT, 1µl RNAseOUT Recombinant Ribosomeclease

inhibitor and 1µl SuperScript II. The first tube is heated to 65°C for 5min and quick chilled on ice before adding the second tube component into the first one. This is then incubated at 25°C for 10min, 42°C for 50min, and 70°C for 15min.

For SuperScript III the first tube includes Xµl up to 5µg RNA; 1 to 5µl random hexamers (50ng/µl); 1µl 10mM dNTP mix; DEPC-treated water up to 13µl. The second one is RT mix in which there are 4µl 5X First-Strand buffer, 1µl 0.1M DTT, 1µl RNAseOUT Recombinant Ribosomeclease inhibitor and 1µl SuperScript III. The first tube is heated to 65°C for 5min and quick chilled on ice for at least 1min. centrifuged and the second tube added. The mix is incubated at 25°C for 5min, 50°C for 50min, and 70°C for 15min. More description is given in Invitrogen First-Strand Synthesis Protocol.

2.2.4 POLYMERASE CHAIN REACTION (PCR)

Taq DNA Polymerase from Invitrogen plays an important role in this process. Adding 10µl 10X PCR buffer, 2µl 10mM dNTP mix, 3µl 50mM $MgCl_2$, 5µl primer mix (10µM each), 1 to 20µl cDNA, 0.5µl *Taq* DNA Polymerase and up to 100µl solution by molecular water in a PCR-Specific tube (500µl). Centrifuging the tube and putting in PCR machine in a process of 94 °C for 3min, 20-35 cycles of PCR amplification which includes denature (94 °C for 45s), anneal (50°C for 30s) and extend (72°C for 1min), incubating for an additional 10min at 72 °C and maintaining the reaction at 4°C, then storing PCR products in -80 °C molecular level freezer. The PCR products are analysed

by agarose gel electrophoresis and visualized by ethidium bromide staining.

2.2.5 PCR AGAROSE GEL ELECTROPHORESIS

Agarose gel powder from Sigma Company was used for molecular biological experiments. There are two different concentrations of agarose gels used in PCR gel running. One is 1.2% in which 0.36g gel power is mixed with 3ml TBE buffer and 27ml distilled water for a small gel tank. The other one is 1.5% in which 1.5g gel powder is mixed with 10ml TBE buffer and 90ml distill water. Ethidium bromide is diluted in equal volume (v/v). To 1.2% PCR gel 2μl ethidium bromide is added for DNA staining and to 1.5% PCR gel 4μl ethidium bromide is used for DNA staining. Standard DNA ladder is used to check PCR products' size. Bands on the gel are analysed automatically by Gel Dock system (Bio-Rad), in the details of which have been described in Bio-Rad User Introduction Booklet.

2.2.6 PCR GEL-SPIN DNA PURIFICATION

PCR Gel-Spin DNA purification protocol provided by *MO BIO* Laboratories Inc: All of the centrifugation steps are 10,000g in this process. The desired DNA band is cut from TBE agarose gel. 3 volumes of GelBind (300μl /100μg) is added to the gel slice and the gel is submerged in the GelBind buffer, incubated for 2min at 55-65 °C, inverted once, and incubated one minute more or until gel is melted. The tube is inverted once to mix and centrifuged for 10second at 10,000g. Spin filter is removed and the collection tube

vortex mixed for 5 seconds to mix the flow through. All liquid is reloaded back onto the spin filter and centrifuged for 10 seconds at 10,000g. The flow through liquid is discarded and spin filter basket replaced. 300µl GelWash buffer is added and the tube spun for 10 seconds at 10,000g. The flow through is discarded and the tube spun again for 30 seconds before carefully transferring the filter basket to a clean collection tube. 50µl Elution buffer (10mM Tris) is added (or water) directly onto the centre of the white spin filter membrane. The Tube is centrifuged for 30 seconds at 10,000g and the spin filter basket discarded. PCR products are then ready to be sequenced.

2.2.7 PCR CLEANUP DNA PURIFICATION

PCR Clean-Up protocol provided by *MO BIO* Laboratories Inc: Add 5 volumes of SpinBind to PCR reaction; transfer the mixture of PCR and SpinBind to a spin filter unit; centrifuge them in a tabletop microcentrifuge at a minimum 10,000g; remove the spin filter basket an discard the liquid from the tube by decanting; add 300 µl SpinClean buffer to the spin filter and centrifuge at a minimum 10,000g for 10 to 30 seconds; remove and discard the liquid from the tube by decanting and centrifuge at a minimum 10,000g for 30 to 60 seconds; transfer spin filter to a clean collection tube; add 50 µl molecular water directly onto the centre of the white spin filter membrane; centrifuge at a minimum 10,000g for 30 to 60 seconds; discard the spin filter basket and store PCR products at –20°C for sequencing.

2.2.8 ExoSAP-IT DNA purification

Information provided by ExoSAP-IT PCR CLEAN-UP PROTOCOL: ExoSAP-IT includes Exonuclease I and Shrimp Alkaline Phosphatase. It is stored at –20°C and kept on ice while pipeting. Take 5 µl of PCR Products and 2 µl of ExoSAP-IT (when treating 10 µl or more of PCR products, increase the amount of ExoSAP-IT proportionally); mix and incubate at 37°C for 15 minutes; inactivate ExoSAP-IT by heating to 80°C for 15 minutes and the PCR products are ready to be sequenced.

2.2.9 SEQUENCING PROCESS

BigDye Terminator v3.1 Cycle Sequencing protocol supported by *PE* Applied Biosystems, California, USA: PCR products treated by PCR GelSpin kit, PCR ClearUp kit and ExoSAP-IT are used in the sequencing process. This process was performed in Institute of Medical & Veterinary Science (IMVS) by GeneAmp PCR System 9600 of *PE* Applied Biosystems Company. The sequencing reaction mix includes 4µl of 2.5X Ready Reaction Premix, 2µl of 5X BigDye Sequencing Buffer, 3.2µl primer, Xµl PCR products depending on their concentration, and molecular water up to 20µl. This is subjected to 25 cycles of rapid thermal ramp to 96 °C for 10 seconds, rapid thermal ramp to 50 °C for 5 seconds and rapid thermal ramp to 60 °C for 4 minutes. At the end, rapid thermal ramp to 4 °C and hold for purifying the extension products. In the process of precipitating in PCR sequencing tubes add 80µl of 75% isopropanol into the tube and vortex briefly. Leave the tubes at room temperature for 15min to precipitate the extension products. Mark their

orientation of the tubes which are placed in a microcentrifuge and spin the tubes for 20min at maximum speed. Discard the supernatants with separate pipette tip for each sample. Add 250µl of 75% isopropanol to the tubes and vortex again. Spin the tubes for 20min at maximum speed in microcentrifuge. Discard the supernatants carefully and dry the samples in a heat block or thermal cycle 90 °C for 1min. The dry pellet was sent to IMVS for sequencing.

2.2.10 REAL-TIME PCR

Real-time PCR is performed by GeneAmp® 5700 Sequence Detection System (SDS) provided by *PE* Applied Biosystems, California, USA and analytic real-time PCR software is 5700 SDS ver 3.0. SYBR Green PCR Master Mix is purchased from *PE* Applied Biosystems, California, USA. Each 25µl SYBR Green tube includes 2.5µl cDNA, 1.0µl of 10µM sense primer, 1.0µl of 10µM antisense primer, 12.5µl SYBR Green PCR Master Mix, and 8µl molecular level water up to 25µl. The sample tube is placed in a PCR process of 95 °C for 10min and 40 cycles of 60 °C for 1min and 95 °C for 15 seconds. More details are given in SYBR Green PCR protocol and GeneAmp® 5700 SDS Compendium. The data from 5700 will be transformed into SSPS software for statistical application. The calculation method applied for the initial quantity of mRNA in sample tissue has been introduced meticulously in Liu and Saint (2002b). The ratio of $[mRNA]_{optimal\ gene}$ and $[mRNA]_{internal\ control}$ is used to express the amount of mRNA in the different samples. GAPDH is selected as an internal control, whose stable expression in

human cardiac tissue has been published by Goulter et al., (2004).

2.2.11 WESTERN BLOT

2.2.11.1 PROTEIN EXTRACTION

1. Retrieve tissue from -80° C freezers and keep on dry ice. Use the tissue hammer to break up stock tissue while in the bag. Place sample tube on balance and zero the balance. Use the scalpel to cut tissue on the chopping board, and weigh approx. 100mg of tissue into sample tube. Record exact weight, and store on dry ice. Stock tissues should be returned to the minus 80°C freezer ASAP
2. To each sample tube, add 1mL of homogenizing buffer, and homogenize each sample with rotor to full speed. Make sure to rinse the homogenizing probe in dH_2O between each sample.
3. Pour the samples from the white-capped tubes into the centrifuge tubes - there will be a little foam left over in the white-capped tubes, therefore they should be discarded in the biohazard bin. Cap the centrifuge tubes, and spin in the Beckman J6 Centrifuge for 30 minutes at 1800rpm (Pre-cool centrifuge to $4^{\circ}C$).
4. Remove tubes from centrifuge and place on ice again. Slowly pour off the supernatant layer from the sample and place into a labeled centrifuge tube. The pellet can be discarded. The extracted protein can be stored at minus 20°C if being used in the short term, or -80°C for long-term storage. Proceed with a Bradford Micro-assay, to determine the concentration of the stock protein samples.

2.2.11.2 SDS-POLYACRYLAMIDE GEL ELECTROPHORESIS

GEL FORMULATIONS (10ML - ENOUGH FOR 2 MINI-GELS)

Percent Gel	MilliQ Water (ml) (for 30% acryl)	30% Acrylamide/ Bisoln (ml)	MilliQ Water (ml) (for 40% acryl)	40% Acrylamide/ Bisoln (ml)	Gel buffer (ml) (* see below)	20% SDS (µl)
4.0	6.1	1.3	6.4	1.0	2.5	50.0
5.0	5.7	1.7	6.1	1.3	2.5	50.0
6.0	5.4	2.0	5.9	1.5	2.5	50.0
7.0	5.1	2.3	5.7	1.7	2.5	50.0

Prepare the stacking gel and resolving gel in 10ml tubes. Mix thoroughly after adding each component. Prepare 300-500µl 10% APS. Add 10µl TEMED to the resolving gel and immediately add 100µl 10% APS solution. Mix quickly by inverting to ensure no bubbles are formed. Slowly pour the resolving gel in between the glass plates up to the texta mark (~3cm from top). Carefully overlay the resolving gel with iso-propanol (or iso-butanol). Add it slowly, so it doesn't mix into the gel layer. Seal the tube with the remainder of the solution and wait for it (gel in tube and in casting plates) to set (~30min). As for resolving gel, add 10µl TEMED & 100µl 10% APS solution to the stacking gel, Mix quickly by inverting to ensure no bubbles are formed. Use a glass pasteur pipette, slowly add the stacking gel in between the glass plates, allowing air bubbles to escape. Once the apparatus is filled, slowly and evenly push the comb the rest of the way in.

Allow the gel layer to set fully (about 30 minutes). Remove the combs when the gel is set, clean all the equipment & rinse in MilliQ H_2O. Pre-heat the heating block to 95-100°C. Add sample buffer (SB) containing 5% β-mercaptoethanol to protein samples in a 1:1 ratio. If using 14 well combs, then load approx 10 µl per lane, i.e. 5 µl protein : 5 µl SB. Add to the heating block. Denature at 95^0C for 5 minutes and cool on ice. Put molecular marker into the well.

2.2.11.3 WESTERN TRANSFER PROTOCOL

1. Use a spatula to separate the glass plates (very carefully), remove the gel and place it in a plastic container. Pour on 1 x Western Buffer + 20% methanol (WBM) to cover the gel and wash for ~10 min to remove the electrode buffer and equilibrate the gel. Cut the nitrocellulose membrane and 2 X pieces of filter paper and soak in 1X WBM along with 2 filter paper.
2. On the transfer cassette, place one of the pre-wetted filter pads and place a piece of filter paper on this. Place the gel on the filter paper being careful not to tear the gel, and roll the glass rod over the gel to remove air bubbles. Place the nitrocellulose membrane on the gel, roll with the glass rod, place the other piece of chromatography paper on top of the membrane, roll with the glass rod, and place the filter pad on top of this. Close the transfer cassette.
3. Place the transfer cassette into the Transfer tank, positioning the 'Bio-ice' cooling unit next to it. Place a magnetic stir flea in the base of the tank, and place the tank

on a magnetic stirrer pad. Fill the tank with the 1XWNM and place the lid on the tank.

4. Connect up the power supply: 300 milliamps for 90min.
5. When transfer is complete, disassemble the transfer cassette, discard the gel and chromatography paper and precede to the immunodetection procedures.

2.2.11.4 WESTERN IMMUNODETECTION PROTOCOL

1. Wash membrane 3 X 5 minutes in TBS (1X) in small tray (i.e. lid of 200µl pipette ART tip box).
2. Block the membrane in TBS-T (1xTBS + 0.1% Tween-20) + 5% MILK (powder form) blocking solution for 1hr at room temperature.
3. Wash 3 X 5 minutes in TBS-T.
4. Dilute Primary Antibody
5. Incubate overnight at 4°C on the shaker in the cold room.
6. Wash membrane 3 X 5 minutes in TBS-T.
7. Dilute the 2° AB (HRP conjugated-Anti-rabbit IgG). Use secondary that came with primary, i.e. Cell Signaling secondary AB
8. Pour over membrane in the small tray. Make sure there are no air bubbles under membrane.
9. Incubate for 1hr at room temperature.
10. Wash membrane 3 X 5 minutes in TBS-T.

11. Make ECL reagents

12. Mix solutions A + B together and incubate membrane for 1 min with agitation. Place membrane in plastic wrap and into film cassette ready for exposure of x-ray film (usually 30s, 1 min, 2.5 m and/or 5 min).

13. If membrane is to be used again, it must be stripped immediately. Add 350 µl of ß-mercaptoethanol to 50 ml of stripping solution.

14. Incubate for 30 min at 50^0C.

15. Wash membrane 3 X 5 minutes in TBS.

16. Repeat step 2 with appropriate blocking solution.

17. Membrane can be stored. After stripping and washing in TBS place the blot between 2 sheets of Whatman paper. Place between 2 sheets of card and clip along edges without touching the blot. Lace into a sealed plastic bag and store at 4^0C for 2 weeks, -20^0C for 2 months or -80^0C long term.

2.2.12 COMPUTER PROGRAMES

Primer design is analysed using ABI Primer Express v2.0 and Gene Jockey. Databases used are GeneBank, EMBL, SWISS-PROT, and NCBI (http://www.ncbi.nlm.nih.gov). Photographs are performed by Biorad scanner and Gel Doc System.

CHAPTER 3

EXPRESSION OF TREK-1 & TRAAK

IN

NORMAL HUMAN HEART

3.1 INTRODUCTION

TREK-1, TREK-2 and TRAAK have been found in the human central nervous system by many groups (Lesage and Lazdunski, 2000; Meadows et al., 2000; Gray et al., 2000). The sequences have also been published in Gene bank of NCBI (http://www.ncbi.num.nih.gov), in which TREK-1 is AF171068, TREK-2 is AF279890 and TRAAK is AF247042.

TREK-1 and TREK-2 have 7 exons and TRAAK has 11 exons. All the two-pore potassium channels have a conserved amino acid sequence T-X-G-X-G on the pore structure. This occurs in the 3rd, 4th and 5th exon of TREK-1 and TRAAK. Table 6 shows the details of the three sequences.

TABLE 5. MOLECULAR DETAILS OF TREK-1, TREK-2 AND TRAAK

Categories	TREK-1	TREK-2	TRAAK
Organism	Homo sapiens	Homo sapiens	Homo sapiens
Tissue source	Brain	Unknown	Frontal lobe
Gene name	KCNK2	KCNK10	KCNK4
Chromosome location	1q41	14q31	11
mRNA length	1252bp	2733bp	2733bp
Exons	7	7	11
Coding area	15thbp to 1250bp	473rdbp to 2089bp	64thbp to 1323bp
Amino Acid length	411AA	538AA	419 AA
Reference	Meadows et al., (2001)	Lesage et al., (2000)	Gray et al., (2000)

More details about exons and introns of these three channels are shown in Table 6 and 7.

TABLE 6. MOLECULAR STRUCTURES OF TREK-1, TREK-2 AND TRAAK

Exons (bp)	TREK-1 (AF171068)	TREK-2 (AF279890)	TRAAK (AF247042)
Exon 1	15	489	64
Exon 2	311	350	266
Exon 3	118	118	124
Exon 4	161	161	161
Exon 5	187	187	187
Exon 6	140	143	140
Exon 7	320	1254	1086
Exon 8			331
Exon 9			80
Exon 10			67
Exon 11			227

TABLE 7. THE DISTANCE BETWEEN EACH EXON IN TREK-1, TREK-2 AND TRAAK

Introns (bp)	TREK-1	TREK-2	TRAAK
$Intron_{1-2}$	3061	62868	1157
$Intron_{2-3}$	37955	22382	3794
$Intron_{3-4}$	44449	13168	278
$Intron_{4-5}$	2638	34965	374
$Intron_{5-6}$	22770	4115	596
$Intron_{6-7}$	39736	1812	182
$Intron_{7-8}$			556
$Intron_{8-9}$			2574
$Intron_{9-10}$			278
$Intron_{10-11}$			930

In both humans and animals, TREK-1 has been shown to be highly expressed in brain, ovary and small intestine, and is expressed at slightly lower levels in kidney, testis, prostate and skeletal muscle, while TRAAK is mostly expressed in brain and placenta and at lower levels in testis, prostate and small intestine (Lesage et al., 2000). Although they have been shown to be expressed in cardiac tissue in animals (Terrenoire et al., 2001; Tan et al., 2004 a; 2004b; Liu and Saint, 2004), it is currently thought that none of these mechanosensitive K^+ channels are present in the human heart (Lesage et al., 2000; Kim, 2003).

However, there is no doubt that electrophysiological responses consistent with the presence of mechanosensitive K^+ channels can be observed in human atria and ventricles (Eckardt et al., 2000). In human atrium, increases in atrial pressure shorten atrial refractoriness (Calkins et al., 1991; Klein et al., 1990). Similarly, in human ventricle, action potential shortening can be induced by increases in ventricular loading either during cardiopulmonary bypass or induced by brief aortic occlusion (Taggart et al., 1988; 1992). These observations in humans, along with similar observations in animals, and the demonstration of expression of TREK-1 in animal heart, strongly suggest that TREK-1 is present in human heart.

3.2 MATERIALS AND METHODS

All procedures in this study were following guidelines of approval from the University of Adelaide Human Ethics Committee, the Royal Adelaide Hospital Ethics Committee and the University of Sydney Human Ethics Committee as appropriate.

Tissue - Human atrial tissue samples (right atrial appendage) were obtained from patients undergoing coronary bypass surgery. The samples used in these experiments were from patients without other cardiac diseases except for coronary artery disease. Atrial tissue samples kept in oxygenated physiological solution were frozen in liquid nitrogen within 20min of being excised at room temperature and then stored at –80°C. Human ventricular tissue samples were obtained from explanted hearts from the transplant program at St Vincent's Hospital, Sydney. Hearts had been maintained in liquid nitrogen for various times since being explanted. Positive control was human testicular tissue stored in oxygenated physiological solution, frozen less than 30min after excision at room temperature from a patient undergoing orchidectomy for prostate cancer in which the testicular tissue was normal in histology.

RNA Extraction - Total RNA was isolated from human atrial, ventricular and testicle tissues with either TRI-Reagent (SIGMA-ALDRICH, Australia) or RNA kit (BIO-RAD, Sydney, Australia). TRI-Reagent-treated RNA isolation was used to prepare cDNA for normal PCR, whereas BIO-RAD-treated RNA extraction was used to prepare cDNA for real-time PCR. Reverse transcriptase was from Invitrogen, (Australia). SYBR Green real-time PCR reagent was from BIO-RAD (Australia) and Applied Biosystems (US). The quantity of RNA in all the samples was detected by spectrophotometer (Eppendorf, Australia), and the same amount of RNA (370ng) from each sample was used in PCR and real-time PCR.

Primer Design - Primers were designed from published human sequences (GeneBank codes AF171068 for TREK-1) using Primer Express software (PE Applied Biosystems, Foster city, CA, USA). Initial PCR was performed for TREK-1 in human

samples and was then followed by nested PCR, in which another pair of sense and antisense primers are designed within the segment of such a PCR product. If the second PCR product with a desired size occurs on the Gel, it means the initial PCR product is obtained from the designed sequence. The products were sequenced and real-time PCR performed to quantify the expression of TREK-1 in normal and diseased human hearts, relative to the expression level of GAPDH. Primers for TREK-1 and GAPDH are shown on the following Tables.

TABLE 8. TREK-1 PRIMER

Primers of TREK-1			
	Sense Primer (5' - 3')	Antisense Primer (3' - 5')	Size
Initial PCR	GAGGACCACCATTGTGATCCA	TCCCACCTCTTCTTTTGTCTTTTT	697bp
Nested PCR	TTTGGAAAAGGAATTGCCAAA	TCCCACCTCTTCTTTTGTCTTTTT	372bp
Real-time PCR	GCTGTCCTGAGCATGATTGGA	CCCGCTGGAACTTGTCATAAA	169bp

TABLE 9. TRAAK PRIMER

Table 2. Primers of TRAAK			
	Sense Primer (5' - 3')	Antisense Primer (3' - 5')	Size
Initial PCR	ACCATCGGCTATGGCAATGT	GGACACTACTCGCAGCCAGTT	477bp
Nested PCR	CGGCTGCCTGCTCTTTGT	GGACACTACTCGCAGCCAGTT	250bp
Real-time PCR	CGGCTGCCTGCTCTTTGT	AAAGCCCACGGTGGTAAGC	132bp

TABLE 10. GAPDH PRIMER

Table 3. Primers of GAPDH			
	Sense Primer (5' - 3')	Antisense Primer (3' - 5')	Size
Real-time PCR	ATGGAAATCCCATCACCATCTT	GGTGCAGGAGGCATTGCT	252bp

PCR and Real-time PCR processes - PCR products were separated in 1.2% agarose gel and visualised with Gel documentation system from BIO-RAD (Sydney, Australia). Bands cut from the gels were cleaned by UltraClean Kit (MO BIO Laboratories, CA, US) and the product of nested PCR was purified by ExoSAP-IT (USB corporation, Cleveland, Ohio, US). For real-time PCR, 25μL reaction solution includes 12.5μL SYBR Green PCR Master Mixer, 5.5μL cDNA, 1μL of sense primer (10μM), 1μL of antisense primer (10μM), and 5μL of molecular-level water. Real-time PCR assay was performed in 96-well optical plates on an ABI Prism 5700 Sequence Detection System (PE Applied Biosystems, Forster city, CA, US). The process of real-time PCR was 1 cycle of 95^0C for 10min, and then 40 cycles of 60^0C for 1min and 95^0C for 15s. The data from real-time PCR was analysed in Sigmaplot (12.01 Version, SPSS, Richmond, CA, US).

Sequencing process

TABLE 11. SEQUENCING MASTER MIX

Reagent	Concentration	Volume (μl)
Ready Reaction Premix	2.5X	4
BigDye sequencing buffer	5.0X	2
Primer (SP/ASP)	5 μM	1
DNA template	[100-300ng]	1
Molecular water		Up to 20 μl
Final volume	1X	20 μl

(Depending on the different volume, but concentration of Ready Reaction Premix and BigDye Sequencing buffer should be half of the final volume).

Nested PCR was performed with an initial denaturation at 96°C for 1 minute, and then 25 cycles of 96°C for 10 seconds, 50°C for 5 seconds and 60°C for 4 minutes. 80μl of 75% isopropanol was added into sequencing products and the tube closed,

vortex briefly at room temperature for 15 to 30 minutes and spun for 20 minutes at maximum speed. Supernatants were discarded, 250µl of 75% isopropanol added and vortexed briefly, spun at maximum speed for 5 minutes and thermal cycled at 90°C for 1 minute.

Western Blot – human ventricular tissues stored at -80° C were homogenized in buffer solution (50mM Tris (pH=8), 150mM NaCl, 1mM Na Vanadate, 10mM NaF, 0.6% Triton) at room temperature. The concentration of protein was measured by spectrophotometer (Eppendorf, Australia) using a colorimetric method (BIO-RAD, Australia). The same amount of protein from each sample with loading buffer (0.5M Tris-HCl (pH 6.8), 40% (v/v) glycerol, 20% SDS, 0.5% (w/v) Bromophenol Blue dye, 5% (v/v) β-mercaptoethanol) was denatured at 95°C for 5min and run on a SDS-PAGE mini-gel (10% acrylamide). After fractionation, the samples were transferred to nitrocellulose membrane. The membrane was blocked with non-fat milk solution (Bio-Rad, Australia) and probed with anti-TREK-1 antibody (1:500, Alomone, Israel) and HRP-Anti-Rabbit antibody (1:1000, Adelaide University). Visualization of immunoreactivity was by ECL reagents (Sigma-Aldrich, Australia). Exposure time for all samples in western blot was kept the same. Images on X-ray Film (Amersham) were analysed by Gel Dock System (Bio-Rad, Australia).

Analysis of the data obtained from all samples is shown as mean ± standard error and statistical comparison by T-test.

3.3. RESULTS

3.3.1 RT-PCR IN HUMAN ATRIAL TISSUE

Standard RT-PCR with the above primers generated products of the expected size for TREK-1 visualised in 1.2% agarose gel (Fig 19). Nested PCR also produced a product of the predicted size (Fig 20). Sequencing of TREK-1 nested PCR product demonstrated 100% identity to the published human TREK-1 sequence (AF171068). The same methods were used with TRAAK. Standard RT-PCR and nested PCR confirmed the homology of the two PCR products (Fig 21 and 22). Sequencing of TRAAK nested PCR product was 100% homologous to the published human TRAAK sequence (AF247042).

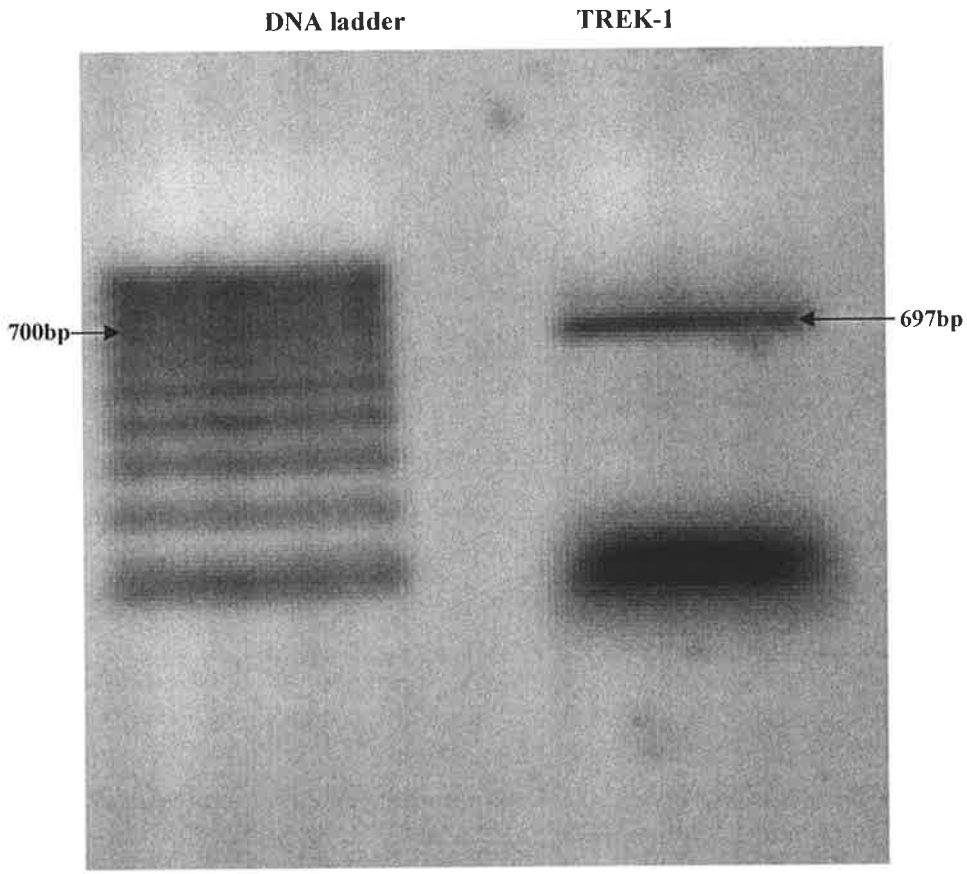

Figure 19. shows a clear band, (theoretic size 697bp), is amplified by specific primers of TREK-1 on 1.2% Agarose gel.

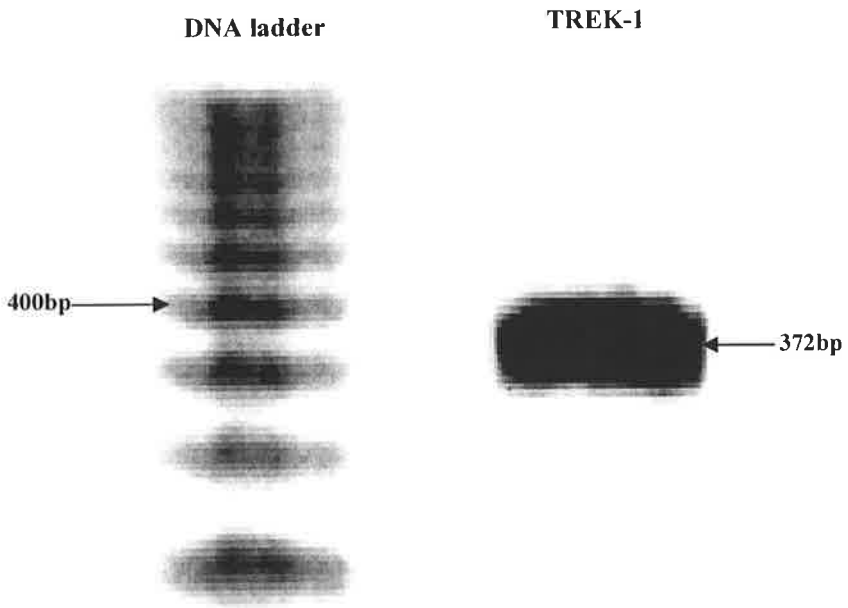

Figure 20. demonstrates that nested PCR produces one band (theoretical size 372bp). Sequencing shows nested PCR product is 100% homologous to the published human TREK-1 sequence.

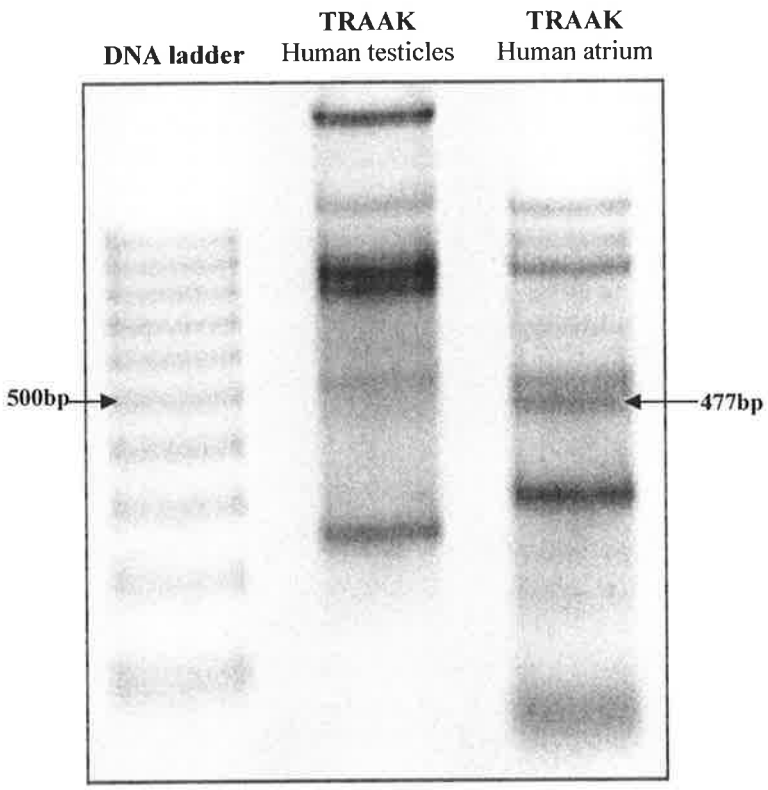

Figure 21. shows that normal PCR for TRAAK in human atrial tissue give a single band (theoretical size 477bp), in which human testicular tissue is chosen as a positive control.

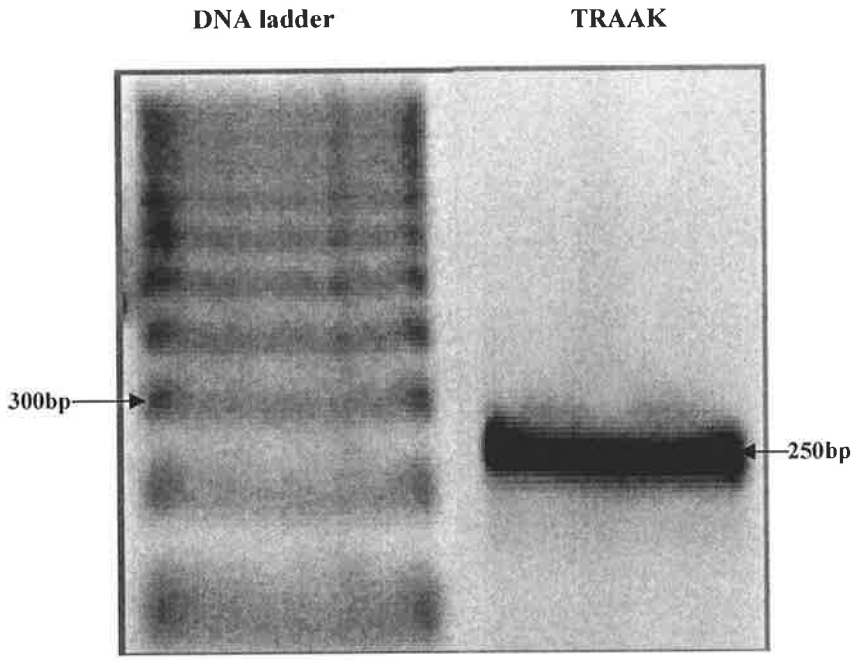

Figure 22. shows that 250-bp nested PCR product is obtained, whose sequencing result is 100% homologous to the published sequence of TRAAK.

3.3.2 SEQUENCING OF TREK-1 (790^{TH} – 1171^{ST})

5′→ ATCATATTTATACTATTTGGCTGTGTACTCTTTGTGGCTCTGCCTGCG

ATCATATTCAAACACATAGAAGGCTGGAGTGCCCTGGACGCCATTTATTTT

GTGGTTATCACTCTAACAACTATTGGATTTGGTGACTACGTTGCAGGTGG

T I G F G

ATCCGATATTGAATATCTGGACTTCTATAAGCCTGTCGTGTGGTTCTGGAT

CCTTGTAGGGCTTGCTTACTTTGCTGCTGTCCTGAGCATGATTGGAGATTG

GCTCCGAGTGATATCTAAAAAGACAAAAGAAGAGGTGGGAGAGTTCAGAG

CACACGCTGCTGAGTGGACAGCCAACGTCACAGCCGAATTCAAAGAAACC

AGGAGGCGACTGAGTGTGGAGATTTATGACAGTTCCCAGCGGGANN-3′

382-bp segment was sequenced from 475bp-PCR product of TREK-1. BLAST illustrated that homology between the sequenced segment and the published sequence in Genebank was 100% identical. The sequenced segment included one pore structure.

3.3.3 SEQUENCING OF TRAAK (702^{ND} – 924^{TH})

5′⟶CAGTTTCGTGTTCTGCTATATGGAGGACTGGAAGCAAGCTGGAGGC

CATCTACTTTGTCATAGTGACGCTTACCACCGTGGGCTTTGGCGACTATG

T V G F G

TGGCCGGCGCGGACCCCAGGCAGGACTCCCCGGCCTATCAGCCGCTGGTG

TGGTTCTGGATCCTGCTCGGCCTGGCTTACTTCGCCTCAGTGCTCACCACC

ATCGGGAACTGGCTGCGAGTAGTGTCCAGNNNNNN⟵3′

223-bp segment was sequenced from 250bp-PCR product of TRAAK. BLAST illustrated that homology between the sequenced segment and sequence in Genebank was 100% identical. The sequenced segment included one pore structure.

3.3.4 REAL-TIME PCR IN HUMAN ATRIAL TISSUE

Human atrial tissue samples (5 females and 2 males; age 40-50yr; simple coronary disease without any complications in diagnosis) frozen at -80°C for approx 12 months were used in real-time PCR. Fresh human testicular tissue was used as a positive control. Fig 23 shows the specificity and validity of the primers for TREK-1, TRAAK and GAPDH in human heart tissue. The expression level of TREK-1 in the frozen atrial tissue was 44 ± 9% that of GAPDH (n = 7; Fig 24A) whereas much higher expression level, 114 ± 16% times of GAPDH, was found in fresh atrial samples (n = 3; Fig 24A). The expression level of TRAAK was 11 ± 4% (n = 7; Fig 24A) in frozen atrial tissue and 46 ± 16% in fresh atrial tissue (n = 3; Fig 24A). Testicular tissue TREK-1 expression level was 1.85 times of GAPDH expression (n=1; Fig 24A), and TRAAK expression very low.

A

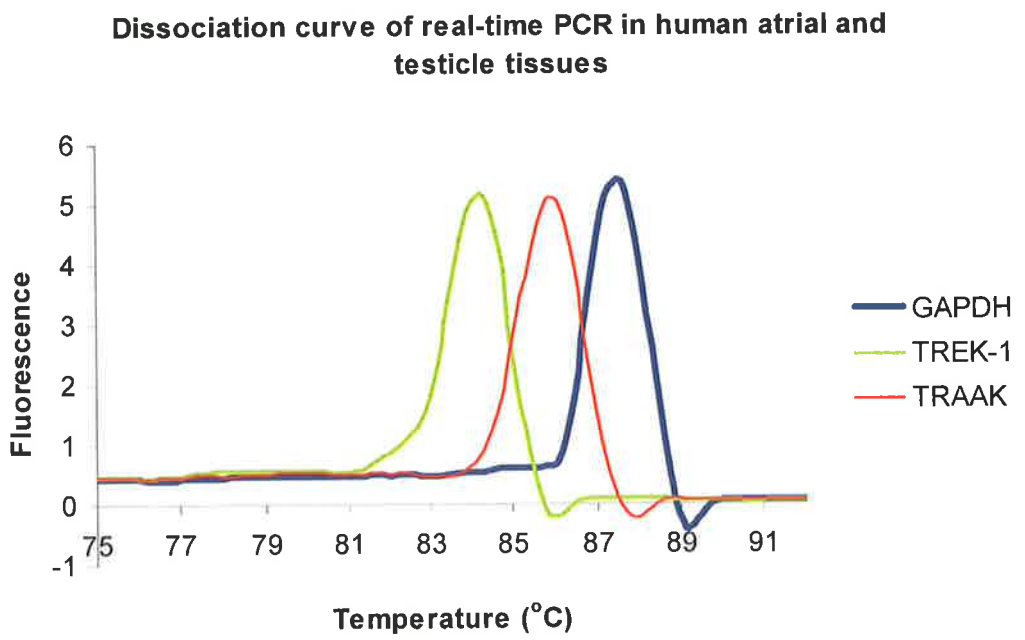

B

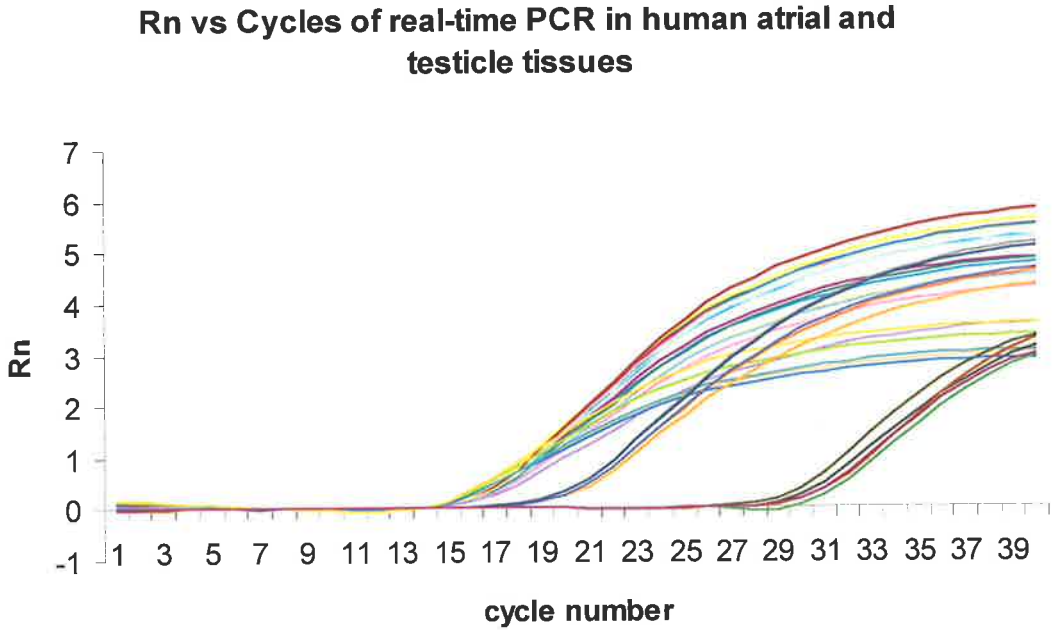

Figure 23. A and B shows that the primers of TREK-1 and TRAAK applied in real-time PCR are specific and valid. The results of real-time PCR are suitable to represent the expression level of TREK-1 and TRAAK in human atrial and ventricular tissues. TREK-1, TRAAK and GAPDH are synthesized in 84, 86 and 87 degree, respectively (A) whereas their fluorescence is dectected by Laster Reader in 27 cycles, 16 cycles and 14 cycles, respectively (B). All curves of the same pair of primers can be traced in a fix initial point that means regression of a single curve is valid to calculate the initial mRNA concentration from a given sample.

A.

Expression level of TREK-1 and TRAAK in fresh human testicular tissue, fresh and frozen human atrial tissues

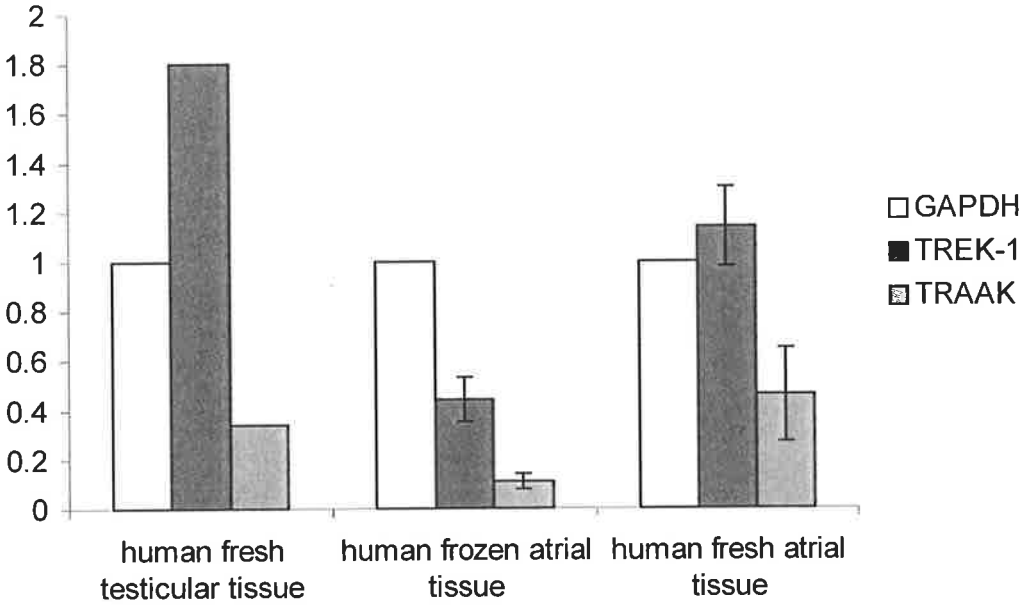

B.

Expression level of TREK-1 and TRAAK in fresh human testicular tissue, frozen human atrial and ventricular tissues

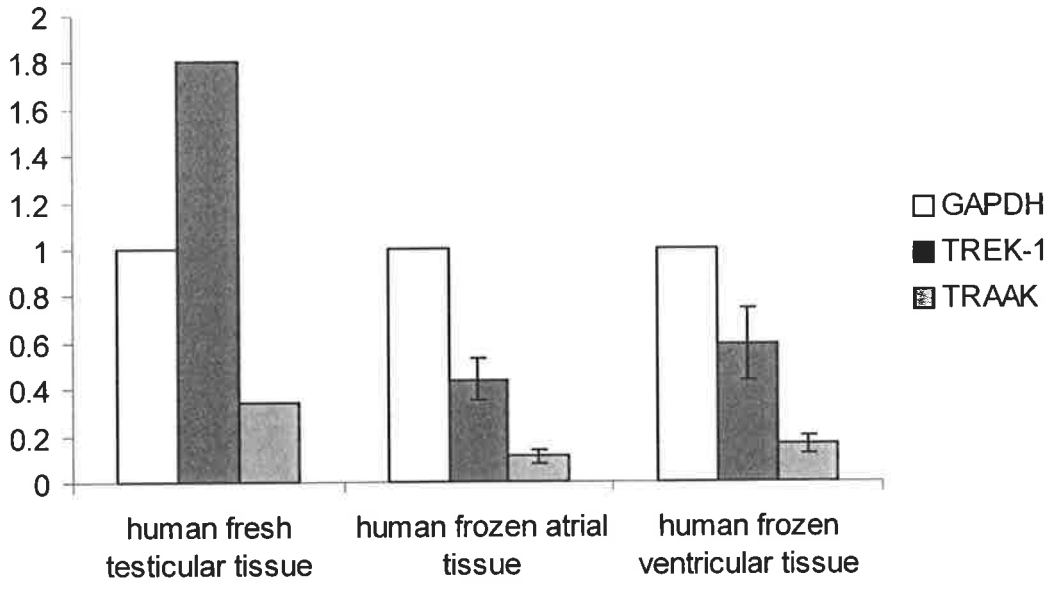

C.

Expression level of TREK-1 and TRAAK in fresh and 3-month-frozen human testicular tissues and fresh human atrial tissue

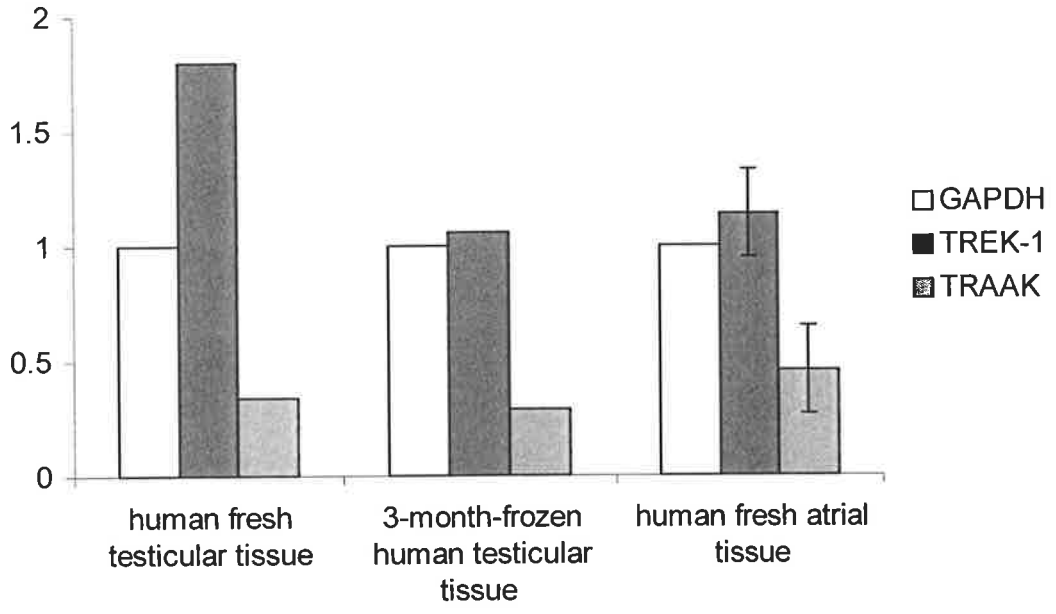

Figure 24. A, Ratio of expression levels of TREK-1 and TRAAK to GAPDH in fresh human testicular tissue (left panel, n=1), frozen human atrial tissue (middle panel, n=7) and fresh human atrial tissue (right panel, n=3). B, Comparison of TREK-1 and TRAAK expression in frozen atrial and ventricular tissue samples. Left panel; fresh human testicular tissue (n=1), middle panel; frozen human atrial tissue (n=7) and right panel; frozen ventricular tissues (n=5). C, Comparison of expression of TREK-1 and TRAAK in fresh human testicular tissue (left panel, n=1), 3-month-frozen human testicular tissue (middle panel, n=1) and fresh human atrial tissues (right panel, n=3).

3.3.5 REAL- TIME PCR IN HUMAN VENTRICULAR TISSUE

Five human ventricular tissue samples (males; age 40-50yr; described as a normal donor heart in physiological structures) were used in real-time PCR. Before use, these tissue samples had been stored for at least 24 months in liquid nitrogen. Relative to GAPDH expression, TREK-1 expression was 59 ± 15% (n = 5; Fig 24B) and TRAAK expression was 16 ± 4% (n =5; Fig 24B).

3.3.6 DEGRADATION OF TREK-1 AND TRAAK mRNA ON STORAGE

To investigate the possible effects of tissue storage on TREK-1 and TRAAK expression levels, two equal-weight samples from the same human testicle sample were used. The first was used immediately after excision in real-time PCR whereas the second was stored at -80°C for 3 months before being used in real-time PCR. The level of expression of TREK-1 in the frozen tissue sample fell noticeably, to 106% compared with 185% in the fresh sample, whereas that of TRAAK remained largely unchanged (34% compared to 29%; Fig 24C).

3.3.7 WESTERN BLOT

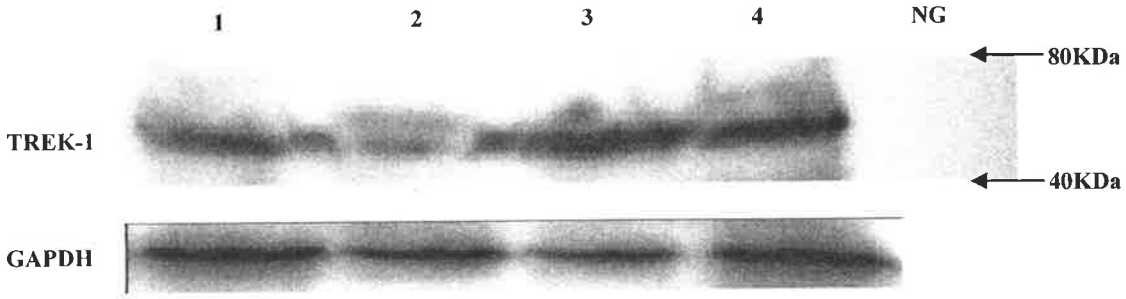

Figure 25. Western Blot analysis of human ventricular samples. 4 ventricular samples are selected from human donor group. GAPDH (36.6KDa) as positive control and TREK-1 (55KDa) are recognized by relative specific antibody. Botanic tissue is selected as negative control (NC). Sample concentration is 20μg/30μL; [primary Ab]$_{TREK-1}$=1:500; [secondary Ab]$_{TREK-1}$=1:1000; [primary Ab]$_{GAPDH}$=1:1000; [secondary Ab]$_{GAPDH}$=1:2000.

Western blot (Fig 25) showed the specific immunoreactivity of GAPDH (positive control) and TREK-1 in human ventricular tissue. TREK-1, 55KDa band, was demonstrated in 4 human ventricle samples used in real-time PCR, which was the same as TREK-1 control picture provided by Alomone Company. The result of Western blot was identical with TREK-1 PCR results in human ventricle.

3.3.8 IMMUNOHISTOCHEMISTRY

Due to the importance of the localization of TREK-1 for analysing the roles of TREK-1 in human cardiomyocytes. Dr. Shiyong Yuan has authorized me to show his results in Appendix.

3.4 Discussion

3.4.1 PRIMER DESIGN

Specificity of Sense Primer (SP) and AntiSense Primer (ASP) was essential to obtain a desired PCR product. Therefore primer design became critical to investigate the expression of TREK-1 in the human heart. However, in this project, we did not know whether or not any of TREK-1, 2 and TRAAK existed in the human heart, and also if they were found in the human heart, what percentage of sequence homogeneity would exist between human heart and central nervous system. Within RNA extraction, it was not possible to prevent genomic DNA contamination completely. Therefore, the distance between SP and ASP was a practical method to test against genomic DNA contamination. Due to the low synthesis rate of DNA polymerase and the size of the introns between SP and SP, a PCR product was only obtained from mRNA.

We applied the whole coding area sequence in primer design. We tried to find a SP around 200bps ahead of 1st-Pore Domain, an ASP between two pores' structure, and one ASP in a range of 200bps behind 2nd-Pore Domain. If the designed primers were specific to the sequences of TREK-1 and TRAAK in human heart, at least one pore coding segment was expressed in sequencing result. For TREK-1, the distance between SP and ASP was at least 20 thousand bp, and the rate of DNA polymerase was 1000bp/min. This prevented the production of genomic DNA contamination completely in relative PCR products. Due to no more than 1300bp of the maximal

distance between each exon in TRAAK, it was difficult to prevent genomic DNA contamination. However if the size of designed PCR product was much lower than 1000bp, it was possible to recognize and separate individual band on the gel for sequencing.

3.4.2 DATA ANALYSIS

Tissue distribution studies have shown TREK-1 to be expressed at high levels in the brain and, at somewhat lower levels, in a variety of peripheral tissues. As yet, no clear role has yet been ascribed to TREK-1 in any these tissues. Nevertheless, it has been the subject of intense research. The possible roles of TREK-1 in the heart have been neglected, since no data of TREK-1 expression in human heart have been reported to date. However, since TREK-1 is sensitive to mechanical stresses, it is reasonable to suppose that it would play an important role in the modulation of electrical activity in organs and tissues subjected to mechanical forces. Certainly, the heart is subjected to constantly varying mechanical forces and there is now a large body of evidence to show that these forces can alter the electrical properties of the myocardium. For example, in animals rapid stretch of the ventricles can produce either rapid depolarisations or hyperpolarizations, depending on the timing (Zabel et al., 1996). Mechanosensitive channels which presumably give rise to these responses have been recorded directly in myocardial cells, one type of which is a potassium selective channel which has properties similar to those exhibited by channels formed when TREK-1 constructs are expressed in heterologous systems (Hu et al., 1996).

Similar electrophysiological responses to those in animals have been demonstrated in human heart (Eckardt et al., 2001). For example, in human atrium,

Calkins et al., (1992) noted that acute increases in atrial pressure induced by varying the atrioventricular interval shortened atrial refractoriness. In a similar human model, Klein et al., (1990) demonstrated that increases in right atrial pressure significantly attenuated (> 20 ms) atrial refractory periods. In human ventricle, Taggart et al, (1988) observed a progressive shortening of repolarization as left ventricular pressure and volume increased in patients during the process of weaning off cardiopulmonary bypass. In another group of patients undergoing cardiac surgery, Taggart et al., (1992) showed that action potential duration shortened during ventricular loading induced by aortic occlusion and returned to control values within 1 – 3 beats after release. A similar result was reported by Levine et al., (1988) in right ventricle during transient occlusion of the right ventricular outflow tract. It has been suggested that this shortening of the action potential by stretch plays an important role in protection from arrhythmias, which could otherwise arise because of heterogeneous action potential propagation velocities in the myocardium (Lab, 1999). The mechanism of such shortening of the action potential by stretch is a matter of dispute, but it is entirely consistent with our imminohistochemical results, in which most of TREK-1 was illustrated on the membrane of cardiomyocyte in both atrial and ventricular tissues. Hence, changes in the expression level of TREK-1, or modulation of the channel activity, may be very important in arrhythmias.

As noted above, TREK-1 and TRAAK also respond to a variety of other stimuli as well as stretch. For example, they are opened by arachidonic acid and by polyunsaturated fatty acids (Fink et al., 1998; Maingret et al., 1999; 2000; Kim, 1992). One of the primary events in cardiac ischaemia is the release of phospholipids from the cell membrane by activation of phospholipases (Mancuso et al., 2003).

Hence, TREK-1 may have a protective role in ischaemia, since its activation would shorten the action potential in a way similar to activation of K_{ATP} channels. In addition, it has been shown that TREK-1 is activated by intracellular acidosis: lowering intracellular pH shifts the pressure / activation relationship so that, at lower pH levels, TREK-1 is converted into a background channel (Maingret et al., 1999; Honoré et al., 2002). In ischaemia, this effect would be synergistic with the activation due to polyunsaturated fatty acids acting on the membrane of cardiomyocytes. These are parallel with the localization of TREK-1 on cardial myocytes by immunohistochemistry.

TREK-1 is also modulated by protein kinase A mediated phosphorylation, which closes the channel and it has been suggested that this protein kinase A dependent phosphorylation may induce a reversible conversion of the channel between a voltage-dependent and stretch-dependent form (Bockenhauer et al., 2001). Hence, it is possible that TREK-1 existing in human heart would be subject to complex and interacting modulation by hormonal, biochemical and physiological influences, with consequent effects on cardiac electrophysiology.

In these studies we used fresh atrial appendage from patients undergoing coronary bypass surgery, and, although they had been frozen, ventricular tissue samples, rather than a cDNA library sourced from a third party. Since it seems that TREK-1 mRNA may be preferentially degraded on storage, this may be part of the reason why we see substantial expression whereas the few publications on TREK-1 expression in heart have failed to do so. In addition, real-time PCR used for the quantification of TREK-1 is more sensitive than Northern blot techniques. Our

discoveries not only identify that TREK-1 channels are notably expressed on human cardiomyocyte membrane but also expose the altered quantification of TREK-1 in human ventricle and atrium. These observations may explore the roles of TREK-1 channels as a mechnosensor in stretch-induced arrhythmogenesis and cardiac hypertrophy.

Because of practical limitations, the ventricular samples were taken from various parts of the ventricle and it was not always possible to document the position (apex/base and epicardial/endocardial). We have previously shown that TREK-1 is differentially expressed across the ventricular wall in rats, and we assume that a similar heterogeneous distribution exists in humans. In this case, it is possible that some tissue samples are from areas of the ventricle with low expression. Similarly, the atrial appendage may not be the part of the atria expressing the highest levels of TREK-1.

The existence of TREK-1 and TRAAK in the human heart was confirmed by RT-PCR, sequencing, Western blot and Immunohistochemistry. Real-time PCR demonstrated that the expression of TREK-1 was higher than TRAAK in the human donor atrial and ventricular samples, which suggested that TREK-1 and TRAAK may play different roles in the regulation of cardiac physiology. Varying amounts of TREK-1 provided a reasonable explanation why the previous experiments did not discover the existence of TREK-1 and TRAAK in human heart (both atrium and ventricle).

CHAPTER 4

QUANTITATION OF TREK-1

IN

NORMAL AND PATHOLOGICAL

HUMAN HEART

4.1 INTRODUCTION

Since 2-Pore-4-Transmembrane domain (2-P-4-TD) potassium channels were first cloned in mice (Fink et al., 1996), they have been discovered in a wide variety of animals. In humans, 2P potassium channels are not only expressed in central nervous system but are also found in peripheral organs (Lesage and Lazdunski, 2000; Meadows et al., 2000; Medhurst et al., 2001). 2P potassium channels are members of the KCNK gene family that control background potassium conductance for regulating resting membrane potential and cell excitability (Lesage and Lazdunski, 2000; Patel and Honore, 2001). Similar arrangement of conserved amino acid sequence (T-x-G-x-G) was shown on the two-pore structure, which contributed to a typical K+-selectivity. Based on the unique physiological and pharmacological characteristics, TREK-1 (Twik-RElated K^+ channel; KCNK2), TREK-2 (KCNK10) and TRAAK (Twik-Related Arachidonic Acid-stimulated K^+ channel; KCNK4) were distinguished from other members of 2P potassium channels.

TREK-1, TREK-2 and TRAAK are sensitive to membrane stretch, pH, temperature and polyunsaturated fatty acids (Patel et al., 1998; Kim, 2003; Kang et al., 2005; Maingret et al., 1999; Patel and Honore, 2002). TREK-1 is also activated by lysophospholipids (Maingret et al., 2000; Han et al., 2003) and inhaled anaesthetics (Kindler et al., 1999; Patel et al., 1999). The functions of TREK-1 are regulated by neurotransmitters and receptor-dependent signalling mechanisms, for example, TREK-1 activity is enhanced by phosphorylating Ser-351 of C-terminus by a cGMP-activated protein kinase (PKG) (Koh et al., 2001); TREK-1 is inactivated by phosphorylating Ser-300 and Ser-333 of C-terminus by protein kinase A (PKA) and C (PKC) (Patel et al., 1998; Murbartian et al., 2005); The action of $G\alpha_s$-couple receptor

pathways preventing TREK-1 activity is similar to PKA (Patel et al., 1998; Koh et al., 2001) whereas inhibition of $G\alpha_q$-coupled receptors to TREK-1 is similar to PKC (Chemin et al., 2003; 2005; Lopes et al., 2005). TREK-1 is also largely inhibited by prostaglandin E_2 (PGE_2) (Maingret et al., 2000). In addition, TREK-1 is notably insensitive to typical potassium channel inhibitors such as tetraethylammonium (TEA), 4-aminopyridine (4-AP) and Ba^{2+} (Patel et al., 1998; Meadows et al., 2000; Lesage, 2003). Furthermore, TREK-1 is not inactivated by Gd^{3+} (Kim, 2003), which is not only a widely-applied blocker of stretch-activated channels (Hansen et al., 1991; Takagi et al., 1999) but also a potent inhibitor of L-type Ca^{2+} channels (Lacampagne et al., 1994). Recently, TREK-1 knockout mice demonstrate that polyunsaturated fatty acid-activated neuroprotection is weakened in ischemia and the sensitivity to volatile anaesthetics was reduced (Heurteaux et al., 2004).

Despite the fact that TREK-1 expression is shown in many kinds of human tissues and organs (Lesage and Lazdunski, 2000), especially in brain (Meadows et al., 2000; Medhurst et al., 2001), at present TREK-1 has not been demonstrated in human heart. With TREK-1 expressed in cardiomyocytes of mice and rat (Fink et al., 1996; Aimond et al., 2000; Tan et al., 2004a; 2004b; Li et al., 2005) and TREK-1-like potassium currents found in human atrial tissue (Terrenoire et al., 2001), these observations strongly indicated the existence of TREK-1 in human heart. This study applied PCR, sequencing, real-time PCR, Western blot and immunohistochemistry to investigate the expression, localization and quantification of TREK-1 in normal and diseased human heart and likely functions of TREK-1 in human heart under different physiological and pathological conditions.

4.2 MATERIALS AND METHODS

The procedures and materials of Real-time PCR and Western Blot were the same as described in Chapter 2. Normal and pathological human ventricular samples were obtained from Prof. Cris dos Remedios under the rules of The University of Adelaide Ethics Committee and The University of Sydney Ethics Committee.

TABLE 12 DETAILS OF NORMAL AND PATHOLOGICAL HUMAN VENTRICULAR SAMPLES

NUMBER	DATE OF BIOPSIS	S/A	SAMPLE CODE	DISEASE
1	5/05/1997	M/44	2-149	DONOR
2	24/07/1997	M/23	2-152	DONOR
3	23/11/1997	F/45	3-007	IC
4	20/04/1999	M/59	3-037	IDC
5	9/08/2000	M/61	3-071	IC
6	11/08/2000	F/41	3-073	DONOR
7	14/08/2001	F/49	3-104	IDC
8	8/11/2001	M/52	3-106	IC
9	30/11/2001	M/43	3-107	IDC
10	27/12/2001	M/08	3-109	DONOR
11	17/01/2002	M/43	3-111	IDC
12	25/03/2002	M/61	3-117	VALVULAR DISEASE
13	18/04/2002	M/46	3-123	IC
14	25/05/2002	F/51	3-131	DONOR
15	14/08/2002	F/51	3-131	DONOR
16	19/10/2002	M/26	3-135	DONOR
17	17/11/2002	M/52	3-141	DONOR
18	1/04/2003	M/21	3-160	DONOR
19	5/05/2003	M/61	3-164	DONOR
20	20/09/2003	M/54	4-007	IDC
21	4-017	M/51	4-017	IDC
22	25/05/2004	M/53	4-068	IDC
23	21/09/1998	F/41	3-027	IC
24	09/01/2003	M/59	3-151	IC
25	18/05/2001	M/52	3-101	IC
26	07/07/2001	M/44	3-103	IC

Donor ventricular samples (n=10) were those in which no cardiac disease history was described. Pathological samples were divided into 3 groups, which included IC (Ischemic Cardiomyopathy; n=8), IDC (Idiopathic Dilated Cardiomyopathy; n=7) and valvular disease (n=1).

Tissue - Human atrial tissue samples (right atrial appendage) were obtained from patients undergoing coronary bypass surgery. The samples used in these experiments were from patients with no underlying disease other than coronary artery disease. Atrial tissue samples were frozen in liquid nitrogen within one hour of being excised and then stored at –80°C. Human ventricular tissue samples were obtained from explanted hearts from the transplant program at St Vincent's Hospital, Sydney. Hearts had been maintained in liquid nitrogen for various times since being explanted. Positive control was human testicular tissue, frozen less than one hour after excision from a patient undergoing orchidectomy for prostate cancer in which the testicular tissue was normal in histology.

RNA Extraction - Total RNA was isolated from human atrial, ventricular and testicle tissues with either TRI-Reagent (SIGMA-ALDRICH, Australia) or RNA kit (BIO-RAD, Sydney, Australia). TRI-Reagent-treated RNA isolation was used to prepare cDNA for normal PCR, whereas BIO-RAD-treated RNA extraction was used to prepare cDNA for real-time PCR. Reverse transcriptase was from Invitrogen, (Australia). SYBR Green real-time PCR reagent was from BIO-RAD (Australia) and Applied Biosystems (US). The quantity of RNA in all the samples was detected by spectrophotometer (Eppendorf, Australia), and the same amount of RNA (370ng) from each sample was used in PCR and real-time PCR.

Primer Design - Primers were designed from published human sequences (GeneBank codes AF171068 for TREK-1) using Primer Express software (PE Applied Biosystems, Foster city, CA, USA). Initial PCR was performed for TREK-1 in human samples and was then followed by nested PCR to confirm the homology between

PCR products and the published sequences. The products were sequenced and real-time PCR performed to quantify the expression of TREK-1 in normal and diseased human hearts, relative to the expression level of GAPDH. Primers for TREK-1 and GAPDH were shown on Table12.

TABLE 13. Primer sequences

Primers of TREK-1 and GAPDH applied in PCR and real-time PCR			
	Sense Primer (5' - 3')	Antisense Primer (3' - 5')	Size
TREK-1	GCTGTCCTGAGCATGATTGGA	CCCGCTGGAACTTGTCATAAA	169bp
GAPDH	ATGGAAATCCCATCACCATCTT	GGTGCAGGAGGCATTGCT	252bp

PCR and Real-time PCR processes - PCR products were separated in 1.2% agarose gel and visualised with Gel documentation system from BIO-RAD (Sydney, Australia). Bands cut from the gels were cleaned by UltraClean Kit (MO BIO Laboratories, CA, US) and the product of nested PCR was purified by ExoSAP-IT (USB corporation, Cleveland, Ohio, US). For real-time PCR, 25μL reaction solution includes 12.5μL SYBR Green PCR Master Mixer, 5.5μL cDNA, 1μL of sense primer (10μM), 1μL of antisense primer (10μM), and 5μL of molecular-level water. Real-time PCR assay was performed in 96-well optical plates on an ABI Prism 5700 Sequence Detection System (PE Applied Biosystems, Forster city, CA, US). The process of real-time PCR was 1 cycle of 95^0C for 10min, and then 40 cycles of 60^0C for 1min and 95^0C for 15s. The data from real-time PCR was analysed in Sigmaplot (12.01 Version, SPSS, Richmond, CA, US).

Western Blot – normal and diseased human ventricular tissues stored below -80°C were homogenized in buffer solution (50mM Tris (pH=8), 150mM NaCl, 1mM Na Vanadate, 10mM NaF, 0.6% Triton) at room temperature. Concentration of protein was measured by spectrophotometer (Eppendorf, Australia) using colorimetric method (BIO-RAD, Australia). The same amount of protein from each sample with loading buffer (0.5M Tris-HCl (pH 6.8), 40% (v/v) glycerol, 20% SDS, 0.5% (w/v) Bromophenol Blue dye, 5% (v/v) β-mercaptoethanol) was denatured at 95^0C for 5min and run on a SDS-PAGE mini-gel (10% acrylamide). After fractionation, the samples were transferred to a nitrocellulose membrane. The membrane was blocked with non-fat milk solution (Bio-Rad, Australia) and probed with anti-TREK-1 antibody (1:500, Alomone, Israel) and HRP-Anti-Rabbit antibody (1:1000, Adelaide University). Visualization of immunoreactivity was by ECL reagents (Sigma-Aldrich, Australia). Exposure time for all samples in western blot was kept the same. Images on X-ray Film (Amersham) were analysed by Gel Dock System (Bio-Rad, Australia).

Normal and diseased human ventricular samples applied in real-time PCR and Western blot were in an age range of 40 to 60 years old. Analysis of all data was shown as mean ± standard error and statistical comparison by T-test.

4.3 Results

4.3.1 PCR OF TREK-1 IN HUMAN NORMAL AND DISEASED HEART

RT-PCR was used to demonstrate the existence of TREK-1 in normal human atrial and ventricular samples (Fig 27). Human testicles were selected as positive control. Single band of TREK-1 and GAPDH with predicted size (169bp and 252bp, respectively) was detected in human heart and testicles whereas no other bands were

shown on the Agarose gel (1.2%). PCR results confirmed that genomic DNA contamination was prevented and the primers of TREK-1 and GAPDH were specific and valid to be used in real-time PCR.

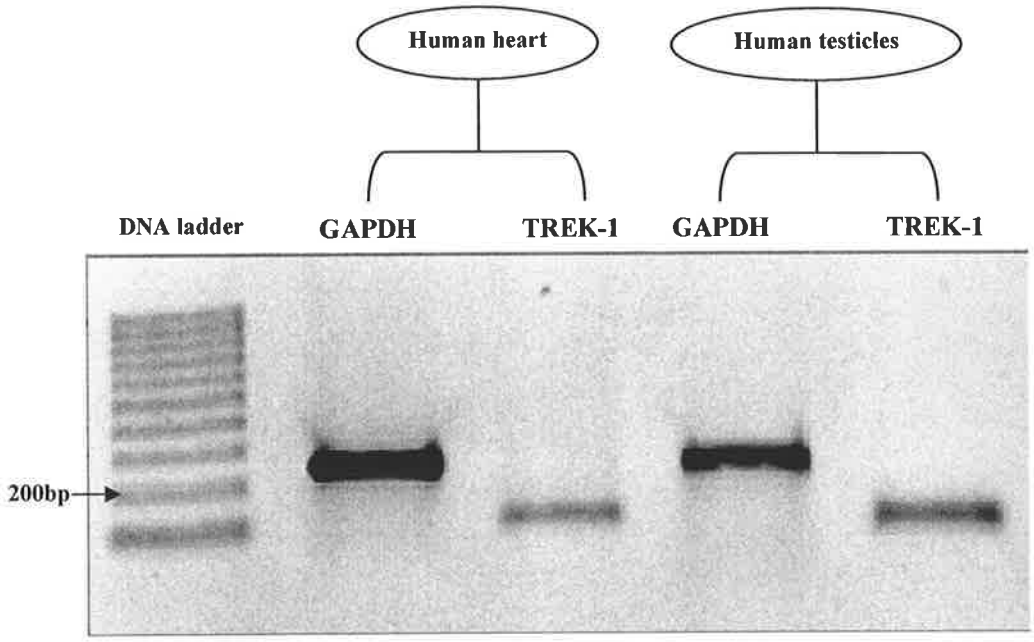

Figure 27. PCR results of real-time primer. Human testicle tissue is selected as positive control.

4.3.2 WESTERN OF TREK-1 IN HUMAN NORMAL AND DISEASED HEART

Western blot was used to investigate the expression of TREK-1 at the protein level in human normal ventricular samples (Donor; n=4), human idiopathic dilated cardiomyopathy (IDC; n=7) and human ischemic cardiomyopathy (IC; n=7). The supernatant of each sample used in Western blot was at 20μg/30μL. GAPDH was used as a housekeeping gene to ensure the validity of protein extraction of all samples. TREK-1 (56KDa) and GAPDH (37KDa) were recognized by specific antibodies (Alomone and Geneworks, respectively; Fig. 28A). No band was shown in negative control applied with the same concentration of TREK-1 antibody. Protein levels of

TREK-1 expressed in IDC (Fig. 28B) and IC (Fig. 28C) were remarkably higher than that in Donor group.

A:

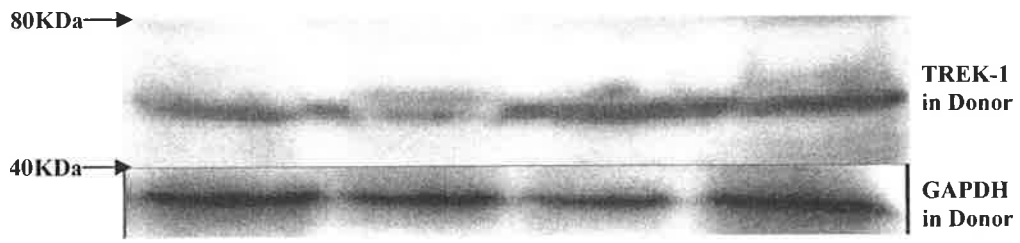

B:

C:

Figure 28. Western blot of TREK-1 and GAPDH in human donor, IDC and IC groups. A: TREK-1 (55KDa) and GAPDH (37KDa) as positive control are identified by specific antibodies from normal human ventricular samples (n=4). [Supernatant concentration]=20μg/30μL. [Primary Ab] =1:500; [Secondary Ab] =1:1000; B and C: TREK-1 and GAPDH were expressed in idiopathic dilated cardiopathy samples (n=7) and ischemia cardiopathy samples (n=7). [Supernatant concentration]=20μg/30μL. [primary Ab]$_{TREK-1}$=1:500; [secondary Ab]$_{TREK-1}$=1:1000; [primary Ab]$_{GAPDH}$=1:1000; [secondary Ab]$_{GAPDH}$=1:2000.

4.3.3 QUANTIFICATION OF TREK-1 IN NORMAL AND DISEASED HUMAN VENTRICLES

Real-time PCR showed that there were significant differences in the expression level of TREK-1/GAPDH in Donor, IDC and IC samples. The quantity of TREK-1 in IDC (0.44±11.47%; n=7) was 5 times to that of Donor group (0.08±1.56%; n=4) whereas TREK-1 in IC (0.23±7.96%; n=7) was 3 times to that of Donor group (P≤0.001; Fig. 30A). Protein level of TREK-1 was parallel with real-time PCR results. Intensity of TREK-1 protein in IDC (1.82±14.26%; n=7) was 2.2 times to that of TREK-1 in Donor group (0.84±7.46%; n=4) whereas TREK-1 in IC (1.51±10.44%; n=7) was 1.78 times to that of TREK-1 in donor group (P≤0.00028; Fig. 30B). Real-time PCR and Western blot made it clear that TREK-1 was expressed at higher levels in diseased human ventricles with respect to normal human hearts.

A:

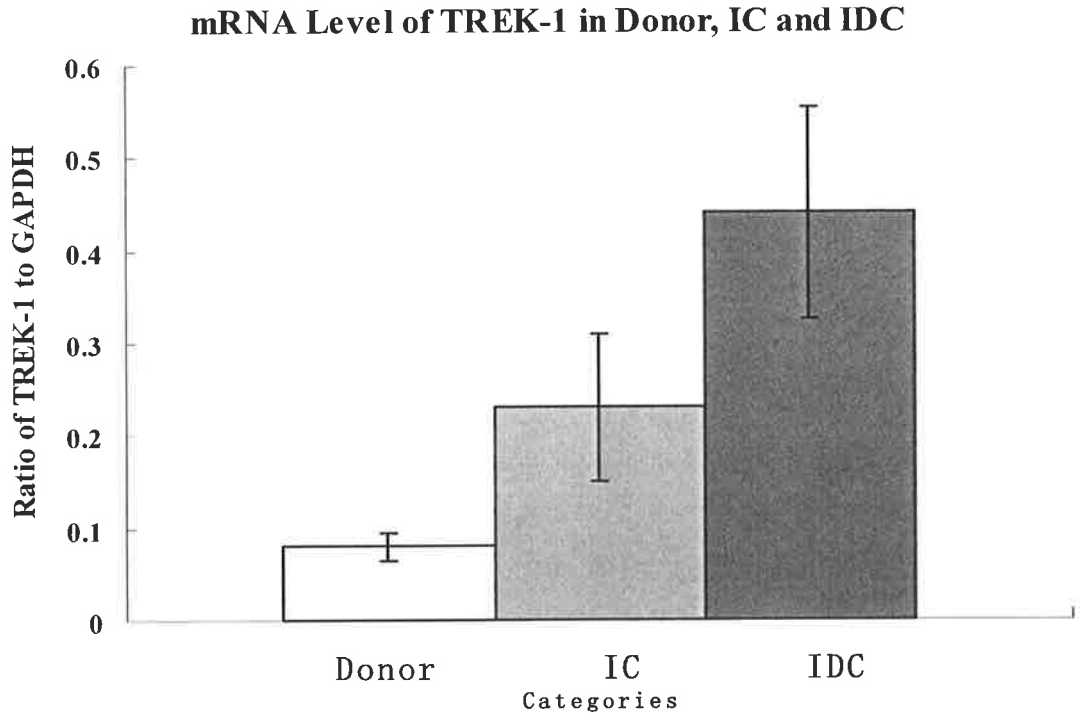

B:

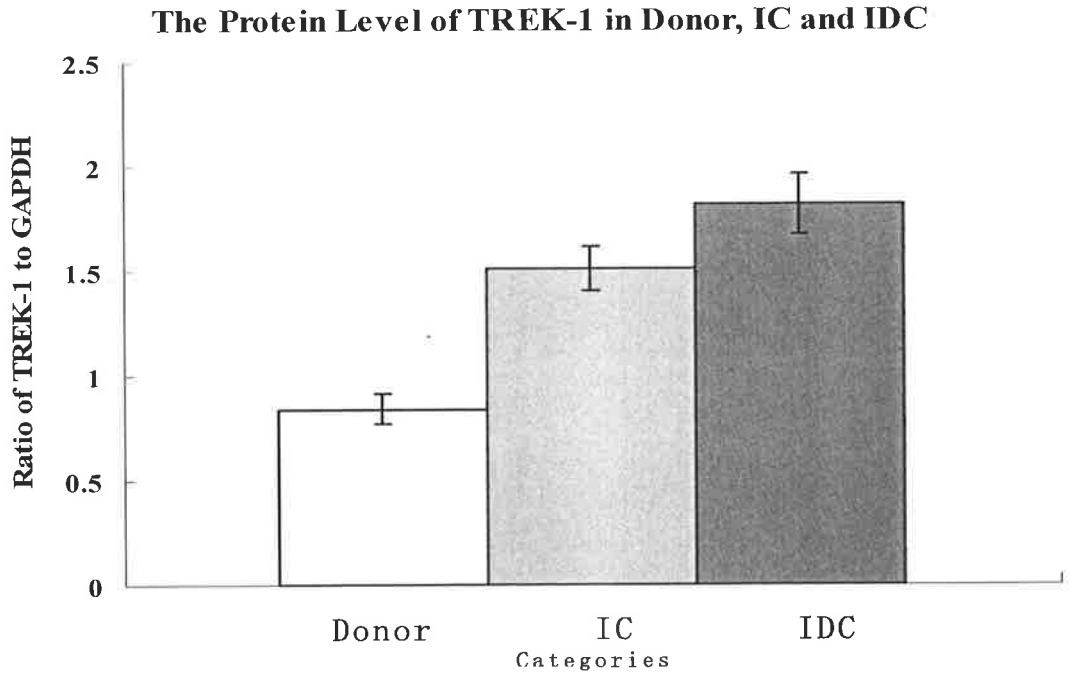

Figure 29. The expression of TREK-1 in Donor, IC and IDC at mRNA and protein levels. A: summary data of real-time PCR of TREK-1 in Donor, IC and IDC; B: data collection of Western blots of TREK-1 in Donor, IC and IDC, in which density ratio of TREK-1 and GAPDH obtained by Gel Dock System is used to represent the amount of TREK-1 protein in each group. Mean values of TREK-1 protein in IDC and IC are compared with those in Donor.

4.4 DISCUSSION

Stretch-induced arrhythmia depending on the activation of stretch-activated channels (SACs) has been shown in heart (Franz et al., 1992; Zabel et al., 1996; Janse et al., 2003). Recently, the studies has shown that stretch of isolated cardiac myocytes increases the occurrence of pacemaker-like afterdeploarizations (Ravens, 2003; Kamkin et al., 2000; Isenberg et al., 2003) whereas stretch in isolated hearts produces premature beats and ventricular arrhythmia. Many reviews conclude that non-selective cation SAC and potassium-specific SAC in heart contribute to the production of most of the above phenomena (Zeng et al., 2000; Kamkin et al., 2000; Kim, 1992; Niu et al., 2003; Isenberg et al., 2003). In a study of SAC-activated 2-D ventricular models, Garny and Kohl (2004) demonstrated that non-selective cation

SAC may trigger sudden arrhythmia whereas K^+-specific SAC was essential for the development and maintenance of ventricular arrhythmia. In 3-D ventricle models of rabbit, Li et al., (2004) showed that K^+-specific SAC, maintained ventricular arrhythmia triggered by non-selective cation SAC. Garan et al., (2005) confirmed Garny's and Li's speculations, where Garan showed that streptomycin, a blocker of non-selective cation SAC (Eckardt et al., 2000; Salmon et al., 1997), did not prevent the production of sustained ventricular arrhythmia stimulated by altering mechanical loadings in porcine models.

These observations are entirely consistent with our results, in which TREK-1, a K^+-specific SAC, is expressed in human atrium and ventricle and is localized on cardiomyocyte membrane and arranged in longitudinal stripes along myocardium. These patterns are suitable for sensing and transferring stretch in cardiac muscle. In addition, our data show that the levels of cDNA and protein of TREK-1 expressed in IDC were obviously higher than those of normal human ventricles. Overexpression of TREK-1 in IDC is, at least in part, matching the description of tachycardiomyopathy model, a subtype of IDC (Shinbane et al., 1997), where the changes of hemodynamics may induce sustained supraventricular arrhythmia by stretch based on TREK-1-sensitive cardiac remodelling.

Altering mechanical loading on cardiac muscle results in the activation of a number of immediate-early (IE) genes and cardiac hypertrophy *in vivo* and *in vitro* (Sadoshima et al., 1992a). Stretch of cultivated cardiac cells on a deformable silicon membrane enhanced protein synthesis independent of exogenous neurohormonal factors (Vandenburgh and Kaufman, 1979; Mann et al., 1989; Komuro et al., 1990).

Recently, The studies show that mechanical stretch activates intracellular multi-signal transduction systems in neonatal cardiac myocytes, which are directly or indirectly involved in cardiac hypertrophy (Rozich et al., 1995; Komuro et al., 1996; Yamazaki et al., 1993). Mechanical stretch has become the most essential activator in the development of cardiac hypertrophy (Cooper et al., 1985; Komuro et al., 1990; Sadoshima et al., 1993).

However, it is not clear how stretch is translated into biochemical signals to release hypertrophy-related factors and activate protein kinase cascades. Sadoshima et al., (1992b) demonstrated that [Gd^{3+}] block of non-selective cation SAC did not prevent stretch-induced expression of IE genes and the enhancement of protein synthesis. Stretch may activate TREK-1 on the surface of cardiomyocytes, which transfers the effects of stretch to the nuclei by integrating with cytoskeleton transduction systems or the subunits of other growth factors. Overexpression of TREK-1 by IE genes in IC and IDC may produce a positive feedback where being more dilated causes the myocardium to be more sensitive to mechanical stretch that activates TREK-1-mediated ventricular tachycardia and fibrillation. The activation of p38MAPK and p42/44 MAPK (Mitogen-Activated Protein Kinase) pathway, which is one of the most important protein kinase cascades in cardiac hypertrophy, results in opening TREK-1 in rat cardiomyocytes (Aimond et al., 2000). It may explain the occurrence of idiopathic ventricular arrhythmia in the development of cardiac hypertrophy, IC and IDC without the involvement of stretch.

In rat model, Li et al., (2006) confirmed that TREK-1 not only played an important role in the production of arrhythmia but was involved also in the length-

dependent regulation of contractile force of myocardium. Furthermore, Gd^{3+} neither blocks stretch-induced SAC-mediated phosphorylation of JAK (Janus Kinase)/STAT (Signal Transducers and Activators of Transcription) pathway nor prevents the increase of stretch-induced SAC-dependant IP_3 in rat and mouse ventricle (Pan et al., 1999). Alternatively, TREK-1 may play protective roles in IC. The function of TREK-1 in heart ischemia may be similar as in brain ischemia where endogenous arachidonic acid release and intracellular pH falling in cardiac myocytes around ischemic regions contributes to opening TREK-1 in diastolic repolarization and the following hyperpolarization decreases intracellular $[Ca^{2+}]$ and reduces excitotoxicity (Patel and Honore, 2001; Honore et al., 2002; Buckler and Honore, 2005).

The different levels of TREK-1 expressed in normal, IC and IDC groups and the possible functions of TREK-1 reinforce the importance of TREK-1 in the generation of arrhythmia, cardiac remodelling and cardiac hypertrophy. It is postulated that TREK-1 may be a practical target for clinically relevant applications.

CHAPTER 5

EXPRESSION OF TREK-2

IN

NORMAL AND DISEASED HUMAN

HEART

5.1 INTRODUCTION

Although they share similar functional properties, including mechanosensitivity and activation by polyunsaturated fatty acids (Maingret et al., 2000), and 78% sequence homology, TREK-1 and TREK-2 have different distribution in human CNS and peripheral tissues (Medhurst, et al., 2001). This suggests that TREK-1 and TREK-2 play different roles in the regulation of cell excitation in different areas of the brain even though what these roles may be is still unclear.

While no splice variants of TREK-1 have yet been described, 3 splice variants have been identified for TREK-2; Variant A (Va) (Genebank AF279098) (Lesage et al., 1996), Variant B (AF385399) (Vb) and Variant C (AF385400) (Vc) (Gu et al., 2002). The coding areas of Va, Vb and Vc encode 539, 544 and 544 amino acids respectively. TREK-2 has 7 exons (as does TREK-1), and the splice variants arise because of altered sequences in the first exon.

However, distribution of TREK-2 in human tissues is different from TREK-1 and TRAAK. Va, a splicing variant of TREK-2 found by Lesage et al., (2000) (Fig. 30), is mainly expressed in kidney and pancreas, and also TREK-2 is found in testis, colon, small intestine and brain. No TREK-2 has been shown in human heart.

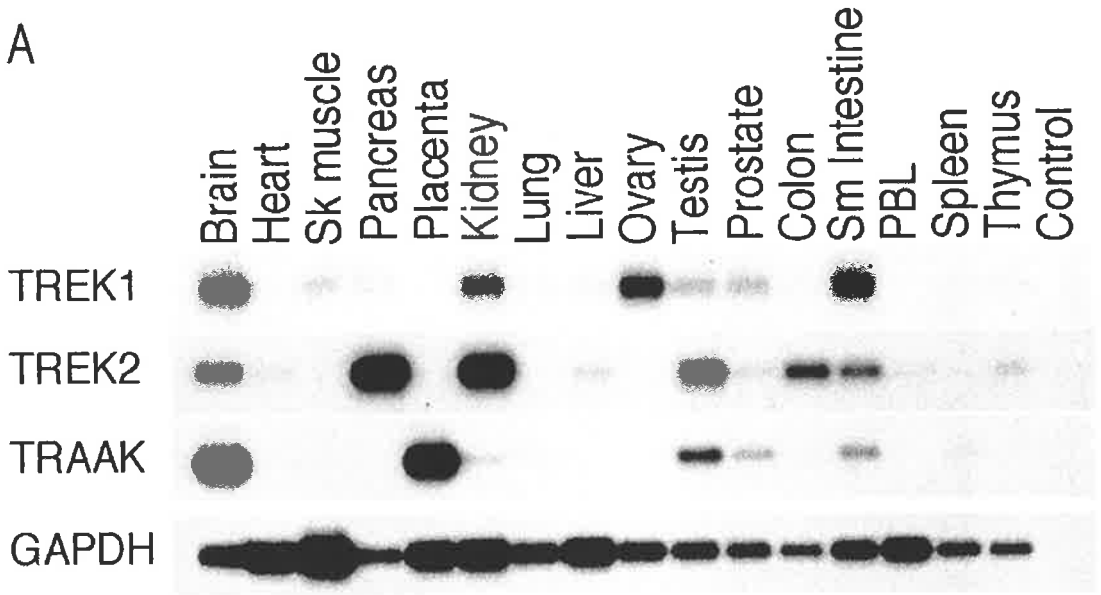

Figure 30. Southern blot of TREK and TRAAK in human cDNA library, Lesage et al., (2000).

Gu et al., (2002) demonstrated that two typical splicing variants of TREK-2, TREK-2b and TREK-2c, were expressed in human embryonic kidney 293 cell lines. TREK-2b (Vb) and TREK-2c (Vc) show similar single channel properties whereas Vb and Vc exhibit the different sensitivities to PKC and PKA. Gu et al., (2002) showed that Vb was largely expressed in kidney and pancreas whereas Vc was mainly expressed in brain. No Vb or Vc is shown in human heart (Fig. 31).

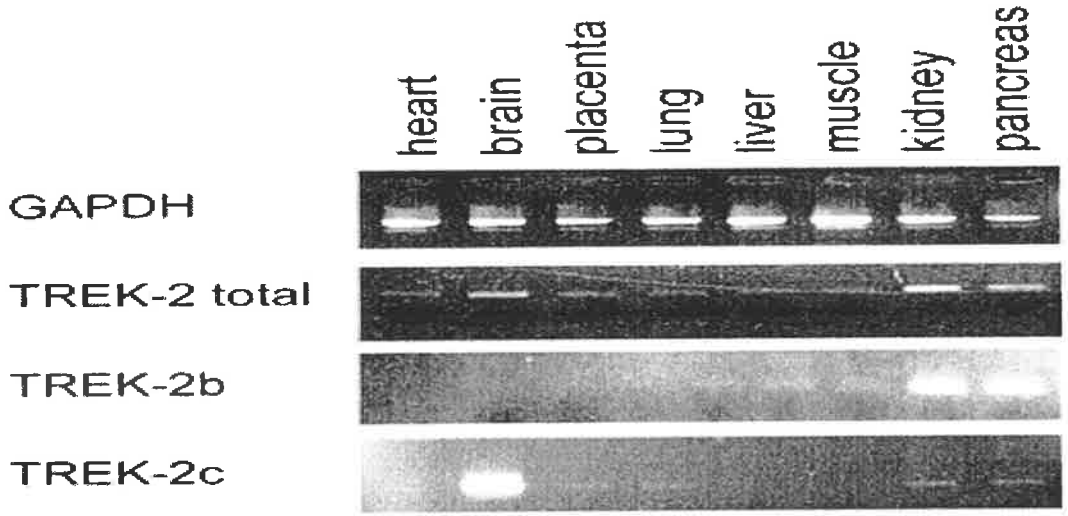

Figure 31. mRNA of TREK-2 is hybridized with human cDNA library, Gu et al., (2002).

Va, Vb and Vc are classified as AF279098, AF385399, and AF385400 respectively in Genebank. There are 7 exons in Va, Vb and Vc. All the exons are identical except for exon1 and exon7. Coding areas of Va, Vb and Vc encode 539AA, 544AA and 544AA individually. More details are shown in the following diagrams (Table. 14).

TABLE 14. SEQUENCE DETAILS OF THREE SPLICING VARIANTS OF TREK-2

Exon size (bp)	TREK-2a (AF279890)	TREK-2b (AF385399)	TREK-2c (AF385400)
Exon 1	509	175	257
Exon 2	350	350	350
Exon 3	118	118	118
Exon 4	161	161	161
Exon 5	187	187	187
Exon 6	143	143	143
Exon 7	1254	1251	1247
Intron size (bp)	**TREK-2a (AF279890)**	**TREK-2b (AF385399)**	**TREK-2c (AF385400)**
$Intron_{1-2}$	62868	62868	62868
$Intron_{2-3}$	22382	22382	22382
$Intron_{3-4}$	13168	13168	13168
$Intron_{4-5}$	34965	34965	34965
$Intron_{5-6}$	4115	4115	4115
$Intron_{6-7}$	1812	1812	1812

In this study, we show that the splice variants of TREK-2 Va and Vc, but not Vb, are expressed in human atrial and ventricular tissues and that TREK-2 channels are located immunohistochemically in the myocytes in both tissues. The proportion of these two splice variants is altered in cardiac disease (ischaemic cardiomyopathy or idiopathic dilated cardiomyopathy) compared to donor hearts.

5.2 METHODS AND MATERIALS

All procedures reported here had the prior approval of the University of Adelaide Human ethics committee and the Royal Adelaide Hospital ethics committee.

Primer design: Sequences of three splice variants of TREK-2 in the human brain have been published in GeneBank (www.ncbi.nlm.nih.gov): access numbers AF279890 (Va), AF385399 (Vb), and AF385400 (Vc). Primers were designed to be specific for each of these variants by Primer Express software (PE Applied Biosystems, Foster city, CA, USA). All primers were purchased from Geneworks (Geneworks, Adelaide, Australia).

Primers of Va for initial PCR in human testicular, atrial and ventricular tissues

Sense: CTGAAGCAATAGCCATGGAAGTT

Antisense: AGGCCAACAAGGATCCAAAA

Primers of Vb for initial PCR in human testicular, atrial and ventricular tissues

Sense: TTGGTATATGGAGGATGGATTTAAGG

Antisense: AGGCCAACAAGGATCCAAAA

Primers of Vc for PCR in human testicular tissue

Sense: CCAATCGAGACGCCAAGAAA

Antisense: CAGGGATCGTCACAAACACAA

Primers of Vc for PCR in human atrial and ventricular tissues

Sense: GGGCAACGAAGCAATGAAAT

Antisense: AGGCCAACAAGGATCCAAAA

Primers of three variants of TREK-2 for nested PCR

Sense: TTGGAGCAGCCCTTTGAGA

Antisense: CAGTGCTCGGAGCAATATTCC

Note that the specificity of the primers for each of the variants relies on the sequence differences in the first exon.

Preparation of mRNA, cDNA, PCR: Fresh human right atrial appendages were obtained from patients undergoing coronary bypass surgery. These patients had no other cardiac disease. Frozen human ventricular tissues were obtained from either transplant donor heart or from explanted hearts with diagnoses of ischaemic cardiomyopathy (IC) or idiopathic dilated cardiomyopathy (IDC). Since all three splice variants of TREK-2 have been reported in human testis tissue, positive control was human testicular tissue from a patient undergoing orchdectomy for prostatic cancer. This tissue was histologically normal. The quantity of mRNA in each sample was detected by spectrophotometer (Eppindorf, Australia). 370ng mRNA was applied in PCR. Fresh tissues were frozen in liquid nitrogen and then stored at -80°C until RNA extraction. Total RNA isolation from human atrial, ventricular and testicle tissues was done with TRI-Reagent (SIGMA-ALDRICH, Australia) and RNA kit (BIO-RAD, Sydney, Australia). TRI-Reagent-treated isolated RNA was used to prepare cDNA for initial PCR by two-step RT-PCR method. The PCR products were detected in 1.2% agarose gel and visualised by a Gel documentation system (BIO-RAD, Sydney, Australia). Selected bands were cleaned by UltraClean Kit (MO BIO Laboratories, CA, US) and used for nested PCR, with the nested PCR product being purified by ExoSAP-IT (USB corporation, Cleveland, Ohio, US), and sequenced.

Preparation of Western Blot experiments: is the same as described in Chapter 4.

5.3 RESULTS

5.3.1 EXPRESSION OF THREE SPLICING VARIANTS OF TREK-2 IN HUMAN TESTICLE AND HEART BY PCR

Sense primers for Va, Vb and Vc were designed from unique sequences in exon 1of each variant. Fig. 32A shows that, although other non-specific PCR products were present, one theoretical-size band was found for each of Va, Vb and Vc in human testis. The predicted-size bands were cut from the gel and used for nested PCR. A single 255bp band was expressed for variants Va, Vb and Vc (Fig. 32B). For human heart tissue Fig. 33A and B showed similar PCR results in atrial and ventricular tissue as those in testis, except that variant Vb was not detected. The existence of Va and Vc in human atrial and ventricular tissues was verified by nested PCR (Fig. 33C). Four 255bp-bands were cut sequenced. BLAST analysis showed that the sequencing results were 100% homologous to AF279098 and AF385400.

A:

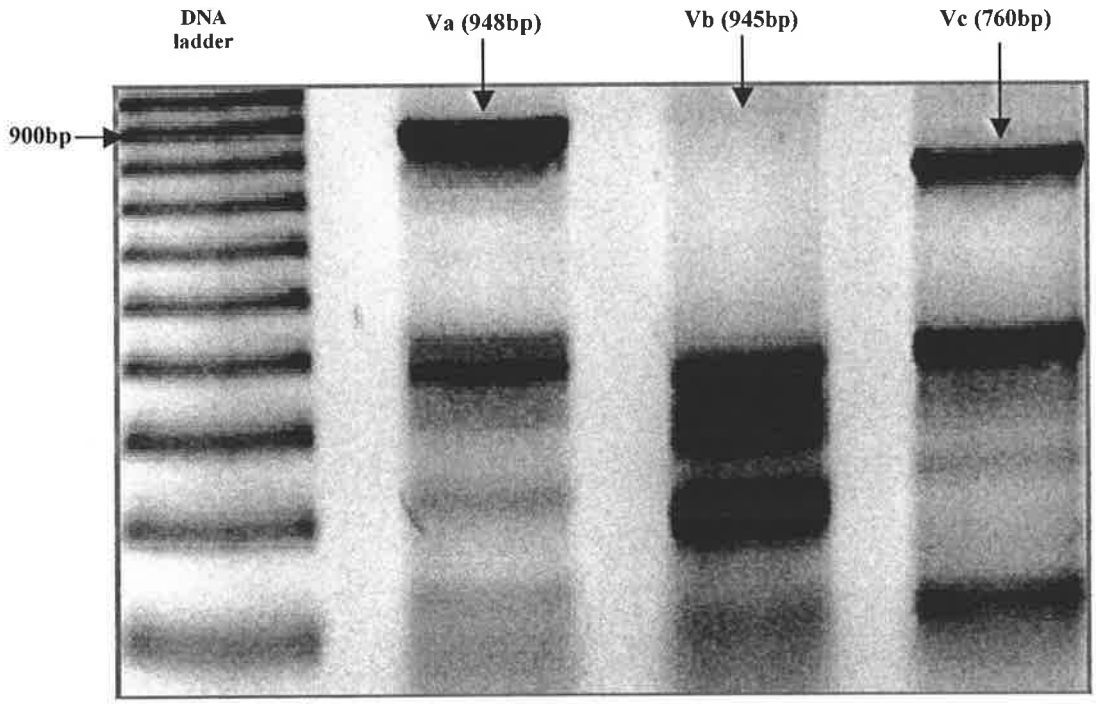

B:

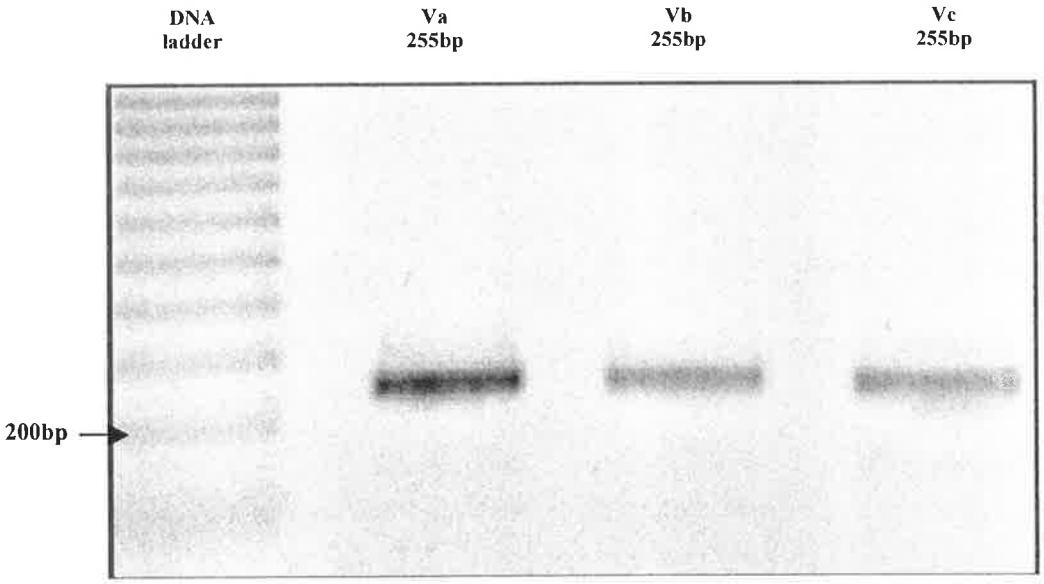

Figure32. PCR and nested PCR of Va, Vb and Vc in human testicular tissue. A shows that one predicted size band was expressed by PCR for Va, Vb and Vc. (sizes were 948bp, 945bp and 760bp respectively). B shows nested PCR results for Va, Vb and Vc. One single-optimal band (255bp) was present in PCR products of Va, Vb and Vc.

A:

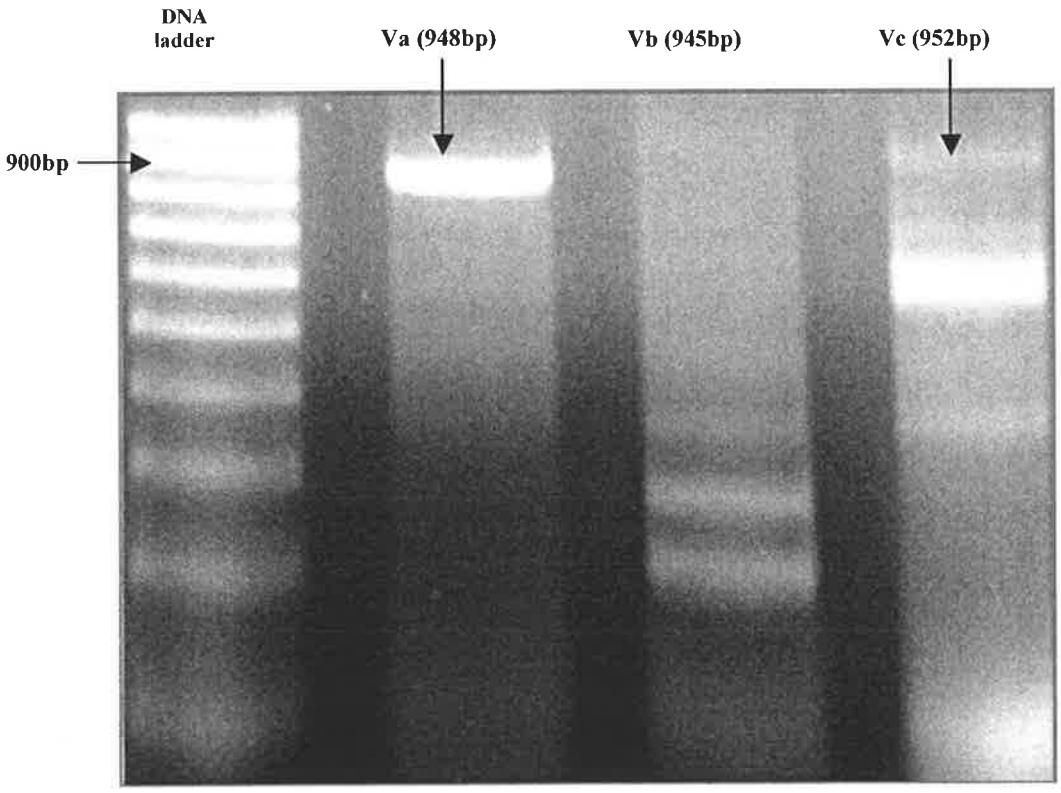

B:

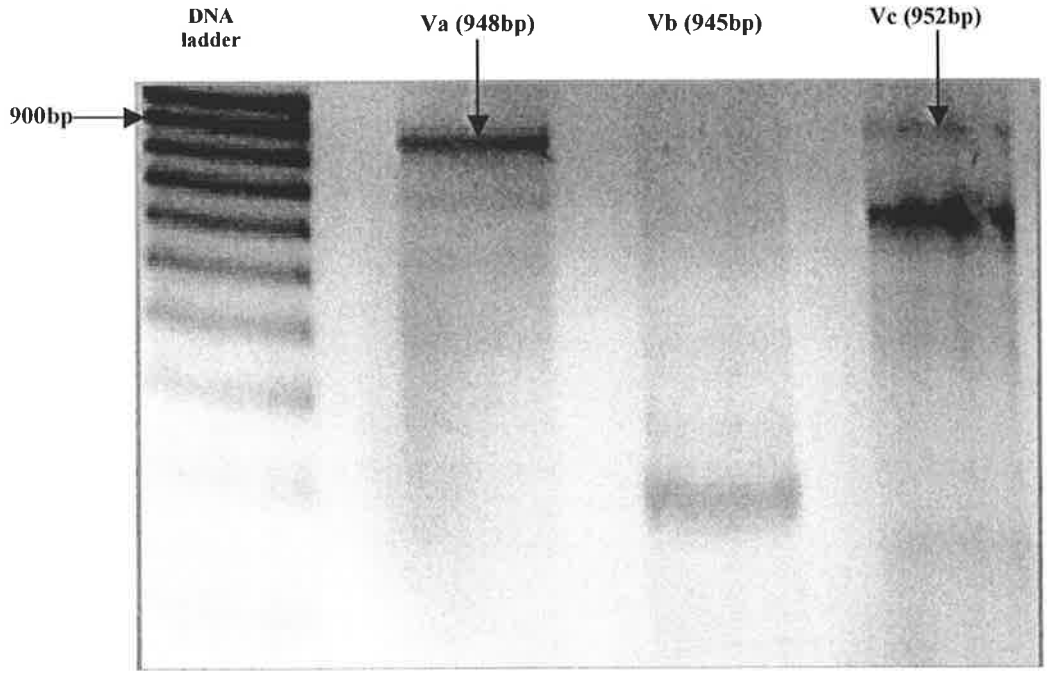

C:

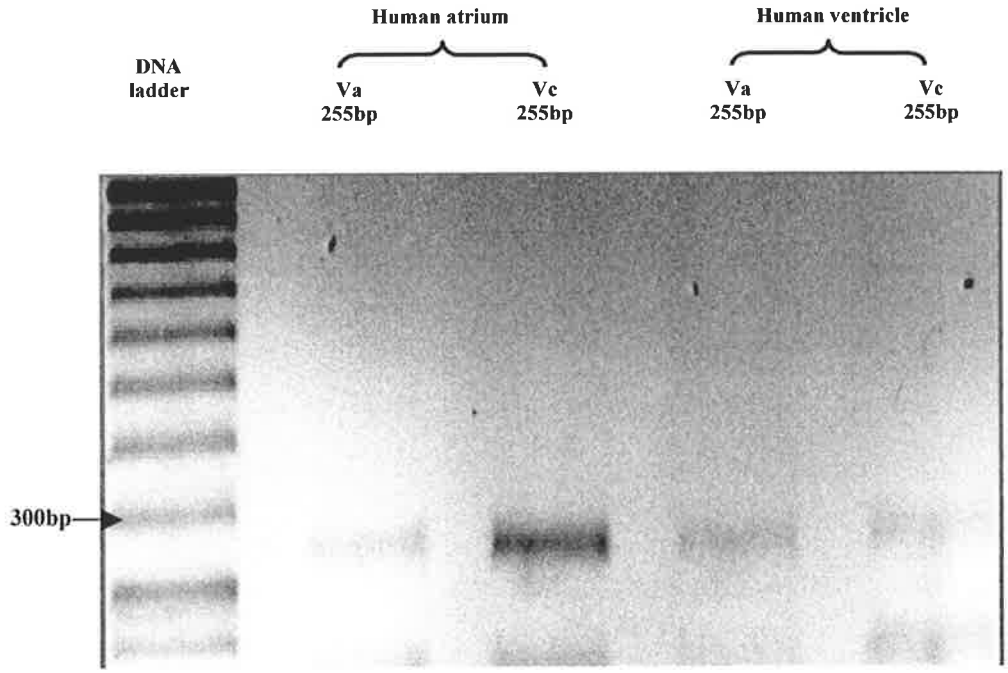

Figure33. PCR and nested PCR of Va, Vb and Vc in human atrial and ventricular tissues. A illustrates PCR products for Va, Vb and Vc in human atrial tissue. A 948bp-product of Va and a 952bp-product of Vc PCR were expressed in human atrial tissue. No Vb expression could be detected. B: PCR products for human ventricular tissue. Similar to atria, Va and Vc variants were detected, but no Vb. Nested PCR results of Va and Vc were shown in C. A single 255bp band occurred in Va and Vc PCR products from human atrial and ventricular tissue.

5.3.2 SEQUENCE DATA

5′→CGAAACATCGCCTTGGAGAAGGCGGAATTCCTGCGGGATCATGTCT

GTGTGAGCCCCCAGGAGCTGGAGACGTTGATCCAGCATGCTCTTGATGCT

GACAATGCGGGAGTCAGTCCAATAGGAAACTCTTCCAACAACAGCAGCCA

CTGGGACCTCGGCAGTGCCTTTTTCTTTGCTGGAACTGTCATTACGACCAT
T I

AGGGTATGGGAATATTGCTCCGAGCACTGANNNNC←3′
G Y G

202-bp sequence obtained from nested PCR of variant A, which contains one pore structure (underlined- amino acid sequence T-I-G-Y-G) and was 100% homologous to the corresponding segment of AF279098 (749–1004).

5′→GGGATGGGCAACGAAGCAATGAAATTTCCAATCGAGACGCCAAG

AAAACAGGTGAACTGGGATCCTAAAGTGGCCGTTCCCGCAGCAGCACC

GGTGTGCCAGCCCAAGAGCGCACTAACGGGCAACCCCCGGCTCCGGCTCG

ATCCAACTCCGCGCCTGTCCATTTCCTCCCGAGCCACAGTGGTAGCCAGGA

TGGAAGGCACCTCCCAAGGGGGCTTGCAGACCGTCATGAAGTGGAAGACG

GTGGTTGCCATCTTTGTGGTTGTGGTGGTCTACCTTGTCACTGGCGGTCTT

GTCTTCCGGGCATTGGAGCAGCCCTTTGAGAGCAGCCAGAAGAATACCAT

CGCCTTGGAGAAGGCGGAATTCCTGCGGGATCATGTCTGTGTGAGCCCCC

AGGAGCTGGAGACGTTGATCCAGCATGCTCTANNNNNNNN←3′

426-bp sequence obtained from nested PCR of variant C, which covers 70-bp variant C-specific fragment (bold) and is 100% homologous to the corresponding segment of AF385400 (192^{nd} – 643^{rd}).

5.3.3 QUANTIFICATION OF VA AND VC IN HUMAN ATRIAL AND VENTRICULAR TISSUE BY WESTERN BLOT EXPERIMENTS

Real-time PCR could not be used to quantify the expression level of the splice variants since specific primers suitable for real-time PCR could not be designed to the different sequences. However, since the variants have different molecular weights, it was possible to quantify them at the protein level using Western blot. 6 human right atrial samples were used. Non-mammalian tissue was used as negative control. The anti-TREK-2 primary antibody recognized Va (59KDa) and Vc (61KDa) (Fig. 34). OD values of Va and Vc in 6 samples demonstrated that the protein expression of Vc was 1.5 times more than that of Va in human atrial tissue (1.85 ± 3% compared to 1.19 ± 5% respectively). For human ventricular samples, different sample concentrations were applied to detect the quantity of Va and Vc, (25μg/30μL, 20μg/30μL and 6μg/20μL). With decreasing gel loading, the level of Va fell below the level of detection before that of Vc (Fig. 35), indicating that the expression level of Vc was higher than that of Va in these tissues. With the sample concentration reducing to 6μg/20μL, Vc was detected on the nitrocellulose membrane whereas Va was not detected. Hence we conclude that Vc is expressed at a higher level in both atrial and ventricular tissue from donor hearts with no obvious cardiac disease.

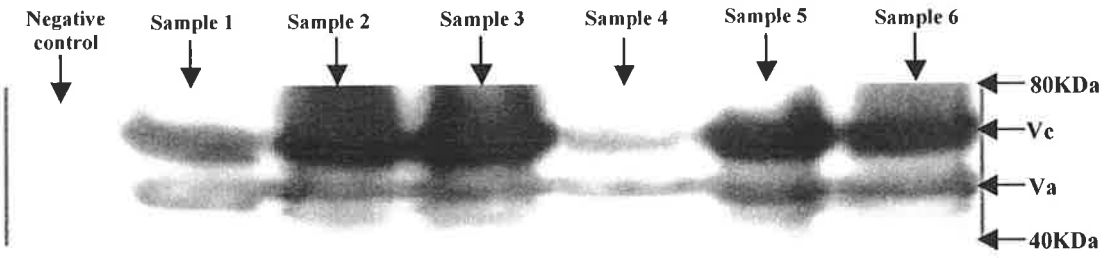

Figure 34. Western Blot of Va and Vc in human atrial tissue. 6 human atrial samples from patients undergoing coronary artery bypass are used for Western Blot experiments. Va (59KDa) and Vc (61KDa) can be readily detected in all the samples. Supernatant concentration of each sample was 25μg/30μL. [primary Ab] =1:500; [secondary Ab] =1:1000

A:

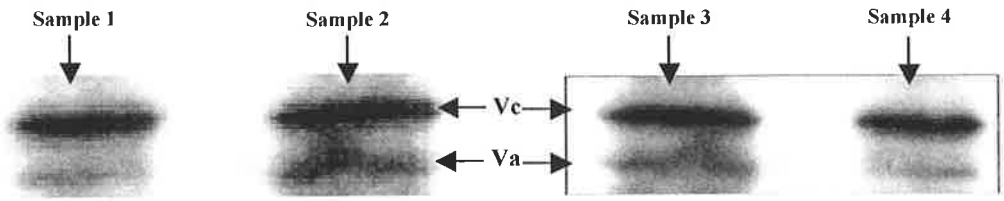

B:

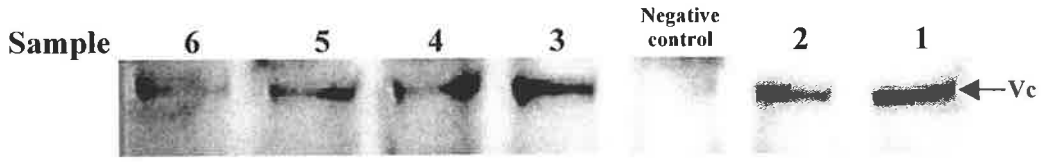

Figure 35. Western Blot of Va and Vc in human ventricular tissue. A shows the expression of Va and Vc in 4 human ventricular samples from donor hearts with sample concentrations of 20µg/30µL. B demonstrates that only Vc was found in 6 human ventricular samples from donor hearts under the sample concentration of 6µg/20µL. [primary Ab] =1:500; [secondary Ab] =1:1000.

However, the protein levels of Va and Vc in ischemia and idiopathic dilated cardiomyopathy groups demonstrated a reverse result with respect to human donor ventricles (Fig. 36 ; 37).

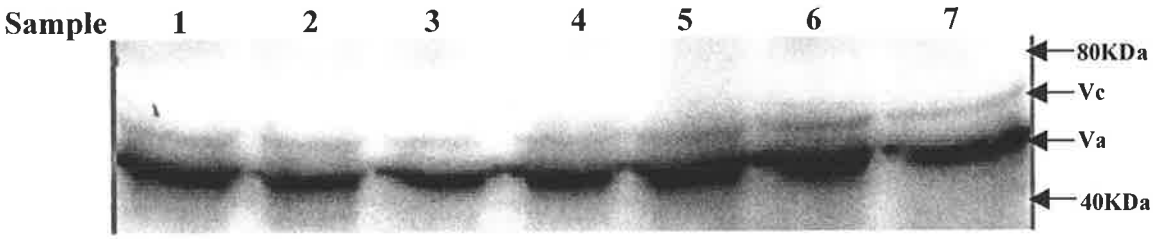

Figure 36. Western Blot of Va and Vc in human disease ventricular tissue. Western blot result of variant A and variant C in 2 ventricular samples of ischemic cardiomyopathy (sample 1&2) and 5 ventricular samples of idiopathic dilated cardiomyopathy (samples 3 to 7) with identical sample concentrations of 20µg/30µL. [primary Ab] =1:500; [secondary Ab] =1:1000.

A:

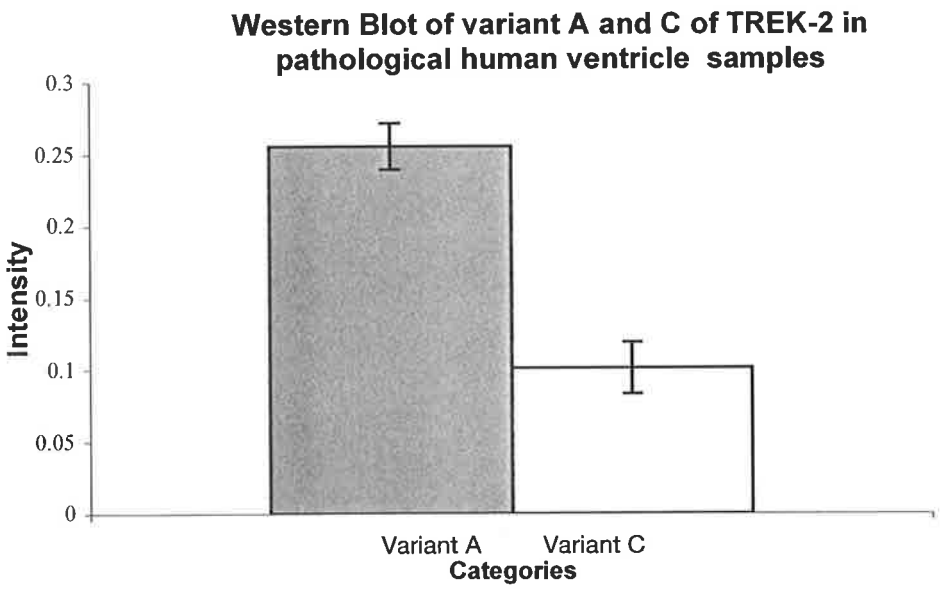

B:

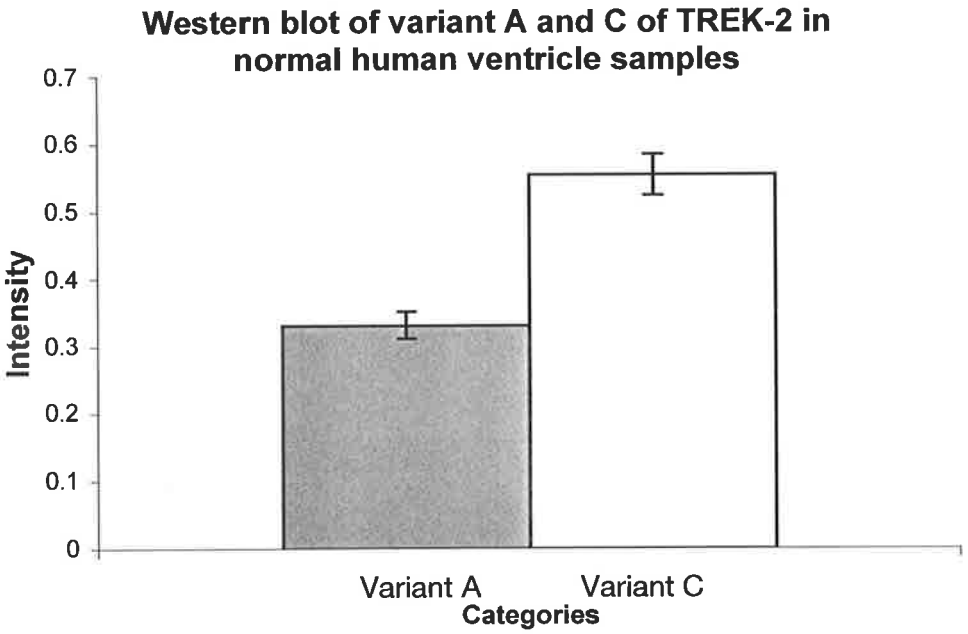

Figure 37. The expression levels of Va and Vc in normal and pathological human ventricular samples. Diagram shows the comparison of expression level of variant A and C between normal human ventricular samples and pathological ventricular samples from Western blot experiments.

5.3.4 IMMUNOHISTOCHEMISTRY

Due to the importance of the localization of TREK-2 for analysing the roles of TREK-2 in human cardiomyocytes. Dr. Shiyong Yuan has authorized me to show his results in Appendix.

5.4 DISCUSSION

As noted above, TREK-2 is one of the mechanosensitive members of the tandem pore family, along with TREK-1 and TRAAK (Lesage et al., 2000). TREK-2 is widely distributed in the brain (Lesage et al., 2000; Gu et al., 2002). Although previous studies have failed to demonstrate the expression of TREK-2 in human heart (Lesage et al., 2000; Gu et al., 2002), channels with very similar properties to TREK-2 have been recorded in animal cardiac cells (Kim, 1992). In humans, TREK-2 is a 539 amino acid protein and shares approx. 65% and 45% amino acid homology with TREK-1 and TRAAK respectively (Lesage and Lazdunski, 2000). TREK-2 has been assigned the gene name KCNK10 and appears to have 7 exons, compared to TREK-1 also with 7 exons (KCNK2), and TRAAK with 11 exons (KCNK4) (Lesage and Lazdunski, 2000; Lesage et al., 1996b). TREK-2 has been reported to have 3 different splice variants arising from alternative splicing of the first exon (the N-terminus of the protein) (Gu et al., 2002).

Although they share a high sequence homology, TREK-1 and TREK-2 have somewhat different functional properties, TREK-1 being outwardly rectifying in high K^+ solution and TREK-2 inwardly rectifying (Kim et al., 2000). However, different splice variants of TREK-2 have only slightly different functional properties. One would not expect fundamental differences in ion selectivity or conductances, since

these are defined by the pore region between M3 and M4 on the subunits, which have identical sequences. Similarly, mechanosensitivity and modulation by fatty acids are properties conferred on the channel by the C-terminus (Lesage et al., 2000), which is also identical between the splice variants. Indeed, deletion of the N terminus does not materially change the properties of TREK-2 channels expressed in heterologous systems (Duprat et al., 2000) and since the differences in the sequence between the splice variants of TREK-2 reside in the first exon (ie the N-terminus) this raises the question of what differences in function may result from such differences.

Like TREK-1, TREK-2 can be modulated by PKA and PKC phosphorylation. All splice variants of TREK-2 can be inhibited by G-protein and regulated by PKA and PKC (Maingret et al., 2000; Gu et al., 2002). However, the potential phosphorylation sites are Ser359 (PKA phosphorylation) and Thr475 (PKC phosphorylation), both located on the C-terminus of the protein (similar to TREK-1), so one would not expect large differences in response or susceptibility to PKA and PKC dependent phosphorylation. There is a possible PKC phosphorylation site at position 7 in the N-terminus of variant b, this not being present in variant A or C (Gu et al., 2002), but since Va and Vc are the two variants that we find in heart, this does not seem a likely candidate for differentiating between the variants in heart. Hence, at present it seems unlikely that there are fundamental differences in the response to PKA of PKC activation of the two variants present in the heart, but this picture may change if it is found that the splice variants have different modulator sub-unit proteins bound to them.

Our immunohistochemical data showed that TREK-2 was widely distributed on the membrane and intracellular area of cardiomyocytes in both human atria and ventricle. Especially, to human ventricular tissue, TREK-2 appeared to be distributed with the same spacing as t-tubule system. Transverse tubules are invaginations of the membrane occurred at Z line along with longitudinal and transverse directions and mainly distributes in human ventricular myocytes (Ayettey and Navaratnam, 1978). Many functional proteins related to excitation-contraction coupling are predominantly expressed at the transverse tubule system (Soeller and Cannell, 1999; Page et al., 1971), which suggests that transverse tubules play an essential role in electrophysiology of cardiomyocytes. However, previous studies have not described any specific K^+ channels in human transverse tubules although $K_{v4.2}$ found in rat transverse tubules (Barry et al., 1955), $K_{ir2.1}$ in mouse (Clark et al., 2001) and TASK-1 in rat (Jones et al., 2002). Also the roles of stretch-activated channels in stretch-induced arrhythmia have been discussed widely (Lab et al., 1993; Hu and Sachs, 1994; 1997). TREK-2, stretch-sensitive channel, found on the membrane and T-tubule system of human cardiomyoctyes predicts that TREK-2 may involve in the electrical responses of the myocardium to mechanical forces (mechanoelectric feedback), which produce some types of arrhythmias.

Most speculation about their functional role, at least in other tissues, has centred on their activation by fatty acids. Hence, it has been suggested that they (TREK-1 and TREK-2) may be protective in ischaemia, on the basis that free fatty acids are released during ischaemia, and the consequent activation of a potassium channel such as TREK-1 or TREK-2 would be protective in a way similar to the opening of K^+-ATP channels (Bazan et al., 1971). Consistent with this idea, the neuroprotective

agent riluzole activates TREK-1 (Duprat et al., 2000). More intriguingly, both TREK-1 and TREK-2 have been shown to be differentially up-regulated in chronic and acute cerebral ischaemia (Li et al., 2005; Xu et al., 2004). If this response to ischemia is indeed part of the role of TREK-2, then the change in the relative expression of the splice variants in the ventricular tissue from patients with IDC and IC may have significance for the progression of these diseases.

CHAPTER 6

EXPRESSION OF TREK-1

IN

ANIMAL HEARTS

6.1 INTRODUCTION

TREK-1 has been cloned in mouse, rat and human (Lesage et al., 19961a; 1996b; 2000). At present, no investigator has demonstrated the expression of TREK-1 in guinea pig heart, rabbit heart and pig heart. The existence of TREK-1 in guinea pig heart, rabbit heart and pig heart strongly reinforces the findings of TREK-1 and TREK-2 in human heart. However, no TREK-1 sequence has been published in guinea pig, rabbit and pig (http://www.ncbi.num.nih.gov). The homology of TREK-1 is 88% between mouse (NM_010607) and human (AF171068) and 88% between rat (AF385402) and human. To confirm the existence of TREK-1 in the hearts of guinea pig, rabbit and pig, the primers are designed from mouse TREK-1 sequence (NM_010607).

6.2 MATERIALS AND METHODS

All procedures in this study were following guidelines of approval from the University of Adelaide Human Ethics Committee, the Royal Adelaide Hospital Ethics Committee and the University of Sydney Human Ethics Committee as appropriate.

Tissue – Atrium and ventricle of rabbit and guinea pig were obtained from the living animals under normal anaesthesia. Pig heart was obtained in abattoir. All cardiac tissues were put in liquid nitrogen immediately and then stored in –80°C freezer.

RNA Extraction – the same as described in Chapter 3.

Primer Design - Primers were designed from published TREK-1 sequences (NM_010607 for mouse TREK-1; AF171068 for human TREK-1) using Primer Express software (PE Applied Biosystems, Foster city, CA, USA).

Mouse primers for TREK-1 expression in guinea pig, rabbit and pig (720bp)

SP: CCTGGTGGTCGTCCTCTACCT

ASP: GCACGCTGGAACTTGTCGTA

Mouse primers for nested PCR of TREK-1 in guinea pig, rabbit and pig (194bp)

SP: CTCGTTGGGCTGGCCTACT

ASP: GCACGCTGGAACTTGTCGTA

PCR and Real-time PCR processes – the same as described in Chapter 3.

6.3 RESULTS

6.3.1 THE EXPRESSION OF TREK-1 IN THE HEARTS OF GUINEA PIG, RABBIT AND PIG

Mouse primers of TREK-1 were applied in the ventricles of guinea pig, rabbit and pig. PCR products similar to the desired size (720bp) were shown in guinea pig, rabbit and pig, respectively (Fig. 39 A, B and C). Nested PCR primers of mouse TREK-1 were applied to the initial PCR products. The same size nested PCR products from guinea pig, rabbit and pig were expressed in nested PCR gel, which were similar to the designed size (194bp; Fig. 39 D). Nested PCR products of guinea pig, rabbit and pig were cleaned and sent to Flinders Medical Centre for sequencing.

A: PCR of mouse TREK-1 primers in guinea pig heart

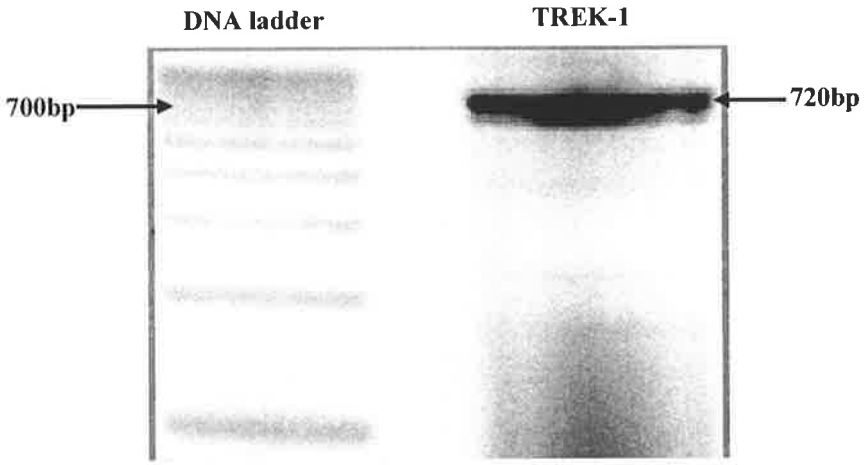

B: PCR of mouse TREK-1 primers in rabbit heart

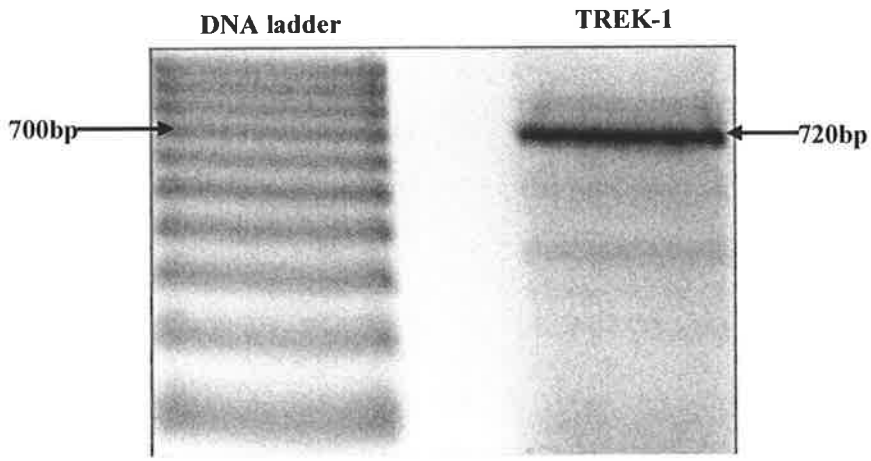

C: PCR of mouse TREK-1 primers in pig heart

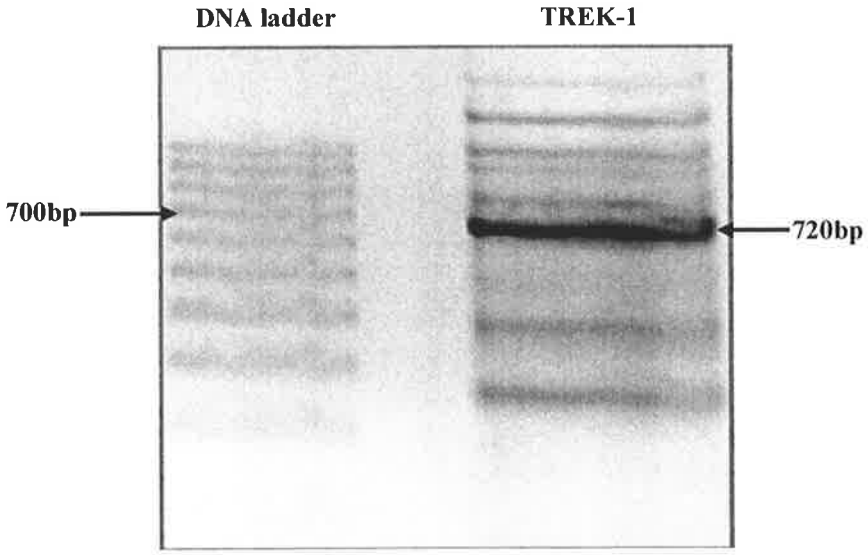

D: Nested PCR of guinea pig, rabbit and pig by mouse TREK-1 primers

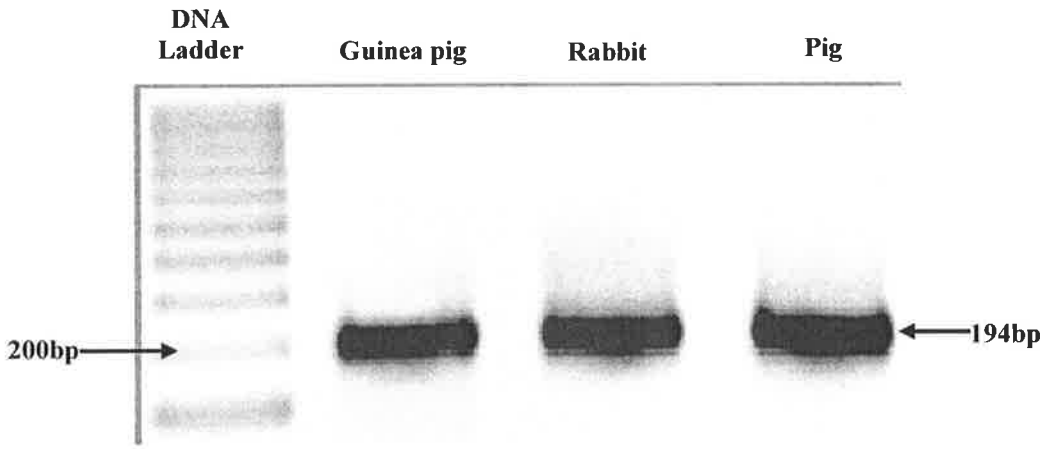

Figure 39. The expression of TREK-1 in guinea pig heart, rabbit heart and pig heart. The bands similar to 720bp are shown on A, B and C, respectively. D shows that the products similar to 194bp are expressed on nested PCR gel.

6.3.2 SEQUENCING

6.3.2.1 SEQUENCING OF NESTED PCR PRODUCT OF GUINEA PIG HEART

3'-GGTTTCTTTGAACTCAGCCGTGACGTTGGCTGTCCACTCAGCAGC
GTGGGCCCTGAACTCTCCTACCTCTTCCTTTGTCTTTTTGGATATCA
CGCGGAGCCAGTCTCCAATCATGCTCAGGACAGCGGCGAAGTATGC
CAGCCCTACAAGGATCCAGAACCACACGACAGGCTTGTAGAAGTCA
GATACTCAATA- 5'

Sequencing showed the 195-bp segment from guinea pig heart is 91% homologous to human TREK-1 sequence (AF171068) and 87% homologous to mouse TREK-1 sequence (NM_010607).

6.3.2.2 SEQUENCING OF NESTED PCR PRODUCT OF RABBIT HEART

5'⟶GGATCCTTGTAGGGCTGGCCTACTTCGCCGCTGTGCTGAGCA
TGATTGGAGACTGGCTCCGCGTGATATCCAAAAAGACAAAGGAAGA
GGTGGGAGAGTTTCTTCCCACGCTGCTGAGTGGACAGCCAACGTCA
CGGCTGAGTTCAAAGAAACCCGCAGGCGGCTAGCGTC⟵ 3'

Sequencing showed the 171-bp segment from rabbit heart is 88% homologous to human TREK-1 sequence (AF171068) and 85% homologous to mouse TREK-1 sequence (NM_010607).

6.3.2.3 SEQUENCING OF NESTED PCR PRODUCT OF PIG HEART

3'-CGCCTCCTGGGTTTCCTTGAATTCGGCCGTGACGTTGGCTGTCCA
CTCCAGCATGGGAAAATAACTCTCCCACCTCTTCTTTTGTCTTTTTG
ATATCACTGGACCAGTCTCCAATCATACTCAGGCAGAGCAAAGTAAG
CA-5'

Sequencing showed the 141-bp segment from pig heart is 87% homologous to human TREK-1 (AF171068) and 92% homologous to mouse TREK-1 (NM_010607).

6.3.3 IMMUNOHISTOCHEMISTRY

Immunohistochemistry showed that the localization of TREK-1 in guinea pig and rabbit heart is very similar to that of human heart, in which TREK-1 is clearly expressed on cardiac myocyte's membrane. (Data by Dr. Shiyong Yuan not shown here.).

6.4 DISCUSSION

The likely functions TREK-1 plays in human heart have been discussed broadly in Chapter 3, 4 and 5. Here, TREK-1 discovered in guinea pig, rabbit and pig heart by RT-PCR, sequencing and immunohistochemistry reinforces the expression of TREK-1 in human heart.

In this study, we have not obtained the whole sequence of each TREK-1 in guinea pig, rabbit or pig. Similarity based on the sequenced segments may not be valid to be used to express the accurate homology of TREK-1 sequence between guinea pig, rabbit, pig, mouse and human being. Since availability of mouse TREK-1 primer has been verified in the expression of TREK-1 in human tissue (Lesage and Lazdunski, 2000) and the existence of TREK-1 in guinea pig and rabbit has been confirmed by immunohistochemistry, the homology of TREK-1 sequenced by mouse primers indicates that TREK-1 channels distributed in human beings and animals are the products of ortholog gene. The existence of TREK-1 in guinea pig, rabbit and pig has provided the opportunities to design the different animal models for the research

of TREK channels in cardiac system, which may lead to the fully understanding of physiological characteristics of TREK channels in normal and diseased heart.

This study shows that TREK-1 channels are broadly distributed in animal and human heart. The possibility of TREK-1 existing in other categories of muscle such as smooth muscle may open a window to speculate the different behaviours of TREK-1 in the regulation of membrane excitability and stretch sensitivity.

CHAPTER 7

GENERAL DISCUSSION

7.1 DISCUSSION

The design of primers has been critical to investigating the expression of stretch-activated 2P-4TMD potassium channels in the human heart. At the beginning of this project, we did not know whether any of TREK or TRAAK channels existed in the human cardiac tissue, and also if they exist in the human heart, what is the percentage of homology between human heart and brain? Based on the published sequences of TREK and TRAAK channels in human brain and the conserved amino acid sequence (T-x-G-x-G) in 2P-4TMD-potassium channels' pore structure, we proposed that TREK and TRAAK channels in human heart would keep the similar arrangement as those in human brain. Based on the unique difference of 3 splicing variants of TREK-2 shown on exon 1, sense primers of 3 splicing variants are designed from exon 1. In this study, we used fresh atrial appendage from patients undergoing coronary bypass surgery, and frozen ventricular tissue samples, rather than a cDNA library sourced from a third party and real-time PCR technique, these may enlighten part of the reason why we see substantial expression whereas the few publications on TREK-1 expression in heart have failed to do so.

Due to degradation of mRNA of TREK-1 in long-term storing, the values of mRNA of TREK-1 in donor and diseased ventricles may not be accurate enough to express the amount of TREK-1 under the different conditions. However, combing with protein expression in donor and diseased group, the sensitivity of qPCR will be corrected at some levels. Since patch clamping to single human cardiomyocyte is not

applied in this study, this enhances the susceptibility of speculating the functions of TREK channels in human heart more and less. These barriers will be eventually overcome with the discoveries of agonist and antagonist of TREK channels.

In spite of sharing a high sequence homology, TREK-1 and TREK-2 have different functional properties, TREK-1 is inactivated by phosphorylating Ser-300 and Ser-333 of C-terminus by protein kinase A (PKA) and C (PKC) (Patel et al., 1998; Murbartian et al., 2005); The action of $G\alpha_s$-couple receptor pathways preventing TREK-1 activity was similar to PKA (Patel et al., 1998; Kohl et al., 2001) whereas inhibition of $G\alpha_q$-coupled receptors to TREK-1 was similar to PKC (Chemin et al., 2003; 2005; Lopes et al., 2005). All splice variants of TREK-2 can be inhibited by G-protein and regulated by PKA and PKC (Maingret et al., 2000; Gu et al., 2002). However, the potential phosphorylation sites are Ser359 (PKA phosphorylation) and Thr475 (PKC phosphorylation), both located on the C-terminus of the protein (similar to TREK-1), so one would not expect large differences in response or susceptibilty to PKA and PKC dependent phosphorylation. There is a possible PKC phosphorylation site at position 7 in the N-terminus of variant b, this not being present in variant A or C (Gu et al., 2002), but since Va and Vc are the two variants that we find in heart, this does not seem a likely candidate for differentiating between the variants in heart. Hence, at present it seems unlikely that there are fundamental differences in the response to PKA of PKC activation of the two variants present in the heart, but this picture may change if it is found that the splice variants are coupled with regulatory

proteins such as G-protein bound to them.

Based on the pore region between M3 and M4 on the subunits with identical sequences, three splice variants of TREK-2 may have only slightly different functional properties in ion selectivity or conductance. Similarly, mechanosensitivity and modulation by fatty acids are properties conferred on the channel by the C-terminus (Lesage et al., 2000), which is also identical between the splice variants. The sequence between the splice variants of TREK-2 shows the obvious difference in the first exon (N-terminus), however, deletion of the N terminus does not materially change the properties of TREK-2 channels expressed in heterologous systems (Duprat et al., 2000). This raises the question of what specificity in function depending on the difference of genetic sequence.

Tissue distribution studies have shown TREK-1 and TREK-2 to be expressed at high levels in the brain and, at somewhat lower levels, in a variety of peripheral tissues. As yet, no clear role has yet been ascribed to TREK channels in any of these tissues. Nevertheless, it has been the subject of intense research. The roles of TREK channels in the heart have been neglected, since no data of TREK channels expressed in human heart have been reported to date (Lesage et al., 2000; Gu et al., 2002). However, since TREK channels are sensitive to mechanical stresses, it is reasonable to suppose that they would play an important role in the modulation of electrical activity in organs and tissues subjected to mechanical forces. Certainly,

the heart is subjected to constantly varying mechanical forces and there is now a large body of evidence to show that these forces can alter the electrical properties of the myocardium. For example, in animals rapid stretch of the ventricles can produce either rapid depolarisations or hyperpolarizations, depending on the timing (Zabel et al., 1996).

Mechanosensitive channels which presumably give rise to these responses have been recorded directly in myocardial cells, one type of which is a potassium selective channel which has properties similar to those exhibited by channels formed when TREK-1 constructs are expressed in heterologous systems (Hu et al., 1997). Similar electrophysiological responses to those in animals have been demonstrated in human heart (Eckardt et al., 2001). For example, in human atrium, Calkins et al., (1992) noted that acute increases in atrial pressure induced by varying the atrioventricular interval shortened atrial refractoriness. In a similar human model, Klein et al., (1990) demonstrated that increases in right atrial pressure significantly attenuated (> 20 ms) atrial refractory periods. In human ventricle, Taggart et al., (1998) observed a progressive shortening of repolarization as left ventricular pressure and volume increased in patients during the process of weaning off cardiopulmonary bypass. In another group of patients undergoing cardiac surgery, Taggart et al., (1992) showed that action potential duration shortened during ventricular loading induced by aortic occlusion and returned to control values within 1 – 3 beats after release. A similar result was reported by Levine et al., (1988) in right ventricle duration during transient

occlusion of the right ventricular outflow tract. It has been suggested that this shortening of the action potential by stretch plays an important role in protection from arrhythmias, which could otherwise arise because of heterogeneous action potential propagation velocities in the myocardium (Lab, 1999).

At present, no investigation has clarified the mechanism by which stretch produces arrhythmia. There are three possibilities to explain this phenomenon. (1) Simple mechanical stimulation directly generates MEF that causes the production of arrhythmia; (2) Stretch induces the activation of TREK channels, which may lead to the changes of internal potassium concentration. Such behavior creates an arrhythmia-sensitive environment; (3) Activation of TREK channels by stretch may activate protein kinase pool, which leads to cardiac muscle remodeling. Cardiac remodeling is straightforwardly responsible for the production of ventricular arrhythmia according to pathological conditions such as myocardial infarction, idiopathic dilated cardiomyopathy and cardiac hypertrophy.

The production of arrhythmia by simple mechanical stimulations has been confirmed in experiments (Ravens, 2003; Kamkin et al., 2000; Isenberg et al., 2003), in which mechanical stimulations acting on isolated cardiac myocytes or isolated hearts produce premature beats and ventricular arrhythmia.

Although the role of potassium-specific SACs in arrhythmogenesis have always

been challenged by non-selective cation SACs in heart (Zeng et al., 2000; Kamkin et al., 2000; Kim, 1992; Niu et al., 2003; Isenberg et al., 2003), the studies of SAC-activated 2-D and 3-D ventricular models of rat and rabbit (Garny and Kohl, 2004; Li et al., 2004) demonstrate that non-select cation SACs may trigger sudden arrhythmia and K^+-specific SACs are more essential to the development of continuous ventricular arrhythmia. Without the involvement of K^+-specific SACs, non-selective cation SACs may not produce sustained ventricular arrhythmia. The importance of K^+-specific SACs such as TREK channels in the process of arrhythmogenesis has been shown by Goldstein et al., (2005), in which streptomycin, a blocker of non-selective cation SAC (Eckardt et al., 2000; Salmon et al., 1997), did not prevent the production of sustained ventricular arrhythmia stimulated by altering mechanical loadings in porcine models. Therefore, it seems that the activation of K^+-specific SACs such as TREK channels is a more acceptable explanation for arrhythmogenesis by stretch.

Our immunohistochemistry results show that TREK-1 is expressed in human atrium and ventricle and localized on cardiomyocyte membrane and arranged in longitudinal stripes along myocardium whereas TREK-2 is widely distributed on the membrane and intracellular area of cardiomyocytes in both human atria and ventricle, especially, in human ventricular tissue, TREK-2 appears to be distributed with the same spacing as t-tubule system. Many functional proteins related to excitation-contraction coupling are predominantly expressed at the transverse tubule

system (Soeller and Cannell, 1999; Page et al., 1971), which may suggest that transverse tubules play an essential role in electrophysiology of cardiomyocytes. At present, although we have not identified what variants of TREK-2 existing in T-tubule system, TREK-2 found in the T-tubule system of human cardiomyoctyes predicts that TREK-2 may involve in the electrical responses of the myocardium to mechanical forces (mechanoelectric feedback), which produce some types of arrhythmias.

These characteristics of TREK-1 and TREK-2 are suitable for sensing and transferring stretch in cardiac muscle. In TREK-1-expressed rat model, Li et al., (2005) confirmed that TREK-1 not only played an important role in the production of arrhythmia but was involved also in the length-dependent regulation of contractile force of myocardium. Due to shortening of diastolic repolarization, the activation of most TREK-1 in ventricle induced sustained ventricular arrhythmia by re-entry mechanism (Li et al., 2004). It is likely that one-time high-level mechanical stretch acting on pre-cordial region may explosively activate a large number of TREK channels in human atrium and ventricle, which results in sudden cardiac death caused by fatal ventricular arrhythmia.

In spite of that the functions of stretch in cardiac remodeling are not clear, some interesting discoveries have been reported, for example, altering mechanical loading on cardiac muscle results in the activation of a number of immediate-early (IE) genes

and cardiac hypertrophy *in vivo* and *in vitro* (Sadoshima et al., 1992a); stretch to cultivated cardiac cell on the deformable silicon membrane enhances the protein synthesis independent of exogenous neurohormonal factors (Vandenburgh and Kaufman, 1979; Mann et al., 1989; Komuro et al., 1990); mechanical stretch activates intracellular multi-signal transduction systems in neonatal cardiac myocytes, which are directly or indirectly involved in cardiac hypertrophy (Rozich et al., 1995; Komuro et al., 1996; Yamazaki et al., 1993). These phenomena demonstrate the importance of mechanical stretch in cardiac remodeling. However, it is not clear how stretch is translated into biochemical signals to release remodeling-related factors and activate protein kinase cascades.

Sadoshima et al., (1992b) demonstrated that [Gd^{3+}] block of completely inactivating non-selective cation SACs did not prevent stretch-induced expression of IE genes and the enhancement of protein synthesis. TREK-1 is not inhibited by the blockers of non-selective cation SAC such as Gd^{3+}, streptomycin and tarantula venom (Kim, 2003). Our results show that the levels of cDNA and protein of TREK-1 expressed in IDC are obviously higher than those of normal human ventricles. These suggest that stretch may activate TREK-1 on the surface of cardiomyocytes, which transfers the effects of stretch to the nuclei by integrating with cytoskeleton transduction systems or the subunits of other growth factors. The TREK-1-induced increases of IE gene expression may reversely lead to overexpression of TREK-1 in cardiac myocytes, which is, at least in part, parallel with the clinical descriptions of IC

and IDC where most patients die in ventricular arrhythmia possibly based on TREK-1-sensitive cardiac remodeling. In addition, Aimond et al., (2000) reported that activation of p38MAPK and p42/44 MAPK (Mitogen-Activated Protein Kinase) pathway, which was one of the most important protein kinase cascades in cardiac hypertrophy, resulted in opening TREK-1 of rat cardiomyocytes. This may explain the occurrence of idiopathic ventricular arrhythmia in the development of cardiac remodeling without the involvement of stretch. Differently, TREK-1 and TREK-2 may play protective roles in IC. The action of TREK channels in heart ischemia is similar as in brain ischemia where endogenous arachidonic acid releasing and intracellular pH falling in swelling cardiac myocytes around ischemic regions contribute to opening TREK-1 in systolic repolarization and the following hyperpolarization decreases intracellular [Ca^{2+}] and reduced excitotoxicity (Patel and Honore., 2001; Honore et al., 2002; Buckler and Honore, 2005).

7.2 FUTURE DIRECTIONS

The functions of TREK and TRAAK channels in human heart have been obviously restricted by the current lack of specific agonists and antagonists. Although knockout models are being used to investigate the function of TREK-1 channels in human brain, such techniques may not be enough to explain the accurate mechanisms of TREK-1 or TREK-2 in regulating electrophysiological behaviors of cardiomyocytes and relevant reactions stimulated by hypertrophic factors and protein kinase cascades. Therefore, TREK-1- or 2-specific stimulators and inhibitors based on

small molecule scanning and design may bring breakthrough to the functions of TREK channels in normal and diseased human hearts. In addition, correlation between the activity of TREK channels and the increasing calcium in cardiomyocyte needs to be clarified by the application of specific animal models.

The possibilities of stem cell applied in the treatment of cardiac diseases have been investigated in long time. The likely physiological behaviors of TREK channels in the differentiation of stem cell into cardiomyocytes may provide an answer for the understanding of the functions of stretch-activated 2P-4TMD potassium channels in the development of human normal and diseased heart.

BIBLIOGRAPHY

Aimond, F., Rauzier, J., Bony, C., and Vassort, G. (2000). Simultaneous activation of p38 MAPK and p42/44 MAPK by ATP stimulates the K+ current I_{TREK} in cardiomyocytes. J Biol Chem. 275(50): 39110-39116.

Alexzander, J., and Lassalles, J-P. (1991). Hydrostatic and osmotic pressure activated channel in plant vacuole. Biophys J. 60: 1326-1336.

Andres, O., and Eleazar Vega-Saena de Miera. (2002). Cloning of two transcripts, HKT4.1a and HKT4.1b, from the human two-pore K^+ channels gene KCNK4. Mol Brain Res. 102: 18-27.

Arrighi, I., Lesage, F., Scimeca, J. C., Carle, G. F., and Barhanin, J. (1998). Structure, chromosome localization, and tissue distribution of the mouse TWIK K^+ channel gene. FEBS Lett. 425: 310-316.

Bainbridge, F. (1915). The influence of venous filling upon the rate of the heart. J Physiol. 50: 65–84.

Bang, H., Kim, Y., and Kim, D. (2000). TREK-2, a new member of the mechanosensitive tandem-pore K+ channel family. J Biol Chem 275(23):17412-9.

Barrett, J. S. (1971). Chest thumps and the heart beat. J Medi New England. 17: 284-393.

Barry, D. M., Trimmer, J. S., Merlie, J. P., and Nerbonne, J. M. (1995). Differential expression of voltage-gated K^+ channel subunits in adult rat heart: relation to functional K^+ channel? Circ Res. 77: 361-369.

Bazan, N. G. Jr., de Bazan, H. E., Kennedy, W. G., and Joel, C. D. (1971). Regional distribution and rate of production of free fatty acids in rat brain. J Neurochem 18(8): 1387-93.

Bear, C. E., and Li, C. (1991). Calcium-permeable channels in rat hepatoma cells are activated by extracellular nucleotides. Am J Physiol. 261: C1018-1024.

Ben-Tabou, S., leller, E., and Nussinovitch, I. (1994). Mechanosensitivity of voltage-gated calcium currents in rat anterior pituitary cells. J Physiol. 476 (1): 29-39.

Berrier, C., Coulombe, A., Szabo, I., Zoratti, M., and Ghazi, A. (1992). Gadolinium ion inhibits loss of metabolites induced by osmotic shock and large stretch activated channels in bacteria. Eur J Biochem. 206: 559-565.

Biggin, P. C., Rooslid, T., and Choe, S. (2000). Potassium channel structure: domain by domain. Current Opinion in Structural Biology. 10: 456–461.

Bing, R. J., Puddu, P. E., and Suzuki, H. (1995). Myocardial infarction and nitric oxide. G Ital Cardiol. 25(12): 1621-6.

Bockenhauer, D., Zilberberg, N., and Goldstein, S. A. N. (2001). KCNK2: reversible conversion of a hippocampal potassium leak into a voltage-dependent channel. Nature Neurosci. 4: 486–491.

Bode, F., Sachs, F., and Franz, M. R. (2001). Tarantula peptide inhibits atrial fibrillation during stretch. Nature. 409: 35-36.

Bogoyevitch, M. A., Fuller, S. J., and Sugden, P. H. (1993). cAMP and protein synthesis in isolated adult rat heart preparations. Am J Physiol. 265: C1247–1257.

Boland, L. M., Brown, T. A., and Dingeldine, R. (1991). Gadolinium block of calcium channels: influence of bicarbonate. Brain Res. 563: 142-150.

Brickley, S. G., Revilla, V., Cull-Candy, S. G., Wisden, W., and Farrant, M. (2001). Adaptive regulation of neuronal excitability by a voltage-independent potassium conductance. Nature. 409: 88–92.

Brophy, C. M., Mills, I., Rosales, O., Isales, C., and Sumpio, B. E. (1993). Phospholipase C: a putative mechanotransducer for endothelia cell response to acute hemodynamic changes. Biochem Biophys Res Comm. 109: 576-581.

Buckler, K. J., and Honoré, E. (2005). The lipid-activated two-pore domain K^+ channel TREK-1 is resistant to hypoxia: implication for ischaemic neuroprotection. J Physiol. 562(1): 213-222.

Bustamante, J. O., RuknudinF, A., and Sachs, F. (1991). Stretch-activated channels in heart cells: relevance to cardiac hypertrophy. J Cardiovasc Pharmacol. 17 (Suppl 2): S110–113.

Califf, R. M., Burks, J. M., Behar, V. S., Margolis, J. R., and Wagner, G. S. (1978). Relationships among ventricular arrhythmias, coronary artery disease and angiographic and electrocardiographic indicators of myocardial fibrosis. Circulation. 57: 725–732.

Calkins, H., Levine, J. H., and Kass, D. A. (1991). Electrophysiological effect of varied rate and extent of acute in vivo left ventricular load increase. Cardiovasc Res. 25: 637–644.

Calkins, H., Maughan, W. L., Kass, D. A., Sagawa, K., and Levine, J. H. (1989). Electrophysiological effect of volume load in isolated canine hearts. Am J Physiol 256: H1697- 1706.

Calvert, A., Lown, B., and Gorline, R. (1977). Ventricular premature beats and anatomically defined heart disease. Am J Cardio. 39: 627-634.

Chang, W., and Loretz, C. A. (1992). Activation by membrane stretch and depolarization of an epithelial monovalent cation channel from teleost intestine. J Exp Biol. 169: 87-104.

Chavez, R. A., Gray, A. T., Zhao, B-B., Kindler, C. H., Mazurek, M. J., Mehta, Y., Forsayeth, J. R., and Yost, C. S. (1999). TWIK-2, a new weak inward rectifying member of the tandem pore domain potassium channel family. J Biol Chem. 274: 7887-7892.

Chemin, J., Girard, C., Duprat, F., Lesage, F., Romey, G., and Lazdunski, M. (2003). Mechanisms underlying excitatory effects of group I metabotropic glutamate receptors via inhibition of 2P domain K+ channels. J EMBO. 22: 5403–5411.

Chemin, J., Patel, A. J., Duprat, F., Lauritzen, I., Lazdunski, M., and Honore, E. (2005). A phospholipid sensor controls mechanogating of K+ channel TREK-1. J EMBO. 24: 44–53.

Chomczyznski, P., and Sacchi, N. (1987). Single-step method of RNA isolation by acid guanidinium thiocyanate–phenol–chloroform extraction. Anal Biochem. 162: 156–159.

Christensen, O. (1987). Medication of cell volume by Ca^{2+} influx through stretch activated channels. Nature. 330: 66-68.

Christensen, O., and Hoffmann, E. K. (1992). Cell swelling activates K^+ and Cl^- channels s well as nonselective, stretch-activated cation channels in Ehrlich ascites tumor cells. J Membr Biol.129: 13-26.

Clark, R. B., Tremblay, A., Melnyk, P., Allen, B. G., Giles, W. R., and Fiset, C. (2001). T-tubule localization of the inward-rectifier K^+ channel in mouse ventricular myocytes: a role in K^+ accumulation. J Physiol. 537: 979-992.

Clive, M. B., and Henry, F. C. (2002). Stretch-activated channels and signaling pathways in heart failure. 3rd international workshop on cardiac mechno-electric feedback and arrhythmia. 26-27.

Cooper, G., Kent, R. L., Uboh, C. E., Thompson, E. W., and Marino, T. A. (1985). Hemodynamic versus adrenergic control of cat right ventricular hypertrophy. J Clin Invest. 75:1403–1414.

Craelius, W., Chen, Y., and El-Sherif, N. (1988). Stretch activated ion channels in ventricular myocytes. Biosci Rep. 8: 407-414.

Cranefield, P. F. (1977). Action potentials, afterpotentials, and arrhythmias. Circ Res. 41: 415 – 423.

Cui, O., Smith, D. O., and Adler, J. (1995). Characterization of mechanosensitive channels in *Escherichia coli* cytoplasmic membrane by whole cell patch clamp recording. J Membr Biol. 144: 31-42.

Davidson, R. M. (1993). Membrane stretch activates a high conductance K^+ channel in G292 Osteoblastic-like cells. J Membr Biol. 131: 81-92.

Dean, J. W., and Lab, M. J. (1989). Arrhythmia in heart failure: role of mechanically induced changes in electrophysiology. Lancet. 1: 1309-1312.

Decher, N., Maier, M., Dittrich, W., Gassenhuber, J., Bruggemann, A., Busch, A. E., and Steinmeyer, K. (2001). Characterization of TASK-4, a novel member of the pH-sensitive, two-pore domain potassium channel family. FEBS Lett. 492: 84–89.

Denk. W., and Webb, W. W. (1989). Thermal noise-limited transduction observed in mechnosensory receptors of the inner ear. Phys Rev Lett. 63: 207-210.

Di Diego, J. M., and Antzelevitch, C. (1994). High $[Ca^{2+}]_o$-induced electrical heterogeneity and extrasystolic activity in isolated canine ventricular epicardium: phase 2 reentry. Circulation. 89:1839–1850.

Dick, D. J., and Lab, M. J. (1998). Mechanical modulation of stretch-induced premature ventricular beats: induction of mechanoelectric adaptation period. Cardiovasc Res. 38: 181–191.

Ding, J. P., and Pickard, B. G. (1993). Mechnosensory calcium-sensitive cation channels in epidermal cells. Plant J. 3 (suppl. 1): 83-110.

Duel, J., and Trautwein, W. (1954). Das Aktionpotential and Mechanogramm des Herzmuskels unter dem Einflus der Dhnung. Cardiologie. 25: 344-362.

Duncan, R. L., Hruska, K. A., and Misler, S. (1992). Parathyloid hormone activation of stretch-activated cation channels in osteosarcoma cells (UMR-106.01).FEBS Letts. 307: 219-223.

Duprat, F., Lesage, F., Patel, A. J., Fink, M., Romey, G., and Lazdunski, M. (2000). The neuroprotective agent riluzole activates the two P domain K(+) channels TREK-1 and TRAAK. Mol Pharmacol. 57(5): 906-12.

Duprat, F., Lesage, F., Fink, M., Reyes, R., Heurteaux, C., and Lazdunski, M. (1997). TASK, a human background K^+ channel to sense external pH variations near physiological pH. J EMBO.16: 5464-5471.

Eckardt, L., Kirchof, P., Monnig, G., Breithardt, G., Borggrefe, M., and Haverkamp, W. (2000). Modification of stretch-induced shortening of repolarization by streptomycin in the isolated rabbit heart. J Card. Pharm. 36: 711-721.

Edwards, K. L., and Pickard, B. G. (1987). Detection and transduction of physical stimuli in plants. *In* The Cell Surface and Signal Transduction, ed. By E. Wagner, H.. Greppin, B. Millet, pp. 41-66, Springer-Verlag, Heidelberg, Germany.

Filipovic, D., and Sackin, H. (1991). A calcium permeable stretch-activated cation channel in renal proximal tubule. Am J Physiol. 260: F119-129.

Fink, M., Duprat, F., Lesage, F., Reyes, R., Romey, G., Heurteaux, C., and Lazdunski, M. (1996). Cloning, functional expression and brain localization of a novel unconventional outward rectifier K^+ channel. J EMBO. 15: 6854-6862.

Fink, M., Lesage, F., Duprat, F., Heurteaux, C., Reyes, R., Fosset, M., and Lazdunski, M. (1998). A neuronal two P domain K^+ channel stimulated by arachidonic acid and polyunsaturated fatty acids. J EMBO. 17: 3297-3308.

Franco, A. Jr., and Lansman, J. B. (1990). Stretch-sensitive channels in developing muscle cells from a mouse cell line. J Physiol. 427: 361-368.

Franz, M. R. (1996). Mechano-electrical feedback in ventricular myocardium. Cardiovasc Res. 32: 15–24.

Franz, M. R., Burkhoff, D., Yue, D. T., and Sagawa, K. (1989). Mechanically induced action potential changes and arrhythmia in isolated and in situ canine hearts. Cardiovasc Res. 23: 213–223.

Franz, M. R., Cima, R., Wang, D., Proffitt, D., and Kurtz, R. (1992). Electrophysiological effects of myocardial stretch and mechanical determinants of stretch activated arrhythmias. Circulation. 86: 968–978.

French, A. S. (1992). Mechanotransduction. Ann Rev Physiol. 54: 135-152.

Gallagher, K. P., Gerren, R. A., and Starling, M. C. (1986). The distribution of functional impairment across the lateral border of acutely ischemic myocardium. Circ Res. 58: 570–583.

Garan, A. R., Maron, B. J., Wang, P. J., Esters, N. A 3rd., and Link, M. S. (2005). Role of streptomycin-sensitive stretch-activated channel in chest wall impact induced sudden death (commotio cordis). J Cardiovasc Electrophysiol. 16(4): 433-8.

Garny, A., and Kohl, P. (2004). Mechanical induction of arrhythmias during ventricular repolarisation:modeling cellular mechanisms and their interaction in 2D. Ann NY Acad Sci. 1015: 133–143.

Garrill, A., Jackson, S. L., Lew, R. R., and Heath, I. B. (1993). Ion channel activity andtip growth: tip-localized stretch-activated channels generate an essential Ca^{2+} gradient in the oomycyte *Samrolegia ferax.* Eur J Cell Biol. 60: 358-365.

Goldstein, S. A. N., Bockenhauer, D., O'Kelly, I., and Zilberberg, N. (2001). Potassium leak channels and the KCNK family of two-P-domain subunits. Nature Neurosci. 2: 175–184.

Goulter, B. A., Goddard, J. M., Allan, C. J., and Clark, L. K. (2004). ACE2 gene expression is up-regulated in the human failing heart. BMC medicine. 2: 19-26.

Gradman, A., Deedwania, P., Cody, R., Massie, B., Packer, M., Pitt, B. and Goldstein, S. (1989). Predictors of total mortality and sudden death in mild to moderate heart failure. J Am Coll Cardiol. 14: 564–570.

Gray, A. T., Zhao, B-B., Kindler, C. H., Winegar, B. D., Mazurek, M. J., Xu, J-B. A., Chavez, R. A., Forsayeth, J. R., and Yost, C. S. (2000). Volatile anesthetics activate the human tandem pore domain baseline K+ channel KCNK5. Anes. 92: 1722–1730.

Gu, W-L., Schlichthorl, G., Hirsch, J. R., Engels, H., Karschin, C., Karschin, A., Derst, C., Steinlein, O. K., and Daut, J. (2002). Expression pattern and functional characteristics of two novel splice variants of the two-pore-domain potassium channel TREK-2. J Physiol. 539(3): 657-668.

Guharay, F., and Sachs, F. (1984). Stretch-activated single ion channel currents in tissue cultured embryonic chick skeletal muscle. J Physiol. 352: 685-701.

Gustin, M. C., Zhou, X. L., Martinac, B., and Kung, C. C. (1988). A mechanosensitive ion channel in the yeast plasma membrane. Science (Wash. DC). 242: 762-763.

Hall, S. K., Zhang, J. P., and Lieberma, M. (1995). Cyclic AMP prevents activation of a swelling-induced chloride—sensitive conductance in chick heart cells. J Physiol (London). 488: 359-369.

Hamill, O. P. (1983a). Potassium and chloride channels in red blood cells. *In* Single Channel Recording, Ed. By B. Sakmann, E. Neher, pp. 451-471, Plenum Press, New York.

Hamill, O. P., Marty, A., Neher, E., Sakamnn, G., and Sigworth, F. W. (1981). Imporved patch clamp techniques fro high current resolution from cells and cell-free membrane patches. Pfluegers Arch. 391: 85-100.

Hamill, O. P., and Mcbride, Jr. D. W. (1992). Rapid adaptation of the MG channel in *Xenopus* oocytes. Proc Natl Acad Sci. 89: 7462-7466.

Hamill, O. P., and Mcbride, Jr. D. W. (1994a). The cloning of a mechanomembrane channel. Trends Neurosci. 17: 439-443.

Hamill, O. P., and Mcbride, Jr. D. W. (1995a). Mechanoreceptive membrane ion channels. Am. Sci. 83: 30-37.

Hamill, O. P., and Mcbride, Jr. D. W. (1995b). Pressure/patch clamp methods. *In* Patch Clamp Techniques and Protocols, Ed. By A. A. Boultio, G. B. Baher, W. Walz, pp. 75-87, Humana Press, Totowa, NJ.

Han, J., Gnatenco, C., Sladek, C. D., and Kim, D. (2003). Background and tandem-pore potassium channels in magnocellular neurosecretory cells of the rat supraoptic nucleus. J Physiol. 546:625–639

Hansen, D. E., Borgranelli, M., Stacy, G. P., and Taylor, L. K. (1991). Does-dependent inhibition of stretch-induced arrhythmias by gadolinium in isolated canine ventricles: evidence fro a unique mode of antiarrhythmic action. Circ Res. 69: 820-831.

Hart, G. (1994). Cellular electrophysiology in cardiac hypertrophy and failure. Cardiovasc Res. 28: 933–946.

Hase, C. C., Le Dain, A. C., and Martinac, B. (1995). Purification and functional reconstitution of the recombinant large mechanosensitive ion channel (MscL) of *Escherchia coli.* J Biol Chem. 270: 18329-18334.

Henneckes, R., Kaufmann, R. and Lab, M. (1981). The dependence of cardiac membrane excitation and contractile ability on active muscle shortening (Cat papillary muscle). Pfluegers Arch. 392: 22-28.

Heurteaux, C., Guy, N., Laigle, C., Blondeau, N., Duprat, F., Mazzuca, M., Lang-Lazdunski, L., Widmann, C., Zanzouri, M., Romey, G., and Lazdunski, M. (2004). TREK-1, a K(+) channel involved in neuroprotection and general anesthesia. J EMBO. 23(13): 2684-2695.

Hille, B. (2001). Ion Channels of Excitable Membranes. (3rd ed.). Sinauer Associates Inc. Publishers, Sunderland.

Hirst, B. H. (1989). The gastric mucosal barrier. In: J. Forte, Editor, Handbook of Physiology; Section 6Salivary, Gastric, Pancreatic and Hepatobiliary Secretion vol. III.

Hisads, T., Ordway, R. W., kirber, M. T., Singer, J. J., and Walsh, Jr. J. V. (1991). Hyperpolarixation-activated cationic channels in smooth muscle cells are stretch sensitive. Pfluegers Arch. 417: 493-499.

Holmes, J., Kubo, S. H., Cody, R. J., and Kligfield, P. (1985). Arrhythmias in ischemic and nonischemic dilated cardiomyopathy: prediction of mortality by ambulatory electrocardiography. Am J Cardiol. 55: 146–151.

Honore, E., Maingret, F., Lazdunski, M., and Patel, A. J. (2002). An intracellular proton sensor commands lipid- and mechano-gating of the K^+ channel TREK-1. J EMBO. 21: 2968–2976.

Hougaard, C., Jorgensen, F., and Hoffmann, E. K. (2001). Modulation of volume-sensitive K^+ current in Ehrlich ascites tumour cells by pH. Pflügers Archiv. 442: 622–633.

Howard, J., Roberts, W. M., and Hudspeth, A. J. (1988). Mechanoelectrical transduction by hair cells. Annu Rev Biophys Chem. 17: 99-124.

Hoyer, J., Distler, A., Haase, W., and Gogelein, H. (1994). Ca^{2+}influx through stretch-activated cation channels activate maxi K^+ channels in porcine endocardial endothelium. PNAS. 91: 2367-2371.

Hu, H., and Sachs, F. (1994). Effects of mechanical stimulation on embryonic chick heart cells. Biophys J. 66: A170-177.

Hu. H., and Sachs, F. (1997). Stretch-activated ion channels in the heart. J Mol Cell Cardiol. 9: 1511–1523.

Irina, K., Andre, K., Kay-Dietrich, W., Heinz, T., Axel, L., Holger, S., Joachim, G., and Lab, J. M. (2000). Mechanoelectric feedback after left ventricular infarction in rats.. Cardiovasc Res. 45(2): 370-8.

Isenberg, G., Kazanski, V., Kondratev, D., Gallitelli, M. F., Kiseleva, I., and Kamkin, A. (2003). Differential effects of stretch and compression on membrane currents and $[Na^+]_c$ in ventricular myocytes. Prog Biophys Mol Biol. 82: 43–56.

Janse, M. J., Coronel, R., Wilms-Schopman, F. J., and Groot, J. R. (2003). Mechanical effects on arrhythmogenesis: from pipette to patient. Prog Biophys Mol Biol. 82: 187–195.

Janse, M. J., and Wit, A. L. (1989). Electrophysiological mechanisms of ventricular arrhythmias resulting from myocardial ischemia and infarction. Physiol Rev. 69: 1049–1169.

January, C. T., and Moseucci, A. (1992). Cellular mechanisms of early afterdepolarization. Ann NJ Acad Sci. 644: 23–32.

Jones, S. A., Morton, M. J., Hunter, M., and Boyett, M. R. (2002). Expression of TASK-1, a pH-sensitive Twin-pore domain K+ channel, in rat myocytes. Am J Physiol. 283: H181-185.

Jukka, Y., Lehtonen, A., and kinnunen, P. K. J. (1995). Phospholipase A_2 as a mechanosensor. Biophys J. 68: 1888-1894.

Kamkin, A., Kiseleva, I., and Isenberg, G. (2000). Stretch-activated currents in ventricular myocytes: amplitude and arrhythmogenic effects increase with hypertrophy. Cardiovasc Res. 48(3): 409-20.

Kang, D., Choe, C., and Kim, D. (2005). Thermosensitivity of the two-pore domain K^+ channels TREK-2 and TRAAK. J Physiol. 564:103–116.

Kaufmann, R. L., Lab, M. J., Hennekes, R., and Krause, H. (1970). Feedback interaction of mechanical and electrical events in the isolated mammalian ventricular myocardium

(cat papillary muscle). Pflügers Arch. 324: 100–123.

Kawahara, K., and Matsuzaki, K. (1993). A stretch-activated cation channel in the apical membrane of A6 cells. Jpn J Physiol. 43: 817-832.

Kim, D. (1992). A mechanosensitive K+ channel in heart cells. Activation by arachidonic acid. J Gen Physiol. 100(6): 1021-40.

Kim, Y., Gnatenco, C., Bang, H., and Kim, D. (2001). Localization of TREK-2 K+ channel domains that regulate channel kinetics and sensitivity to pressure, fatty acids and pHi. Pflugers Arch 442(6): 952-60.

Kim, D., Fujita A., Horio Y., and Kurachi, Y. (1998). Cloning and functional expression of a novel cardiac two-pore background K^+ channel (cTBAK-1). Circ Res. 82: 513-518.

Kim, D. (1993). Novel cation-selective mechanosensitive ion channel in the atrial cell membrane. Circ Res. 72: 225-231.

Kim, D., and Fu, Y. (1993). Mechanosensitive ion channels in heart cells. J Gen Physiol. 65(9): 562-571.

Kim, D. (2003). Fatty acid-sensitive two-pore domain K+ channels. Trends Pharmacol Sci. 24(12): 648-654.

Kim, D. H., Sladek, C. D., Aguadovelasco, C., and Mathiasen, J. R. (1995). Arachidonic acid activation of a new family of K+ channels in cultured rat neuronal cells. J Physiol (Lond). 484: 643-660.

Kim, D., and Clapham, D. E. (1989). Potassium channels in cardiac cells activated by arachidonic acid and phospholipid. Science. 244: 1174-1176.

Kim, Y., Bang, H., and Kim, D. (1999). TBAK-1 and TASK-1, two-pore K^+ channel subunits: kinetic properties and expression in rat heart. Am J Physiol. Heart Circ Physiol. 277: H1669-1678.

Kim, Y., Bang, H., and Kim, D. (2000). TASK-3, a new member of the tandem pore K^+ channel family. J Biol Chem. 275: 9340-9347.

Kindler, C. H., Yost, C. S., and Gray, A. T. (1999). Local anesthetic inhibition of baseline potassium channels with two pore domains in tandem. Anesthesiology. 90: 1092-1102.
Kirber, M.T., Ordway, R. W., Clapp, L. H., Walsh, Jr., J. V., and Singer, J. J. (1992). Both

membrane stretch and fatty acids directly activate large conductance Ca^{2+}-acitivated K^+ channels in vascular smooth muscle cells. FEBS Lett. 297: 24-28.

Kjekshus, J. (1990). Arrhythymias and mortality in congestive heart failure. Am J Cardiol. 65: 421–481.

Klein, L. S., Miles, W. M., and Zipes, D. P. (1990). Effect of atrioventricular interval during pacing or reciprocating tachycardia on atrial size, pressure, and refractory period. Contraction-excitation feedback in human atrium. Circulation. 82: 60–68.

Koh, S. D., Monagham, K., Sergeant, G., Ro, S., Walker, R. L., Sanders, K. M., and Horowitz, B. (2001). TREK-1 regulation by nitric oxide and cGMP dependent protein kinase: An essential role in smooth muscle inhibitory neurotransmission. J Biol Chem. 276(47): 44338-44346.

Kohl, P., Day, K., and Noble, D. (1998). Cellular mechanisms of cardiac mechano-electric feedback in a mathematical model. J Cardio Canada. 14: 111-119.

Kohl, P., Hunter, P., and Noble, D. (1999). Stretch-induced changes in heart rate and rhythm: clinical observations, experiments and mathematical models. Prog Bioph Molec Biol. 71(1): 122-128.

Kohl, P., and Noble, D. (1996). Mechanosensitive connective tissue: potential influence on heart rhythm. Cardiovasc Res. 32: 62–68.

Komuro, I., Kaida, T., Shibazaki, Y., Kurabayashi, M., Katoh, Y., Hoh, E., Takaku, F., and Yazaki, Y. (1990). Stretching cardiac myocytes stimulates protooncogene expression. J. Biol Chem. 265(7): 3595–3598.

Komuro, I., Kudo, S., Yamazaki, T., Zou, Y., Shiojima, I., and Yazaki, Y. (1996). Mechanical stretch activates the stress-activated protein kinases in cardiac myocytes. J FASEB. 10: 631–636.

Kramer, C. M., Limaj, J. A. C., and Reichek, N. (1993). Regional differences in function within non-infarcted myocardium during left ventricular remodeling. Circulation. 88: 1279–1288.

Lab, M. J. (1996). Mechanoelectric feedback (transduction) in heart: concepts and implication. Cardiovasc Res. 32: 3–14.

Lab, M. J. (1999). Mechanosensitivity as an integrative system in heart: an audit. Progress in Biophysics & Molecular Biology. 71: 7–27.

Lab, M. J. (1980). Transient depolarisation and action potential alterations following mechanical changes in isolated myocardium. Cardiovasc Res. 14: 624–637.

Lab, M. J. (1982). Contraction-excitation feedback in myocardium. Circ Res. 50: 757-766.

Lab, M. J., Allen, D. G., Orchard, C. H. (1984). The effects of shortening on myoplasmic calcium concentration and on the action potential in mammalian ventricular muscle. Circ Res. 55: 825-829.

Lab, M. J., Zhou, B. Y., Dick, D. J., Horner, S. M., Murphy, C. F., and Harrison, F. G. (1993). Stretch-induced ventricular fibrillation in normal and globally anoxic isolated guinea pig hearts. J Physiol. 473: 183.

Lab, M. J. (1991). Monophasic action potential and the detection and significance of mechanoelectric feedback in vivo. Prog Cardiovasc Dis. 34: 29–35.

Lacampagne, A., Gannier, F., Argibay, J., Garnier, D., and Le Guennec, J. C. (1994). The stretch-activated ion channel blocker gadolinium also blocks L-type calcium channels in isolated ventricular myocytes of the guinea-pig. Biochem Biophys Acta. 1191: 205–208.

Lakatta, E. G., and Fozzard, H. A. (1992). Length modulation of muscle performance. In: The heart and cardiovascular system. 2nd edn. New York: Raven Press. PP: 1325-1349.

Langton, P. D. (1993). Calcium channel currents recorded from isolated myocytes of rat basilar artery are stretch sensitive. J Physiol. 471: 1-11.

Le Guennec, J. Y., White, E., Gannier, F., Argibay, J. A., and Garnier, D. (1991). Stretch-induced increase of resting intracellular calcium concentration in single guinea pig ventricular myocytes. Exp Physiol. 76: 975–978.

Lehrmann, R., and Seelig, J. (1994). Adsorption of Ca^{2+} and La^{3+} to bilayer membranes: measurement of the adsorption enthalpy and binding constant with titration calorimetry. Biochem Biophys Acta. 1189: 89-95.

Leonoudakis, D., Gray, A. T., Winegar, B. D., Kindler, C. H., Harada, M., Taylor, D. M., Chavez, R. A., Forsayeth, J. R., and Yost, C. S. (1998). An open rectifier potassium channel with two-pore domain in tandem cloned from rat cerebellum. J Neurosci. 18: 868–877.

Lerman, B. B., Burkhoff, D., Yue, D. T., and Sagawa, K. (1985). Mechanoelectrical feedback: independent role of preload and contractility in modulation of canine ventricular excitability. J Clin Invest. 76: 1843-1850.

Lesage, F., and Lazdunski, M. (2000). Molecular and functional properties of two-pore-domain potassium channels. Am J Physiol. Renal Physio. 229: F703-801.

Lesage F, Terrenoire C., Romey G., and Lazdunski, M. (2000). Human TREK2, a 2P domain mechano-sensitive K+ channel with multiple regulations by polyunsaturated fatty acids, lysophospholipids, and Gs, Gi, and Gq protein-coupled receptors. J Biol Chem. 275(37): 28398-405.

Lesage, F. (2003). Pharmacology of neuronal background potassium channels. Neuropharmacology. 44(1): 1-7.

Lesage, F., Guillemare, E., Fink, M., Duprat, F., Lazdunski, M., Romey, G., and Barhanin, J. (1996a). A pH-sensitive yeast outward rectifier K^+ channel with two pore domains and novel gating properties. J Biol Chem. 271: 4183-4187.

Lesage, F., Guillemare, E., Fink, M., Duprat, F., Lazdunski, M., Romey, G., and Barhanin, J. (1996b). TWIK-1, a ubiquitous human weakly inward rectifying K^+ channel with a novel structure. J EMBO. 15: 1004-1011.

Lesage, F., Lauritzen, I., Duprat, F., Reyes, R., Fink, M., Heurteaux, C., and Lazdunski, M. (1997). The structure, function and distribution of the mouse TWIK-1 K^+ channel. FEBS Lett. 402: 28-32.

Lesage, F., and Lazdunski, M. (1998). Mapping of human potassium channel genes TREK-1 (KCNK2) and TASK (KCNK3) to chromosomes 1q41 and 2p23. Genomics. 51: 478-479.

Lesage, F., and Lazdunski, M. (1999). Potassium channels with two P-domains. In: Potassium Ion Channels: Molecular Structure, Function and Diseases, edited by Kurachi Y, Jan LY, and Lazdunski M. San Diego, CA: Academic. pp: 199-222.

Lesage, F., Maingret, F., and Lazdunski, M. (2000). Cloning and expression of human TRAAK, a polyunsaturated fatty acids-activated and mechano-sensitive K^+ channel. FEBS Lett. 471: 137-140.

Lesage, F., Mattei, M. G, Fink, M., Barhanin, J., and Lazdunski, M. (1996c). Assignment of the human weak inward rectifier K^+ channel TWIK-1 gene to chromosome 1q42-q43. Genomics. 34: 153-155.

Levine, J. H., Guarnieri, T., Kadish, A. H., White, R. I., Calkins, H., and Khan, J. S. (1988). Changes in myocardial repolarization in patients undergoing balloon valvuloplasty for congenital pulmonary stenosis: evidence fro contraction-excitation feedback in humans. Circulation. 77: 70-77.

Li, Z-B., Zhang, H-X., Li, L-L., and Wang, X-L. (2005). Enhanced expressions of arachidonic acid-sensitive tandem-pore domain potassium channels in rat experimental acute cerebral ischemia. Biochem Biophys Res Commun. 327(4): 1163-9.

Li, W., Kohl, P., and Trayanova, N. (2004). Induction of ventricular arrhythmias following mechanical impact: a simulation study in 3D. J Mol Histol. 35(7): 679-86.

Li, X. T., Dyachenko, V., Zuzarte, M., Putzke, C., Preisig-Müller, R., Isenberg, G., and Daut, J. (2006). The stretch-activated potassium channel TREK-1 in rat cardiac ventricular muscle. Cardiovasc Res. 69(1): 86-97.

Lima, J. A. C., Becker, L. C., and Melin, J. A. (1984). Cardiac - and -myosin heavy chain genes are organized in tandem. Proc. Nat Acad Sci. 81: 2626–2630.

Link, M. S., Wang, P. J., Pandian, N. G., Bharati, S., Udelson, J. E., Lee, M-Y., Vecchiotti, M. A., VanderBrink, B. A., Mirra, G., Marson, B. J., and Estes III M, E. (1998). An experimental model of sudden cardiac death due to low-energy chest-wall impact (Commotio cordis). New Engl J Med. 338: 1805-1811.

Liu, W., and Saint, D. A. (2002a). A new quantitative method of real time reverse transcription polymerase chain reaction assay based on simulation of polymerase chain reaction kinetics. Anal Biochem. 302(1): 52-9.

Liu, W., and Saint, D. A. (2002b). Validation of a quantitative method for real time PCR kinetics. Biochem Biophys Res Commun. 294(2): 347-53.

Liu, W., and Saint, D. A. (2004). Heterogeneous expression of tandem-pore K+ channel genes in adult and embryonic rat heart quantified by real-time polymerase chain reaction. Clin Exp Pharmacol Physiol. 31(3): 174-8.

Lopes, C. M., Gallagher, P. G., Buck, M. E., Butler, M. H., and Goldstein, S. A. N. (2000). Proton block and voltage gating are potassium-dependent in the cardiac leak channel KCNK-3. J Biol Chem. 275: 16969–16978.

Lopes, C. M., Rohacs, T., Czirjak, G., Balla, T., Enyedi, P., and Logothetis, D. E. (2005). J Physiol. 564:117–129.

Lopes, C. M., Zilberberg, N., and Goldstein, S. A. N. (2001). Block of KCNK-3 by protons: evidence that 2-P-domain potassium channel subunits function as homodimers. J Biol Chem. 276: 24449–24452.

Lundbaek, J. A., and Anderson, O. S. (1994). Lysophosphlipids modulate channel function by altering the mechanical properties of lipid bilayers. J Gen Physiol. 104: 645-673.

Maingret, F., Fosset, M., Lesage, F., Lazdunski, M., and Honoré, E. (1999). TRAAK is a mammalian neuronal mechano-gated K^+ channel. J Biol Chem. 274: 1381-1387.

Maingret, F., Lauritzen, I., Patel, A., Heurteaux, C., Reyes, R., Lesage, F., Lazdunskim, M., and Honoré, E. (2000). TREK-1 is a heat-activated background channel. J. EMBO. 19: 2483-2491.

Maingret, F., Patel, A. J., Lesage, F., Lazdunski, M., and Honore, E. (1999). Mechano- or acid stimulation, two interactive modes of activation of the TREK-1 potassium channel. J Biol Chem. 274: 26691-26696.

Maingret, F., Patel, A. J., Lesage, F., Lazdunski, M., and Honore, E. (2000). Lysophospholipids open the two-pore Domain Mechano-gated K+ Channels TREK-1 and TRAAK. J Biol Chem. 275(14): 10128-10133.

Mann, D. L., Kent, R. L., and Cooper, G 4^{th}. (1989). Load regulation of the properties of adult feline cardiocytes: growth induction by cellular deformation. Circ Res. 64(6): 1079–1090.

Mancuso, D. J., Abendschein, D. R., Jenkins, C. M., Han, X., Saffitz, J. E., Schuessler, R. B., and Gross, R. W. (2003). Cardiac ischemia activates calcium-independent phospholipase A2beta, precipitating ventricular tachyarrhythmias in transgenic mice: rescue of the lethal electrophysiologic phenotype by mechanism-based inhibition. J Biol Chem. 278: 22231-6.

Marcotti, W., Sachs, F., Ashmore, J. F., and Kros, C. J. (2001). Effect of a peptide tarantula toxin on mechano-transduction in neonatal mouse cochlear hair cells. Brit J Audio. 5: 156-162.

Markin, V. S., and Martinac, B. (1991). Mechanosensitive ion channels as reporters of bilayer expansion: a theoretical model. Biophys J. 60: 1120-1127.

Martinac, B. (1992). Mechanosensitive ion channels: biophysics and physiology. *In* Thermodynamics of Cell Surface Receptors, ed. By M. B. Jackson, pp. 327-352, CRC Press, Boca Raton, FL.

Martinac, B., Adler, J., and Kung, C. (1990). Mechanosensitive ion channels of *E. coli* activated by amphipaths. Nature. 348: 261-263.

Meadows, H. J., Benham, C. D., and Chapman, C. G. (2000). Cloning, Localisation and functional expression of the human orthologue of the TREK-1 potassium channel. Eur J Physiol. 439: 714-722.

Medhurst, A. D., Chapman, C. G., Meadows, H. J., Godden, R. J., Duckworth, M., Kelsell, R. E., Rennie, G. I., Gloger, I. S., and Pangalos, M. N. (2001). Distribution analysis of human two pore domain potassium channels in tissues of the central nervous system and periphery. Mol Brain Res. 86(1-2): 101-114.

Medina, I. R., and Bregestovski, P. D. (1988). Stretch-activated ion channels modulate the resting potential during early embryogenesis. Proc R Soc London Ser. B. 235: 95-102.

Meizlish, J. L., Berger, H. J., Plankey, M., Errico, D., Levy, W., and Zaret, B. L. (1984). Functional left ventricular aneurysm formation after acute transmural myocardial infarction. N Engl J Med. 311: 1001–1006.

Meola, F. (1879). La commozione toracica. Giornale internazionale della Scienze Mediche. 1: 923-937.

Meves, H. (1994). Modulation of ion channels by arachidonic acid. Prog Neurobiol. 43: 175-186.

Millar, J. A., Barratt, L., Southan, A. P., Page, K. M., Fyffe, R. E. W., Robertson, B., and Mathie, A. (2000). A functional role for the two-pore domain potassium channel TASK-1 in cerebellar granule neurons. Proc Nati Acad Sci. 97: 3614–3618.

Millet, B., and Pickard, B. G. (1988). Gadolinium ion is the inhibitor suitable for testing the putative role of stretch-activated ion channels in geotropism and thigmotropism (abstract). Biophys J. 53: 155a.

Morris, C. E. (1990). Mechanosensitive ion channels. J Membr Biol. 113: 93-107.

Morris, C. E., and Horn, R. (1991). Failure to elicit neuronal macroscopic mechno-sensitive currents anticipated by single channel studies. Science (Wash. DC). 251: 1246-1249.

Murbartian, J., Lei, Q., Sando, J. J., and Bayliss, D. A. (2005). Sequential phosphorylation mediates receptor- and kinase-induced inhibition of TREK-1 background potassium channels. J Biol Chem. 280(34): 30175-84.

Nazir, S. A., and Lab, M. J. (1996). Mechano-electric feedback and atrial arrhythmias. Cardiovasc Res. 32: 52–61.

Nelaton, A. (1876). Elements de Pathologie Chirurgicale. Librairie Germer Bathliere et co. Paris.

Niemeyer, M. I., Cid, L. P., Barros, L. F., and Sepulveda, F. V. (2001). Modulation of the two-pore domain acid-sensitive K^+ channel TASK-2 (KCNK5) by changes in cell volume. J Biol Chem. 276: 43166–43174.

Niu, W., and Sachs, F. (2003). Dynamic properties of stretch-activated K^+ channels in adult rat atrial myocytes. Prog Biophys Mol Biol. 82: 121–135.

O'Connell, A. D., Morton, M. J., and Hunter, M. (2002). Two-pore domain K+ channels-molecular sensors. Biochem Biophys Acta. 1566(1-2): 152-61.

Oike, M., Droogmans, G., and Nilius, G. (1994). The volume-activated chloride current in human endothelial cells depends on intracellular ATP. Pflugers Arch. 427: 184-186.

Olesen, S. P., Clapham, D. E., and Davies, P. F. (1988). Haemodynamic shear stress activates a K^+ current in vascular endothelial cells. Nature. 330: 168-170.

Oliet, S. H. R., and Bourque, C. W. (1994). Mechanosensitive channels transducer osmosensitivity in supraoptic neurons. Nature. 364: 341-343.

Olivetti, G., Capasso, J. M., Meggs, L. G., Sonnenblick, E. H., and Anversa, P. (1991). Cellular basis of chronic ventricular remodeling after myocardium infarction in rats. Circ Res. 68: 856–859.

Opsahl, L., and Webb, W. W. (1994). Transduction of membrane tension by the ion channel alamethicin. Biophys J. 66: 71-74.

Ordway, R. W., Petrou, S., kirber, M. T., Walsh, J. V., and Singer, J. J. (1991). Two distinct mechanisms of ion channel activation by membrane stretch: evidence that

endogenous fatty acids mediate stretch activation of K^+ channel (abstract). Biophys J. 61: A390-397.

Ordway, R. W., Petrou, S., kirber, M. T., Walsh, J. V., and Singer, J. J. (1995). Stretch activation of a toad smooth muscle K^+ channel may be mediated by fatty acids. J Physiol. 484: 3311-3337.

Page, E., Mccallister, L. P., and Power, B. (1971). Sterological measurements of cardiac ultrastructures implicated in excitation-contraction coupling. Proc Natl Acad Sci USA. 68: 1465-1466.

Paintal, A. S. (1964). Effects of drugs on vertebrate mechanoreceptors. Pharmacol Rev. 16: 341-380.

Pan, J., Fukuda, K., Saito, M., Matsuzaki, J., Kodama, H., Sano, M., Takahashi, T., Kato, T., and Ogawa, S. (1999). Mechanical stretch activates the JAK/STAT pathway in rat cardiomyocytes. Circ Res. 84(10): 1127-1136.

Paoletti, P., and Ascher, P. (1994). Mechanosensitivity of NMDA receptors in cultured mouse central neurons. Neuron. 13: 645-655.

Patel, A. J., and Honore, E. (2001). Properties and modulation of mammalian 2P domain K+ channels. Trends Neurosci. 24(6): 339-346.

Patel, A. J., and Honore, E. (2002). The TREK two pore domain K+ channels. J Physiol. 539(3): 647-656.

Patel, A. J., Honoré, E., Maingret, F., Lesage, F., Fink, M., Duprat, F., and Lazdunski, M. (1998). A mammalian two-pore domain mechano-gated S-type K^+ channel. J EMBO. 17: 4283-4290.

Patel, A. J., Honore, E., Maingret, F., Lesage, F., Fink, M., Romey, G., and Lazdunski, M. (1999). Inhalational anaesthetics activate two-pore-domain background K+ channels. Nat Neurosci. 2: 422-427.

Patel, A. J., Lazdunski, M., and Honore, E. (2001). Lipid and mechano-gated 2P domain K+ channels. Curr Opin Cell Biol. 13: 421-428.

Patten, B. M. (1949). Initiation and early changes in the character of the heart beat in vertebrate embryos. Physiolo Rev. 29: 31-47.

Penefsky, Z. J., and Hoffman, B. F. (1963). Effects of stretch on mechanical and electrical properties of cardiac muscle. Am J Physiol. 204: 433-438.

Petrou, S., Ordway, R. W., Hamilton, J. S., Walsh, Jr., J. V., and Singer, J. J. (1994). Structural requirements for charged lipid molecules to directly increase or suppress K^+ channels activity in smooth muscle cells. J Gen Physiol. 103: 471-486.

Petrov, A. G., and Usherwood, P. N. R. (1994). Mechanosensitivity of cell membranes: ion channels, lipid matrix and cytoskeleton. Eur Biophys J. 23: 1-19.

Pye, P., and Cobbe, S. M. (1992). Mechanisms of ventricular arrhythmias in cardiac failure and hypertrophy. Cardiovasc Res. 26: 740–750.

Quasthoff, S. (1994). A mechanosensitive K^+ channel with fast gating kinetics on human axons blocked by gadolinium ions. Neurosci Lett. 169: 39-42.

Rajala, G. M., Kalbfleisch, J. H., and Kaplan, S. (1976). Evidence that blood pressure controls heart rate in the chick embryo prior to neural control. J Embryo Experi Morpho. 36: 685-695.

Rajan, S., Wischmeyer, E., Liu, G. X., Presig-Müller, R., Daut, J., Karschin, A., and Derst, C. (2000). TASK-3, a novel tandem pore domain acid-sensitive K^+ channel. J Biochem. 275: 16650–16657.

Ravens, U. (2003). Mechano-electric feedback and arrhythmias. Prog Biophys Mol Biol. 82:255–266.

Reiter, M. J., Synhorst, D. P., and Mann, D. E. (1988). Electrophysiological effect of acute ventricular dilatation in the isolated rabbit heart. Circ Res. 62: 554–562.

Reiter, M. J. (1996). Effects of mechano-electric feedback: potential arrhythmogenic influence in patients with congestive heart failure. Cardiovasc Res. 32: 44–51.

Reyes, R., Duprat, F., Lesage, F., Fink, M., Salinas, M., Farman, N., and Lazdunski, M. (1998). Cloning and expression of a novel pH-sensitive two pore domain K^+ channel from human kidney. J Biol Chem. 273: 30863-30869.

Riemer, T., Sobie, E., and Tung, L. (1998). Stretch-induced changes in excitability and arrhythmogenesis in experimentally-based heart cell models. Circulation. 111: 111–112.

Rozich, J. D., Barnes, M. A., Schmid, P. G., Zile, M. R., McDermott, P. J., and Cooper, G 4th. (1995). Load effects on gene expression during cardiac hypertrophy. J Mol Cell Cardiol. 27: 485–499.

Ruknudin, A., Sachs, F., and Bustamante, J. O. (1993). Stretch-activated ion channels in tissue-cultured chick heart. Am J Physiol. 264: H960-972.

Sachs, F. (1988). Mechanical transduction in biological systems. CRC Crit Rev Biomed Eng. 16: 141-169.

Sachs, F. (1991). Mechanical transduction by membrane ion channels: a mini review. Mol Cell Biochem. 113: 93–107.

Sachs, F. (1994). Modeling mechanical-electrical transduction in the heart. Springer Verlag, New York. PP: 308-328.

Sachs, F. (2002). Specific stretch-channel blockers: a new class of anti-arrhythmic drugs. 3rd international workshop on cardiac mechano-electric feedback and arrhythmia. PP: 58-59.

Sackin, H. (1989). A stretch-activated K^+ channel sensitive to cell volume. Proc Natl Acad Sci. 86:1731-1735.

Sackin, H. (1995). Mechanosensitive channels. Annu Rev Physiol. 57: 333-353.

Sadoshima, J. I., and Izumo, S. (1993). Mechanotransduction in stretch-induced hypertrophy. Annu Rev Physiol. 23: 428–441.

Sadoshima, J., and Izumo, S. (1993). Mechanical stretch rapidly activates multiple signal transduction pathways in cardiac myocytes: Potential involvement of an autocrine/paracrine mechanism. J EMBO. 12(4): 1681-1692.

Sadoshima, J., Jahn, L., Takahashi, T., Kulik, T. J., and Izumo, S. (1992a). Molecular characterization of the stretch-induced adaptation of cultured cardiac cells. An in vitro model of load-induced cardiac hypertrophy. J Biol Chem. 267(15): 10551–10560.

Sadoshima, J., Takahashi, T., Jahn, L., and Izumo. S. (1992b). Roles of mechano-sensitive ion channels, cytoskeleton, and contractile activity in stretch-induced immediate-early gene expression and hypertrophy of cardiac myocytes. Proc. Natl. Acad. Sci. 89(20): 9905-9.

Salinas, M., Reyes, R., Lesage, F., Fosset, M., Heurteaux, C., Romey, G., and Lazdunski, M. (1999). Cloning of a new mouse two-P domain channel subunit and a human homologue with a unique pore structure. J Biol Chem. 274: 11751-11760.

Salmon, A. H. J., Mays, J. L., Dalton, G. R., Jones, J. V., and Levi, A. J. (1997). Effect of streptomycin on wall-stress-induced arrhythmias in the working rat heart. Cardiovasc Res. 34: 493-503.

Sambrook, J., Fritsch, E. F., and Maniatis, T. (1989). Molecular Cloning: A laboratory manual, (Second Edition). Cold Spring Habour Laboratory Press, USA.

Sasaki, H., Mitsuiye, T., and Noma, A. (1992). Effects of mechanical stretch on membrane currents of single ventricular myocytes of guinea pig heart. Jpn J Physiol. 42: 957-970.

Schlichter, L. C., and Sakellaropoulos, G. (1994). Intracellular Ca^{2+} signaling induced by osmotic shock in human T-lymphocytes. Exp Cell Res. 215: 211-222.

Schlomak, G., and Hinrichs, A. (1932). Experimentelle Untersuchungen uber den EinfluB stumpfer Brustkorbverletzungen auf das elektrokardiogrmm. Zeitschrift fuer die Besamte Experimentelle Medizin. 81: 43-61.

Schmid, A., Feick, P., and Schulz, I. (1997). Inwardly rectifying, voltage-dependent and resting potassium currents in rat pancreatic acinar cells in primary culture. J Physiol (Lond). 504: 259-270.

Schmid, A., and Schulz, I. (1995). Characterization of single potassium channels in mouse pancreatic acinar cells. J Physiol (Lond). 484: 661-676.

Shinbane, J. S., Wood, M. A., and Jensen, D. N. (1997). Tachycardia-induced cardiomyopathy: A review of animal models and clinical studies. J Am Coll Cardiol. 29: 709–715.

Sigurdson, W. J., Ruknudin, A., and Sachs, F. (1992). Calcium imaging of mechanically induced fluxes in tissue cultured chick heart; role for stretch-activated ion channels. Am J Physiol. 262: H1110-1115.

Sigurdson, W. J., Morris, C. E., Brezden, B. L., and Gardner, D. R. (1987). Stretch activation of a K^+ channel in molluscan heart cells. J Exp Biol. 127: 191-209.

Small, D. L., and Morris, C. E. (1995). Pharmacology of stretch-activated channels in Lymnaea neurons. Br J Pharmacol. 114: 180-185.

Soeller, C., and Cannell, M. B. (1999). Examination of the transverse tubular system in living cardiac rat myocytes by 2-photon microscopy and digital image-processing techniques. Circ Res. 84: 266-275.

Sokabe, M., Hasegawa, M., and Yamamori, K. (1993). Blockers and activators for stretch-activated ion channels of chick skeletal muscle. Anne N Y Acad Sci. 707: 417-421.

Sorota, S. (1992). Swelling-induced chloride-sensitive current in canine atrial cells revealed by whole-cell patch-clamp method. Circ Res. 70: 679-687.

Suchyna, T. M. (2000). Identification of a peptide toxin from Grammostola spatulata spider venom that blocks stretch activated channels. J Gen Physiol. 115: 585-598.

Sugiura, S., Hunter, W. C., and Sagawa, K. (1989). Long-term versus intrabeat history of ejection as determinants of canine ventricular end-systolic pressure. Circ Res. 64: 225-264.

Sukharev, S. I., Blount, P., Martinac, G., Blatiner, F. R., and Kung, C. (1994). A large-conductance mechanosensitive channel in *E. coli* encoded by *mscL* alone. Nature. 368: 265-268.

Suleymanian, M., Clemo, H., Cohen, N., and Baumgarten, C. (1995). Stretch-activated channel blockers modulate cell volume in cardiac ventricular myocytes. J Mol Cell Cardiol. 27: 721–728.

Swerdloe, C. D., Winkle, R. A., and Mason, J. W. (1983). Determinants of survival in patients with ventricular tachyarrhythmias. N Engl J Med. 308: 1436–1442.

Taggart, P., Sutton, P. M., Treasure, T., Lab, M., O'Brien, W., Runnalls, M., Swanton, R. H., and Emanuel, R. W. (1988). Monophasic action potentials at discontinuation of cardiopulmonary bypass: evidence for contraction-excitation feedback in man. Circulation. 77: 1266-75.

Taggart, P., Sutton, P., Lab, M., Runnalls, M., O'Brien, W., and Treasure, T. (1992). Effect of abrupt changes in ventricular loading on repolarization induced by transient aortic occlusion in humans. Am J Physiol. 263: H816–823.

Taggart, P., and Sutton, P. M. I. (1999). Cardiac mechano-electric feedback in man: clinical relevance. Prog Biophys Mol Biol. 71(2): 132-141.

Taggart, P., Sutton, P. M. I., Boyett, M. R., Lab, M., and Swanton, H. (1996). Human ventricular action-potential duration during short and long cycles: rapid modulation by ischemia. Circulation. 94: 2526–2534.

Takagi, S., Miyazaki, T., Moritani, K., Miyoshi, S., Furukawa, Y., Ito, S., and Ogawa, S. (1999). Gadolinium suppresses stretch-induced increases in the differences in epicardial and endocardial monophasic action potential durations and ventricular arrhythmias in dogs. J Jpn Circ. 63: 296-302.

Takanashi, H., Sawanobori, T., Kamisaka, K., Maezawa, H., and Hiraoka, M. (1994). Properties of single potassium channels in guinea pig hepatocytes. J Cell Physiol. 161: 537-543.

Talley, E. M., Lei, Q., Sirois, J. E., and Bayliss, D. A. (2000). TASK-1, a two-pore domain K^+ channel is modulated by multiple neurotransmitters in motoneurons. Neuron. 25: 399–410.

Tan, J. H., Liu, W., and Saint, D. A. (2002). Trek-like potassium channels in rat cardiac ventricular myocytes are activated by intracellular ATP. J Membr Biol. 185: 201–207.

Tan, J. H., Liu, W., and Saint, D. A. (2004a). Differential expression of the mechanosensitive potassium channel TREK-1 in epicardial and endocardial myocytes in rat ventricle. Exp Physiol. 89(3): 237-42.

Tan, J. H., Liu, W., and Saint, D. A. (2004b). Trek-like potassium channels in rat cardiac ventricular myocytes are activated by intracellular ATP. J Membr Biol. 185(3): 201-7.

Terrenoire, C., Lauritzen, I., Lesage, F., Romey, G., and Lazdunski, M. (2001). A TREK-1-like potassium channel in atrial cells inhibited by β-adreergic stimulation and activated by volatile anaesthetics. Circ Res. 89: 336-342.

Tseng, G. N. (1992). Cell swelling increases membrane conductance for canine cardiac cells: evidence for a volume-sensitive Cl: channel. Am J Physiol. 262: C1056-1068.

Ubl, J., Murer, H., and Kolb, H. A. (1988). Ion channels activated by osmotic or mechanical stress in membranes of opossum kidney cell. J Membr Biol. 104: 223-232.

Van Wagoner, D. R. (1993). Mechanosensitive gating of atrial ATP-sensitive potassium channels. Circ Res. 72: 973-983.

Vandenburgh, H., and Kaufman, S. (1979). In vitro model for stretch-induced hypertrophy of skeletal muscle. Science. 203(4377): 265–268

Vandorpe, D. H., and Morris, C. E. (1992). Stretch activation of the Aplysia S-channel. J Membr Biol. 127: 205-214.

Vandorpe, D. H., Small, D. H., Dabrowski, A. R., and Morris, C. E. (1994). FMR-Famide and membrane stretch as activation of the *Aplysia S*-channel. Biophys J. 66: 46-58.

Wang, Z. W., Kunkel, M. T., Wei, A., Butler, A., and Salkoff, L. (1999). Genomic organization of nematode 4TM K^+ channels. Ann NY Acad Sci. 868: 286-303.

Watkins, C. S., and Mathie, A. (1996). A non-inactivating K^+ current sensitive to muscarinic receptor activation in rat cultured cerebellar granule neurons. J Physiol. 491: 401–412.

Weaver, W. D., Lorch, G. S., Alvarez, H. A., and Cobb, L. A. (1976). Angiographic findings and prognostic indicators in patients resuscitated from cardiac death. Circulation. 54: 895–900.

Wellner, M. C., and Isenberg, G. (1994). Stretch effects on whole-cell currents of guinea-pig urinary bladder myocytes. J Physiol. 480: 439-448.

White, H. D., Norris, R. N., Brown, M. A., Brandt, P. W., Whitlock, R. M. L., and Wild, C. J. (1987). Left ventricular end systolic volume as the major determinant of survival after recovery from myocardial infarction. Circulation. 76: 44–51.

Wilkinson, M. C., McBride, Jr. D. W., and Hamill, O. P. (1996a). Testing the putative role of a mechano-gated channel in *Xenopus oocytes* maturation, fertilization and tadpole development (abstract). Biophys J. 70: A349.

Wilkinson, M. C., McBride, Jr. D. W., and Hamill, O. P. (1996b). On the role of a mechano-gated cation channel in *Xenopus oocytes*. J Phsiol. 491: P101-102.

Xu, X., Pan, Y., and Wang, X. (2004). Alterations in the expression of lipid and mechano-gated two-pore domain potassium channel genes in rat brain following chronic cerebral ischemia. Mol Brain Res. 120(2): 205-9.

Yamazaki, T., Tobe, K., Hoh, E., Maemura, K., Kaida, T., Komuro, I., Tamemoto, H., Kadowaki, T., Nagai, R., and Yazaki, Y. (1993). Mechanical loading activates mitogen-activated protein kinase and S6 peptide kinase in cultured rat cardiac myocytes. J Biol Chem. 268(16): 12069-12076.

Yang, X-C., and Sachs, F. (1989). Block of stretch-activated ion channels in *Xenopus oocytes* by gadolinium and calcium ions. Science. 243: 1068-1071.

Yu, A., Ermakov, A. Z., Averbakh, V. I., Lobyshev, V. I., and Sukharev, S. I. (1996). Effects of gadolinium on electrostatic and thermodynamic properties of lipid membranes (abstract). J Biophys. 70: A96.

Zabel, M., Koller, B. S., Sachs, F., and Franz, M. R. (1996). Stretch-induced voltage changes in the isolated beating heart: importance of the timing of stretch and implications for stretch-activated ion channels. Cardiovasc Res. 32: 120–130.

Zeng, T., Bett, G. C., and Sachs, F. (2000). Stretch-activated whole cell currents in adult rat cardiac myocytes. Am J Physiol Heart. Circ Physiol. 278: H548–557.

Zhang, J., Hall, S. K., and Lieberman, M. (1993a). An early transient current activates the swelling-induced chloride conductance in cardiac myocytes. J Biophys. 66: A442.

Zhang, J., Rasmusson, R. L., Hall, S. K., and Lieberman, M. (1993b). A chloride current associated with swelling of cultured chick heart cells. J Physiol (London). 472: 801-820.

Zhou, X-L., Stumpf, M. A., Hoch, H. C., and Kung, C. (1991). A mechanosensitive channel in whole cells and in membrane patches of the fungus *Uromyces*. Science. 253: 1415-1417.

Zhou, X-L., Vaillant, B., Loukin, S. H., Kung, C., and Saimi, Y. (1995). YKC1 encodes the depolarization-activated K^+ channel in the plasma membrane of yeast. FEBS Lett. 373: 170-176.

APPENDIX

IMMUNOHISTOCHEMISTRY OF TREK-1 IN HUMAN ATRIUM AND VENTRICLE

The Location of TREK-1 channel in atrial appendage was revealed by immunohistochemical labelling with specific antibody for TREK-1 channels. In paraffin section, human atrial cardiac myocytes are formed in bundles, which are separated by connective tissue (Fig 26A). TREK-1 immunoreactivity was observed as bright punctate granules in most of cardiac myocytes. Many of them were found along the membrane of the cardiac myocytes (Fig 26A). No connective tissue was labelled. No immunoreactivity was found in negative control preparation after omission of primary antibody (Fig 26B) and after preincubation with the control peptide antigen. In human ventricular tissue, cardiac myocytes are also formed in bundles but of larger size. There was much less connective tissue between the muscle bundles. TREK-1 immunoreactivity was also observed as bright punctate granules in ventricular cardiac myocytes, with no connective tissue labelling (Fig 26C). No immunoreactivity was found in negative control preparation after omission of primary antibody (Fig 26D) and after preincubation with the control peptide antigen. Immunohistochemistry was provided by Dr. Shiyong Yuan.

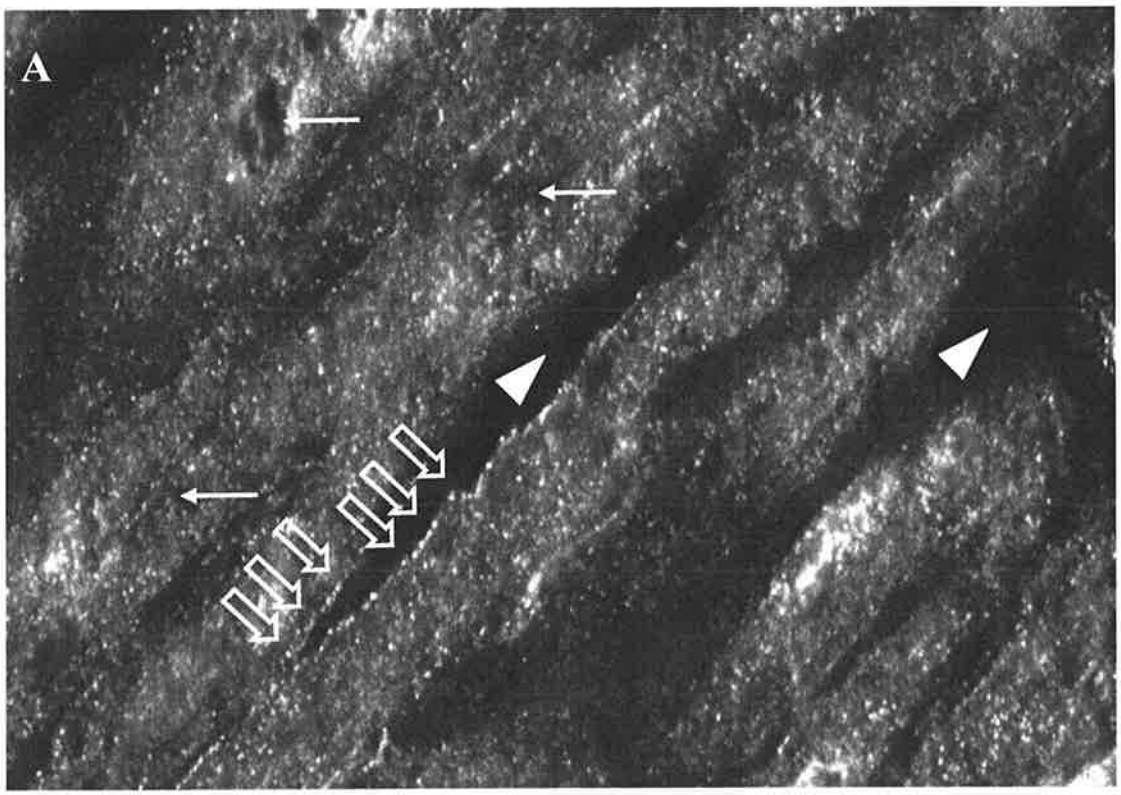

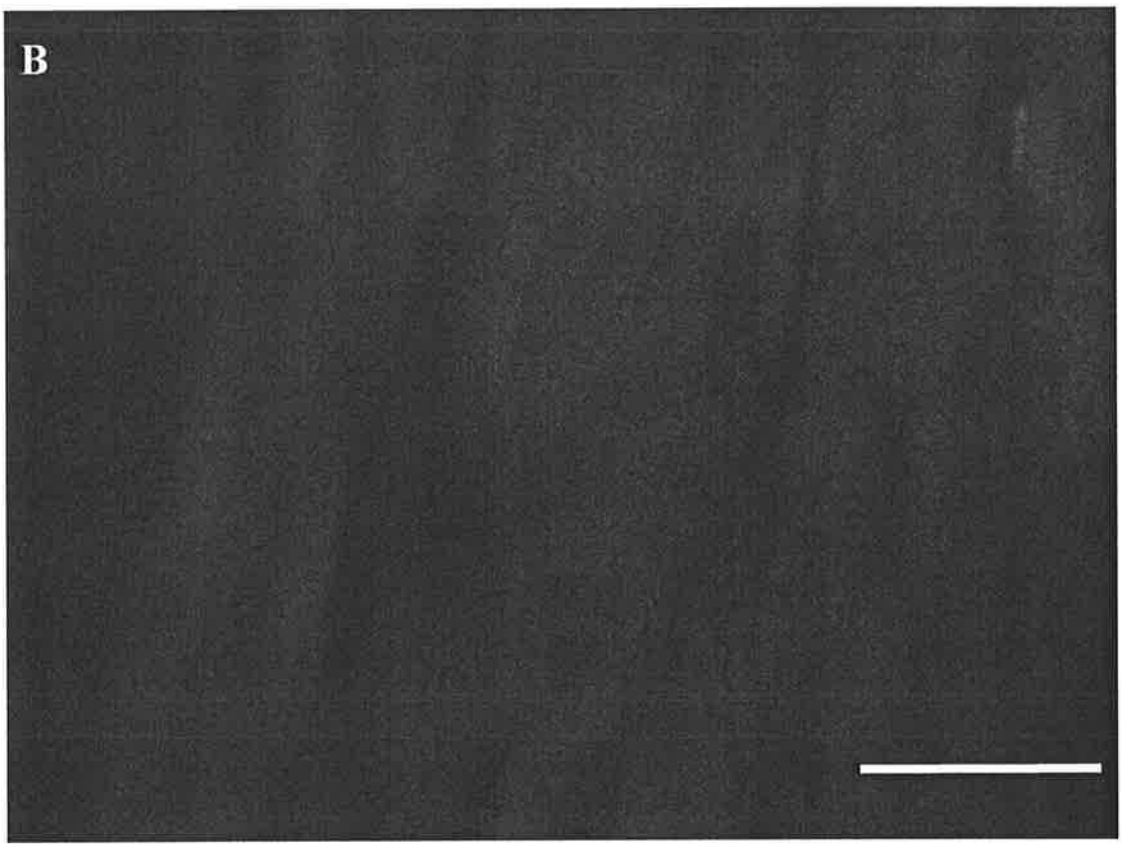
B

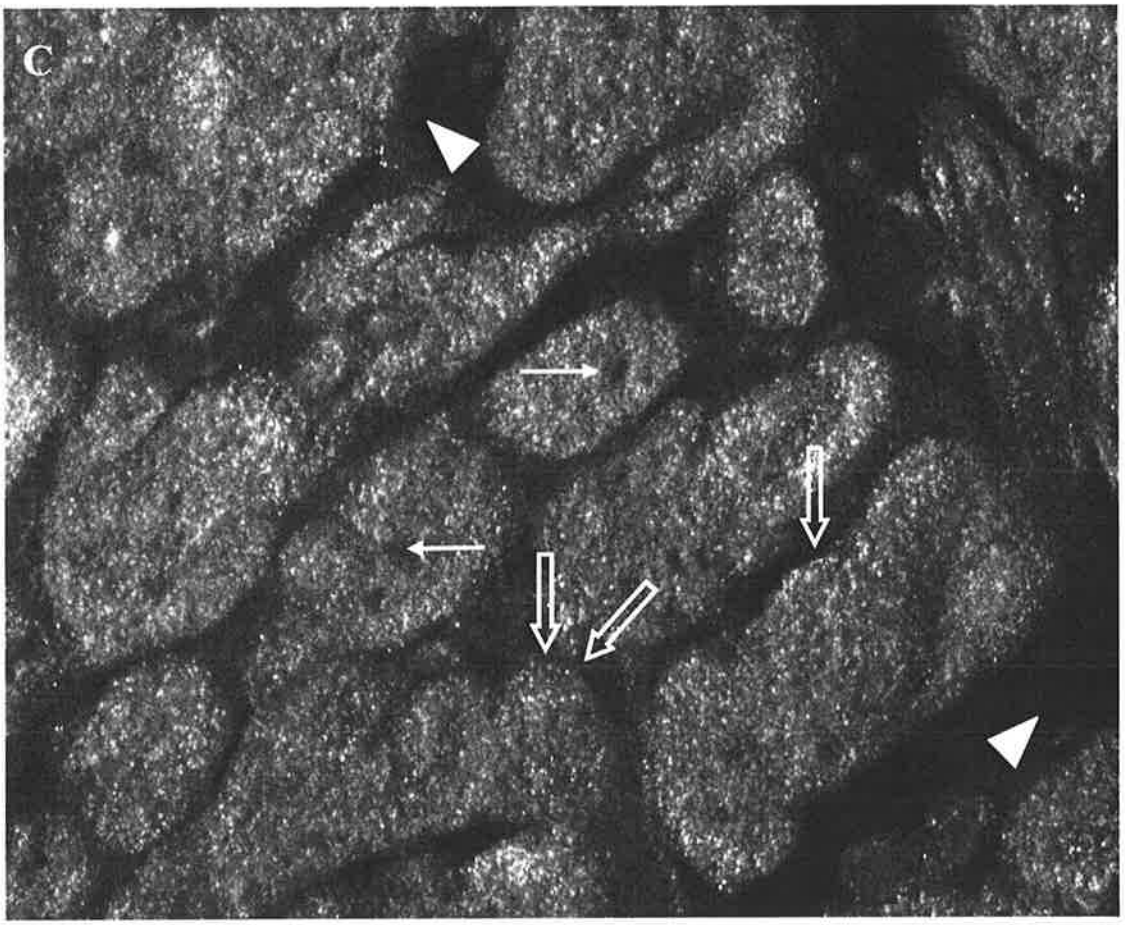
C

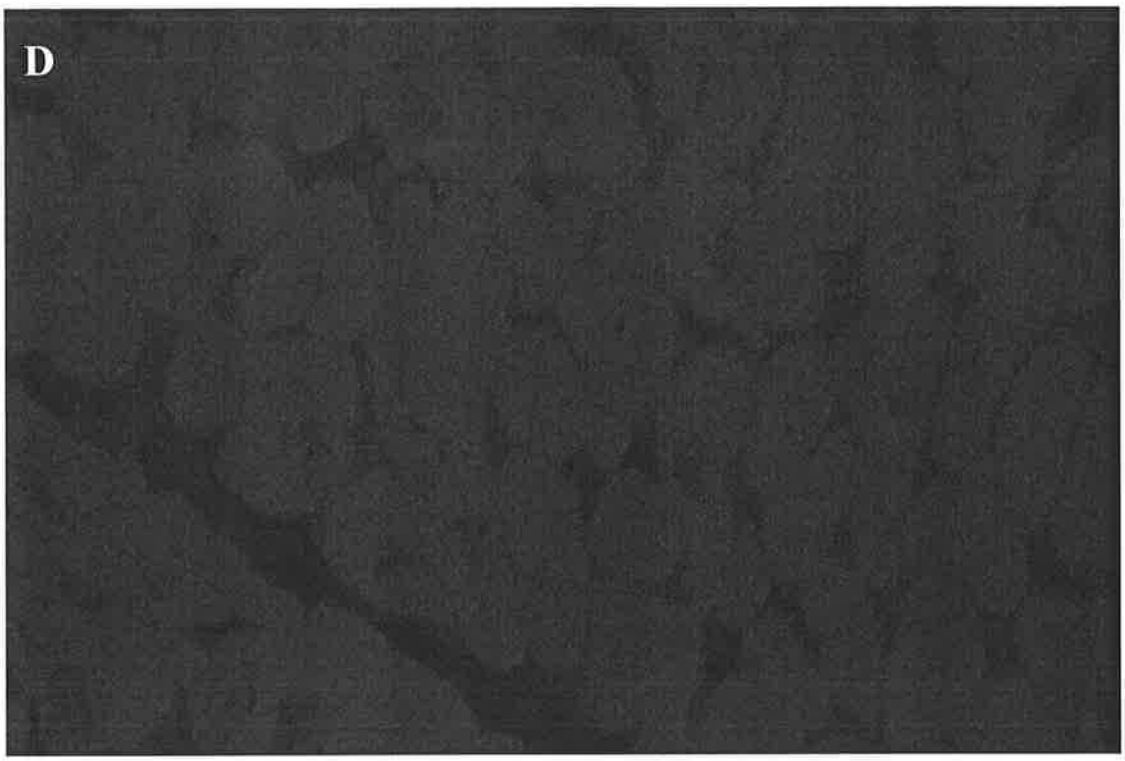

Figure 26. TREK-1 immunoreactivity in paraffin section of human heart. A. Labeled TREK-1 channels in longitudinal section of cardiac myocytes in atrial appendage. TREK-1 immunoreactivity is observed as bright punctate granules in most of cardiac myocytes. Many of them are found along the membrane of the cardiac myocytes (unfilled arrows) and some in the cytoplasm. Connective tissue between the muscle bundles (arrow heads) and the center of nuclear region in cardiac myocytes (filled arrows) are not labeled. No immunoreactivity is found in negative control preparation after omission of primary antibody (B). C: Labeled TREK-1 channels in cross-section of cardiac myocytes in ventricular tissue. Similar distribution of TREK-1 immunoreactivity in atrial tissue is observed in ventricular tissue. Labelled TREK-1 channels can also be found along membrane of cardiac myocytes and in the cytoplasm. No connective tissue and centre of nuclear region of cardiac myocytes are labelled. No positive labelling was observed in negative control preparation (D). Calibration bar: 25 μm for A and B and 50 μm for C and D.

IMMUNOHISTOCHEMISTRY OF TREK-2 IN HUMAN ATRIUM AND VENTRICLE

In order to confirm the tissue localisation of the variants of TREK-2 in atrial and ventricular tissue, immunohistochemistry was performed. In human atrial and ventricular tissue, cardiac myocytes are formed in bundles separated by connective tissue and small blood vessels (Fig. 38A). In paraffin sections of human atrial tissue,

TREK-2 immunohistochemical reactivity was observed as bright punctate granules in the cardiac myocytes, with some of this immunoreactivity along the membrane of the cardiac myocytes. No connective tissue was labelled. No immunoreactivity was found in negative control preparation after omission of primary antibody (Fig. 38B) and preincubation with the control peptide antigen. In human ventrical tissue there was much less connective tissue between the muscle bundles. TREK-2 immunohistochemical reactivity was also observed as bright punctate granules in cardiac myocytes in ventricular tissue, with no connective tissue labelling (Fig. 39C). TREK-2 immunoreactivity appeared to be distributed in the myocytes with the same spacing as the t-tubule system (magnified image in Fig. 39D). No immunoreactivity was found in negative control preparation after omission of primary antibody (Fig. 39E) and preincubation with the control peptide antigen. Immunohistochemistry was provided by Dr. Shiyong Yuan.

A:

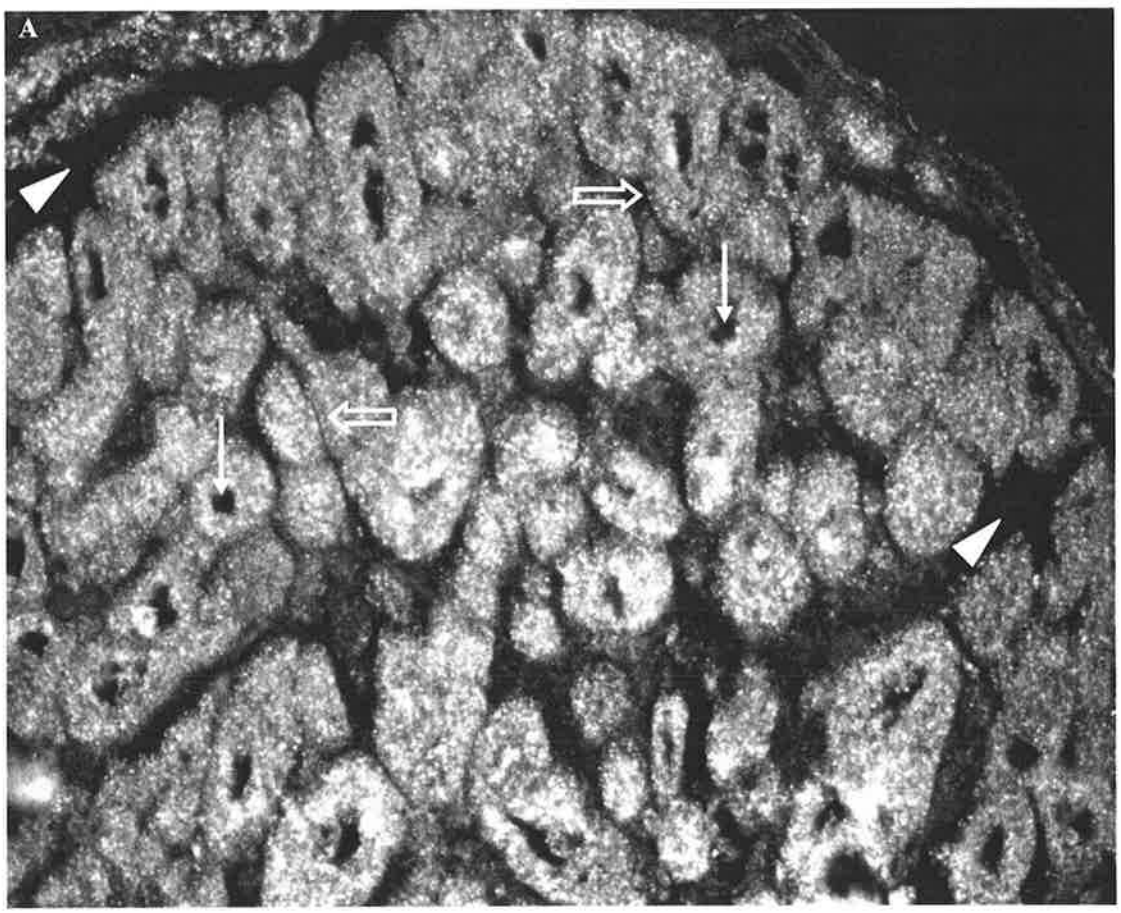

B:

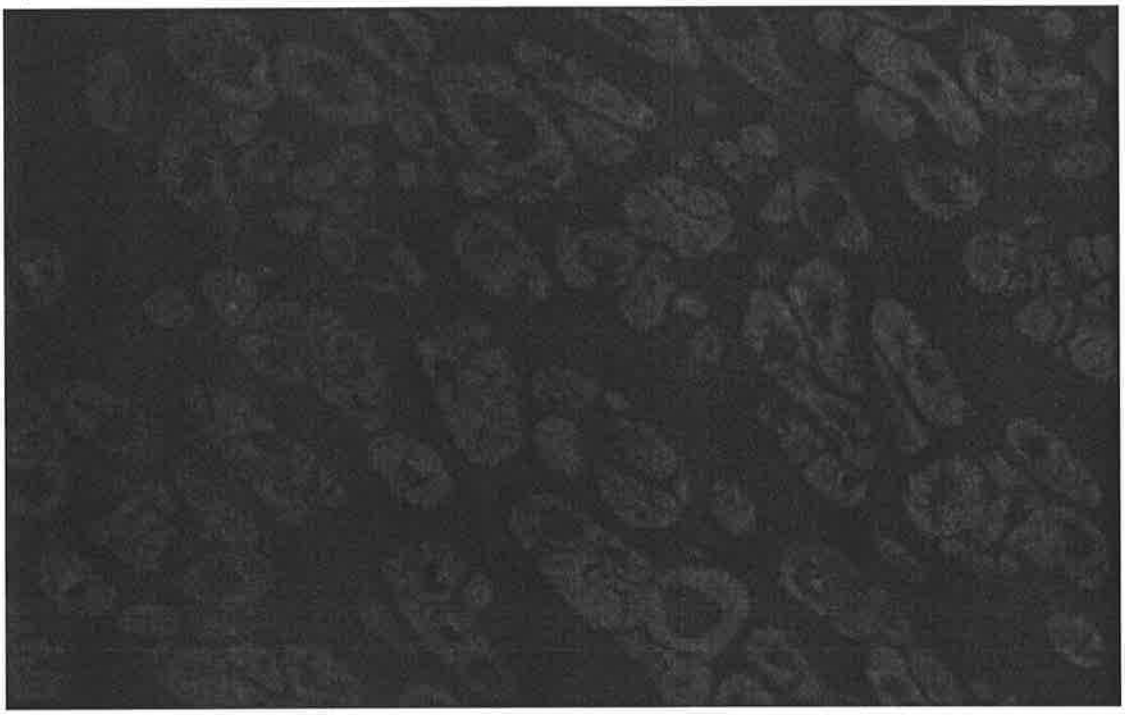

C:

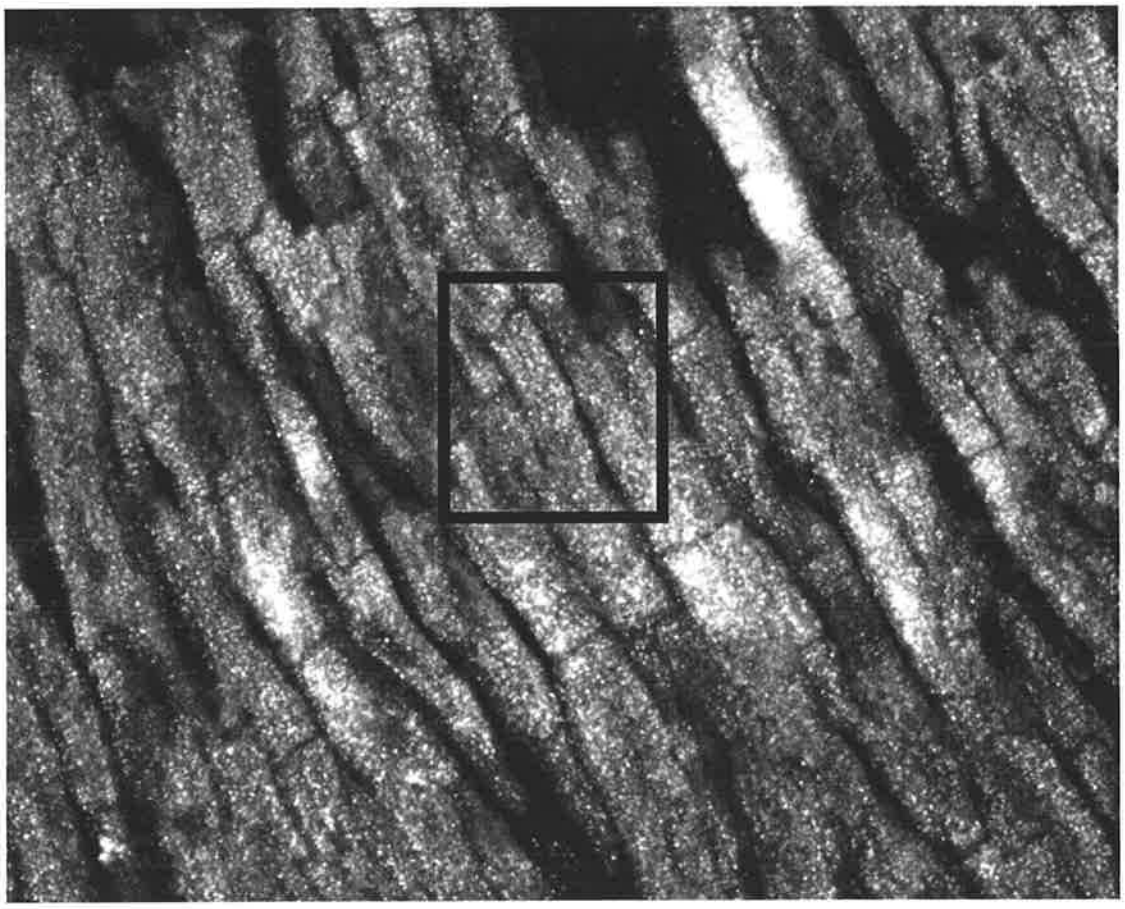

D:

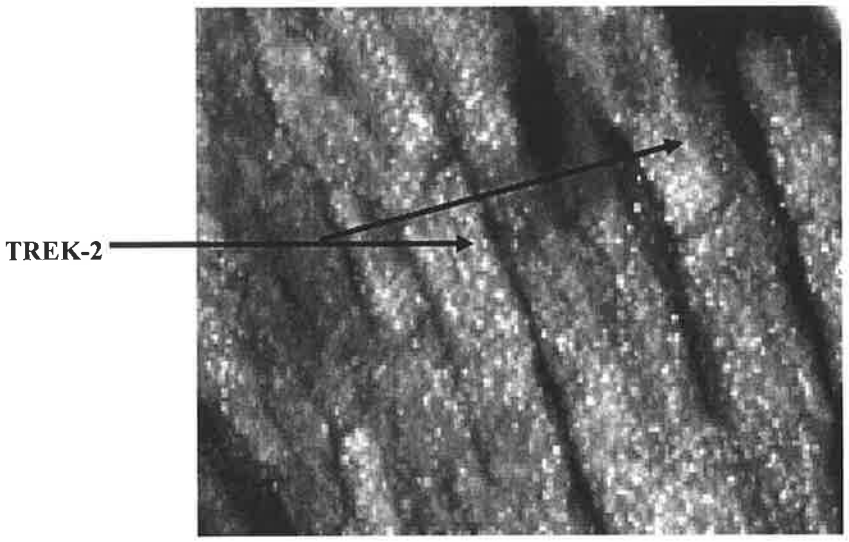

E:

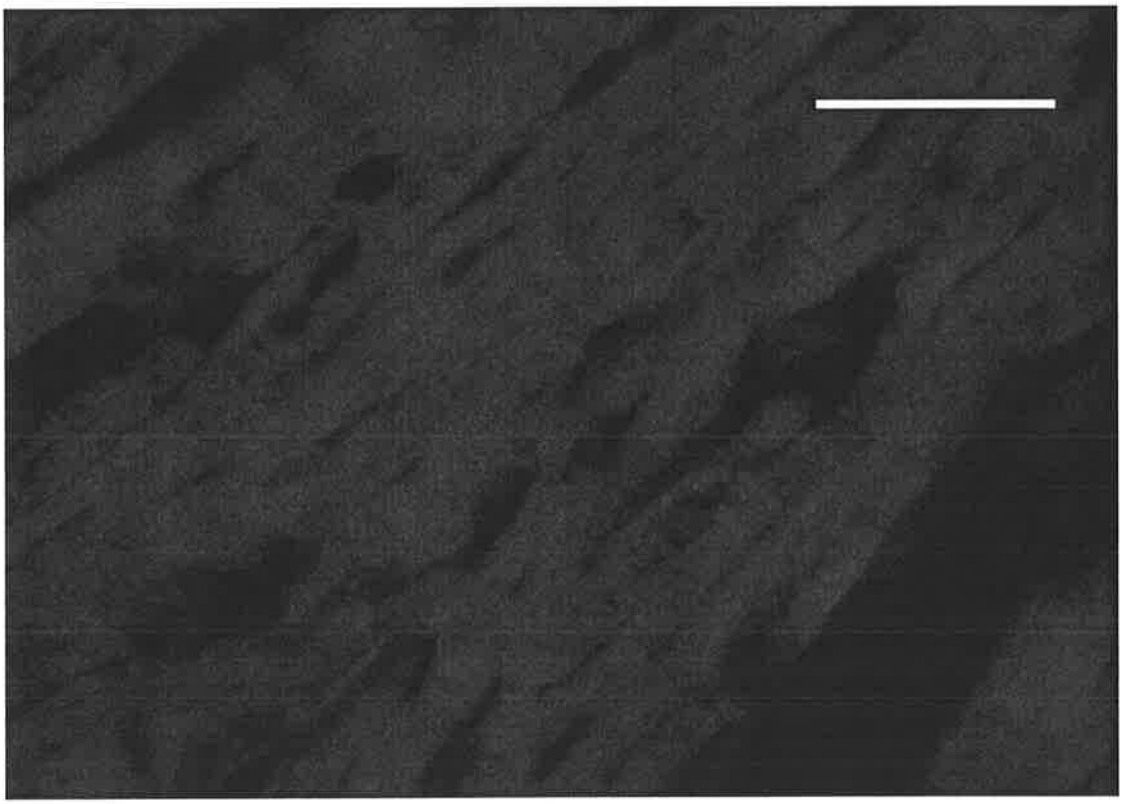

Figure 38. Immunohistochemistry of Va and Vc in human atrial and ventricular tissues. Panel A: TREK-2 immunoreactivity in paraffin section of human atrial appendage. Within the muscle bundle the cardiac myocytes are different in diameter and some of them show an empty area without myofibrils in the nuclear region (filled arrows). Punctate fine granules of TREK-2 immunoreactivity were located in most of cardiac myocytes. Some of TREK-2 positive granules were located along the membrane of the cardiac myocytes (hollow arrow). Connective tissue between the muscle bundles (arrow head) and centre of nuclear region in cardiac myocyte (filled arrows) were not labelled. No immunoreactivity was found in negative control preparation (Panel B). Calibration bar: 50 μm. Panel C: TREK-2 immunoreactivity in paraffin section of human cardiac ventricle. TREK-2 immunoreactivity was located in most of cardiac myocytes and their locations were similar to that in atrial myocytes, along the membrane (hollow arrow) and in the cytoplasm. Connective tissues between the muscle bundles (arrow head) were not immunoreactive. In an expanded view (Panel D) the immunoreactivity appeared to be spaced in striations. No immunoreactivity was found in negative control preparation (Panel E). Calibration bar: 50 μm.

Model 3700
Version 3.7
Basecaller-3700POP6.bc
BC 1.3.0.0

13-4p2_H07_SHT1-31_060.ab1
ZhuHaipengPHYSIOLibmFtextPOweb
SHT1-31
Cap 60

Signal G:65 A:78 T:62 C:41
DT3700POP6{BDv3}v1.mob

Points 2976 to 13000 Pk 1 Loc: 2976

Wed, 14 Apr 2004 9:02
Tue, 13 Apr 2004 22:11
Spacing: 12.34{12.34}

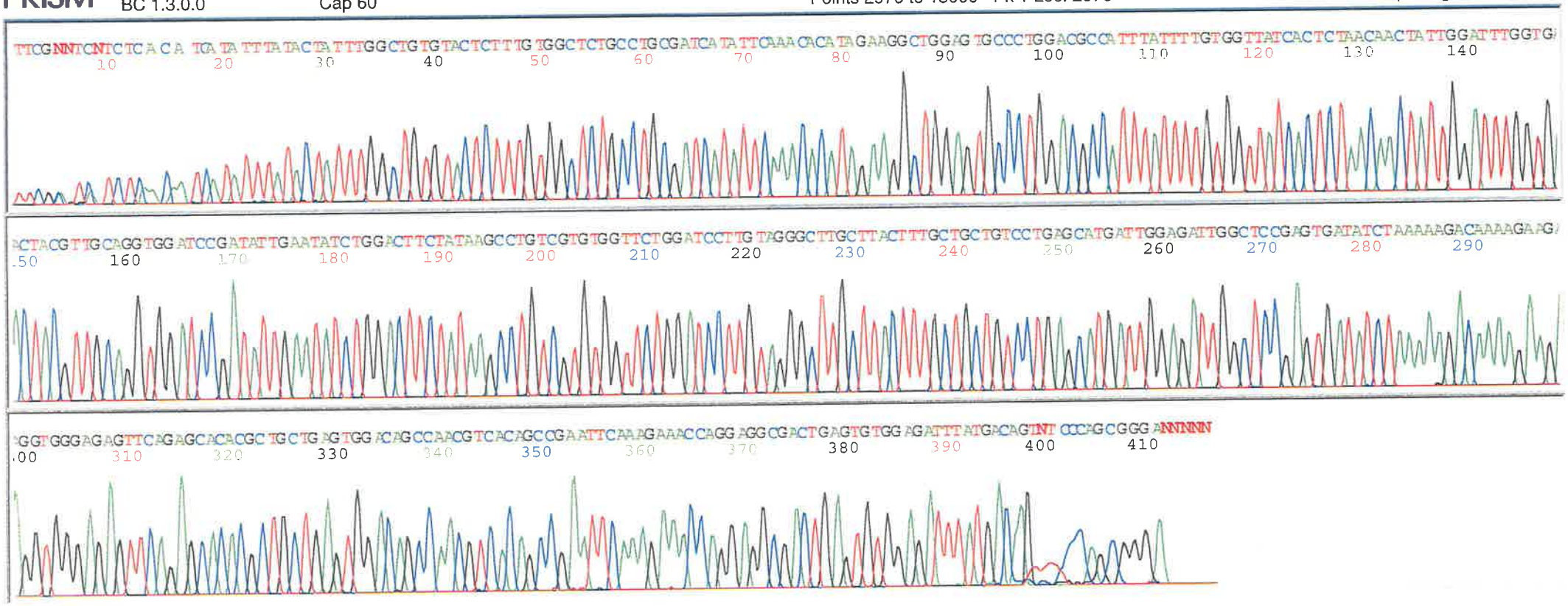

ABI PRISM

Version 3.7 H. Zhu
Basecaller-3100POP4_8HTA41_FHTA41
BC 1.5.0.0 Cap 2

DT3100POP4{BDv3}v1.mob
ABI_3100
Points 1794 to 5488 Pk 1 Loc: 1794

Mon, Feb 07, 2005 11:32 AM
Mon, Jan 31, 2005 4:15 PM
Spacing: 17.66{17.66}

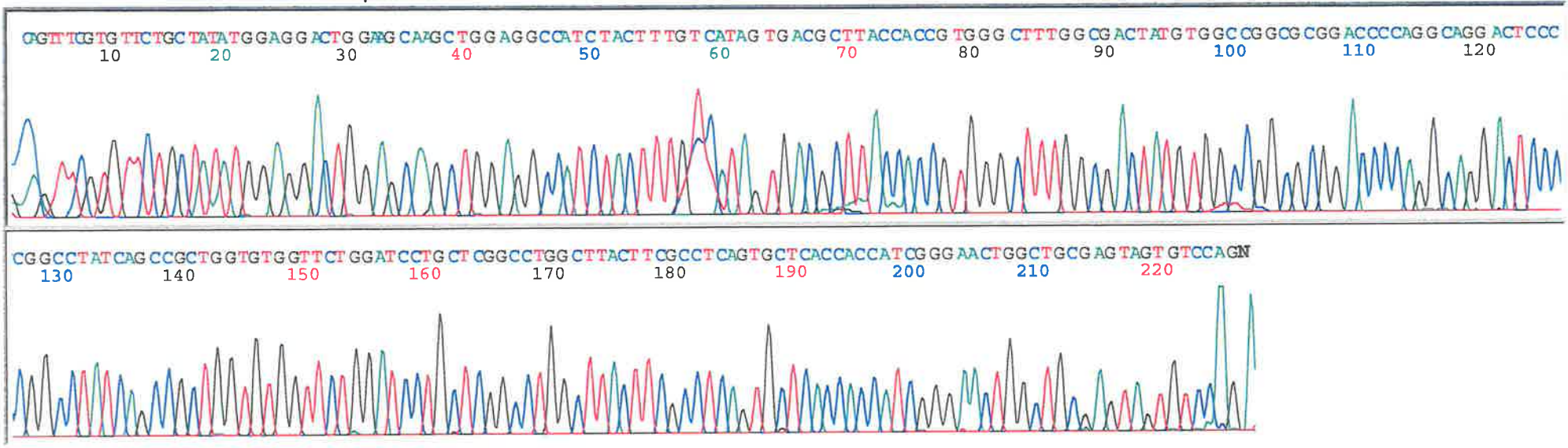

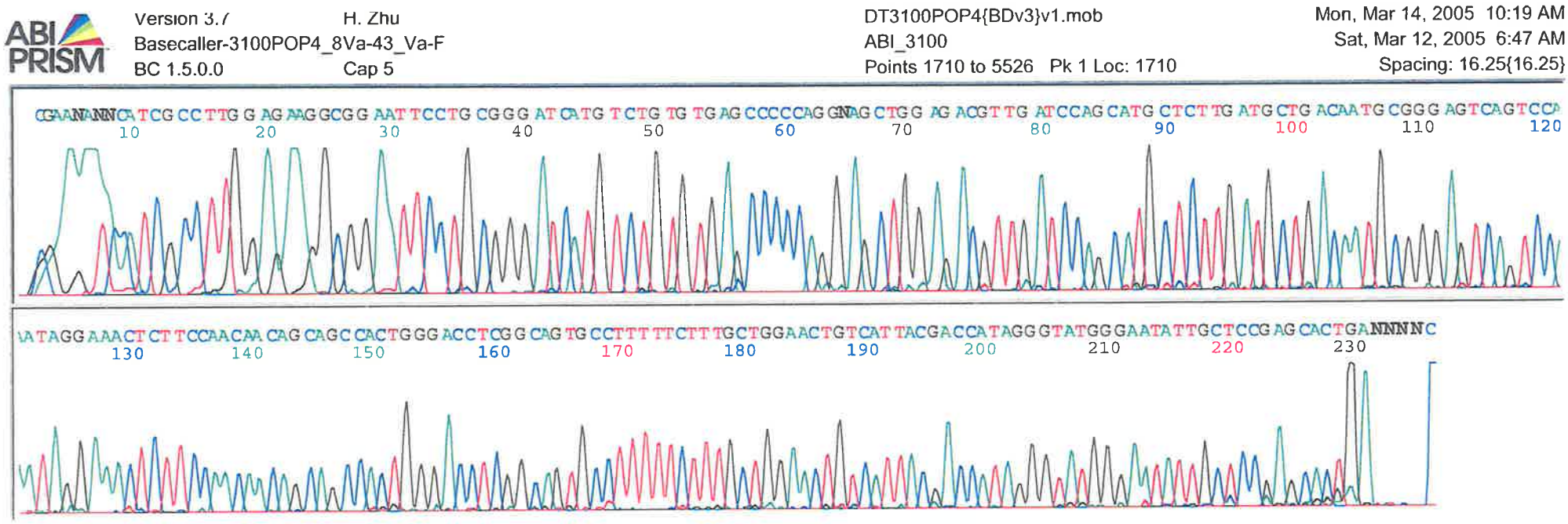
Version 3.7
H. Zhu
Basecaller-3100POP4_8Va-43_Va-F
BC 1.5.0.0
Cap 5
DT3100POP4{BDv3}v1.mob
ABI_3100
Points 1710 to 5526 Pk 1 Loc: 1710
Mon, Mar 14, 2005 10:19 AM
Sat, Mar 12, 2005 6:47 AM
Spacing: 16.25{16.25}

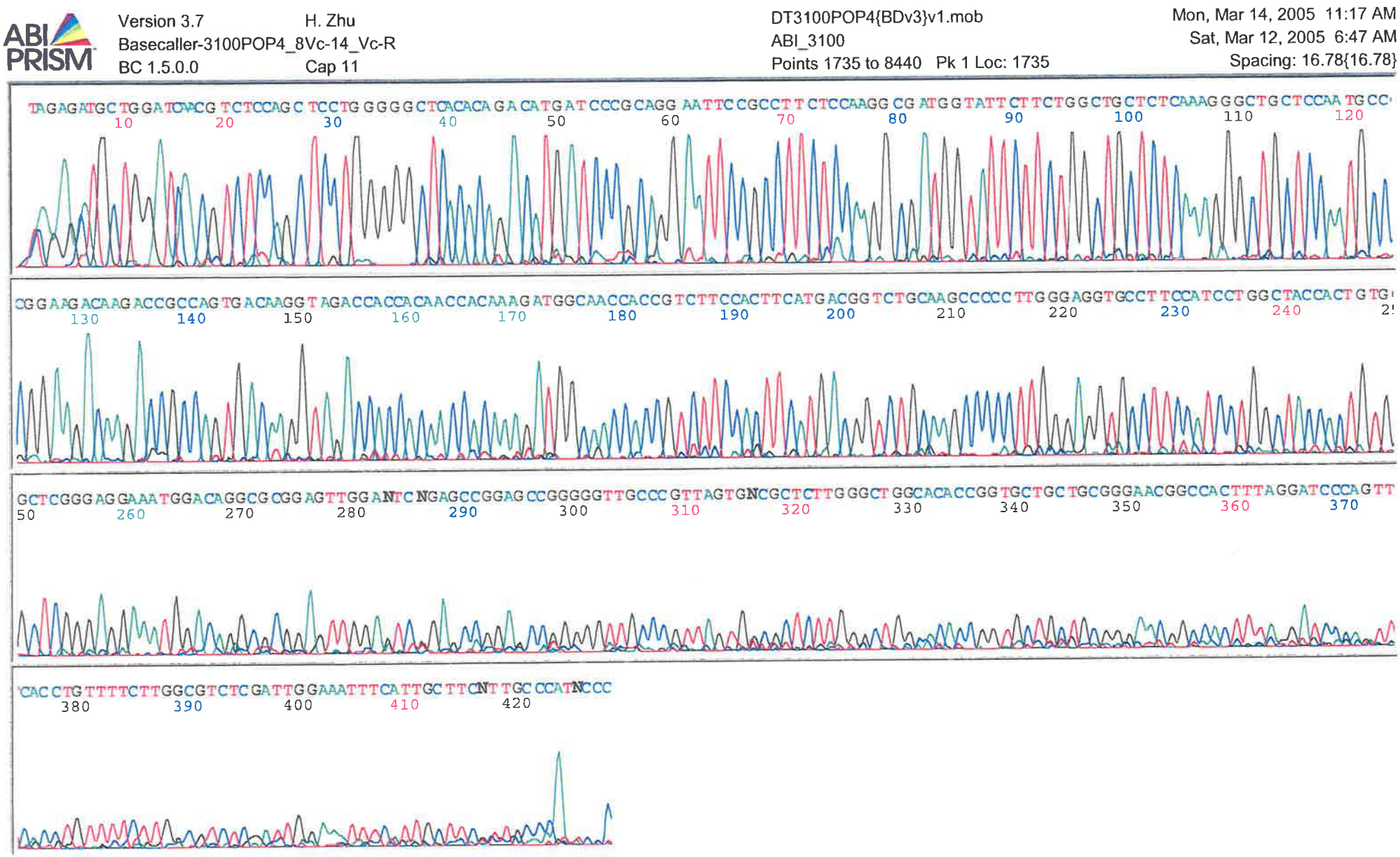
Version 3.7 H. Zhu
Basecaller-3100POP4_8Vc-14_Vc-R
BC 1.5.0.0 Cap 11
DT3100POP4{BDv3}v1.mob
ABI_3100
Points 1735 to 8440 Pk 1 Loc: 1735
Mon, Mar 14, 2005 11:17 AM
Sat, Mar 12, 2005 6:47 AM
Spacing: 16.78{16.78}
TAGAGATGCTGGATCNCG TCTCCAGC TCCTG GGGGCTCACACA GA CATGAT CCCGCAGG AATTCCGCCTT CTCCAAGG CG ATGGTATT CTTCTGGCTGCTCTCAAAGGGCTGCTCCAA TGCC
10 20 30 40 50 60 70 80 90 100 110 120
CGGAAGACAAG ACCGCCAGTGACAAGGT AGACCACCACAACCACAAAG ATGGCAACCACCG TCTTCCACTTCATGACGGTCTGCAAGCCCCC TTGGGAGGTGCCTTCCATCCTGGCTACCACTGTG
130 140 150 160 170 180 190 200 210 220 230 240
GCTCGGGAGGAAATGGACAGGCGCGGAGTTGGANTCNGAGCCGGAGCCGGGGGTTGCCC GTTAGTGNCGCTCTTGGGCTGGCACACCGGTGCTGCTGCGGGAACGGCCACTTTAGGATCCCAGTT
50 260 270 280 290 300 310 320 330 340 350 360 370
CACCTGTTTTCTTGGCGTCTCGATTGGAAATTTCATTGCTTCNTTGCCCATNCCC
380 390 400 410 420

ABI PRISM

Model 3100 2_G32_G32R_C02_06.ab1
Version 3.7 Z. Haipeng
Basecaller-3100POP4_8G32_G32R
BC 1.4.0.0 Cap 6

Signal G:87 A:33 T:40 C:54
DT3100POP4{BDv3}v1 ob
Baldric_3100
Points 1632 to 7850 Pk 1 Loc: 1632

Mon, Nov 08, 2004 1:32 PM
Sun, Nov 07, 2004 9:58 AM
Spacing: 16.52{16.52}

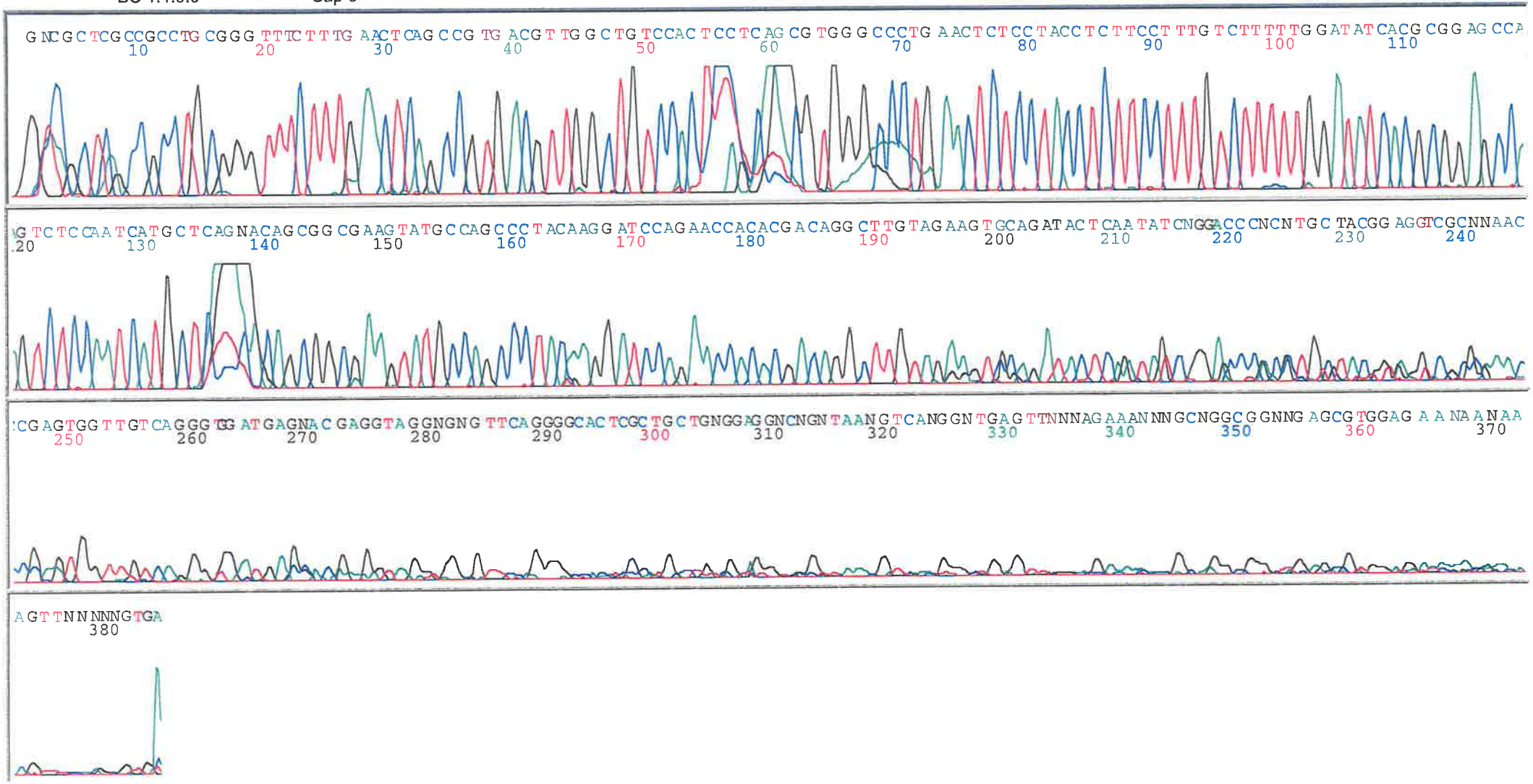

ABI PRISM

Version 3.7 H. Zhu
Basecaller-3100POP4_8R22-22-200_R22-22
BC 1.5.0.0 Cap 7

DT3100POP4{BDv3}v1.mob
ABI_3100
Points 1724 to 4504 Pk 1 Loc: 1724

Mon, Feb 07, 2005 2:53 PM
Mon, Jan 31, 2005 7:55 PM
Spacing: 16.00{16.00}

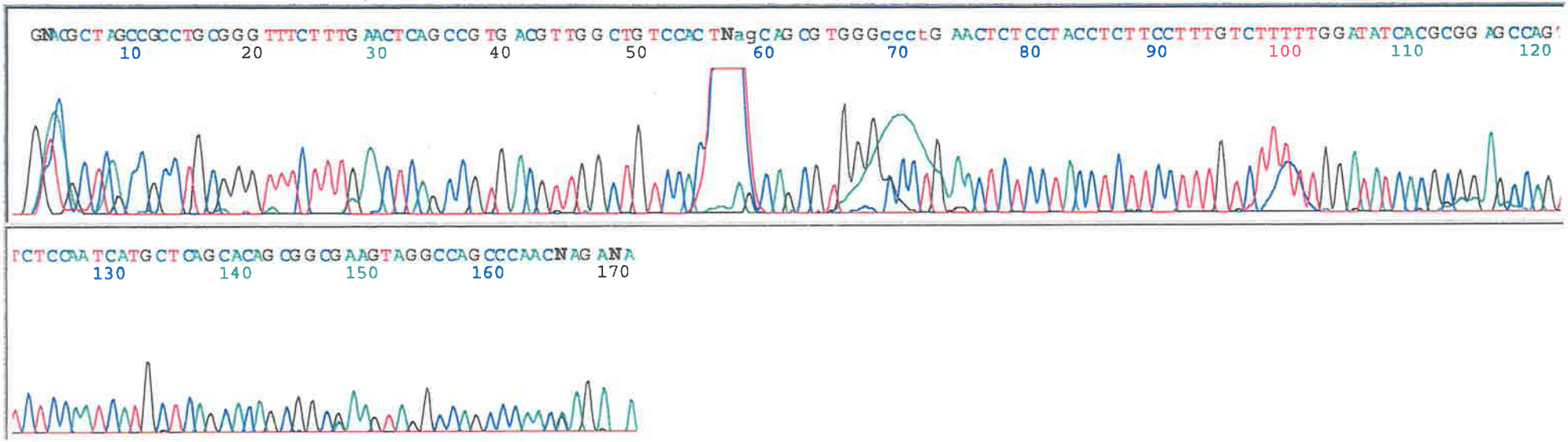

ABI PRISM

Version 3.7 H. Zhu
Basecaller-3100POP4_8Pm32-22_Pm32-22-R
BC 1.5.0.0 Cap 4

DT3100POP4{BDv3}v1.mob
ABI_3100
Points 1793 to 4767 Pk 1 Loc: 1793

Fri, Mar 04, 2005 2:17 PM
Fri, Mar 04, 2005 2:03 AM
Spacing: 16.25{16.25}